von KARMAN INSTITUTE
FOR FLUID DYNAMICS

TECHNICAL NOTE 71

A THEORETICAL STUDY OF WALL COOLING EFFECTS UPON SHOCK WAVE-LAMINAR BOUNDARY LAYER INTERACTION BY THE METHOD OF LEES-REEVES-KLINEBERG

by

B.G. GAUTIER

and

J. J. GINOUX

RHODE-SAINT-GENESE, BELGIUM

MAY 1971

von KARMAN INSTITUTE FOR FLUID DYNAMICS

TECHNICAL NOTE 71

A THEORETICAL STUDY OF WALL COOLING EFFECTS UPON SHOCK WAVE-LAMINAR BOUNDARY LAYER INTERACTION BY THE METHOD OF LEES-REEVES-KLINEBERG

by

Bernard G. GAUTIER *

and

Jean J. GINOUX

May 1971

* This work was conducted by Bernard Gautier, Research Assistant at VKI, under the direction of Professor Ginoux, and will constitute a part of his doctoral thesis.

ACKNOWLEDGEMENTS

The author gratefully acknowledges the guidance of Professor J.J. GINOUX who suggested this research.

Thanks are also due to Dr. H.P. HORTON for his assistance in the theoretical developments, and to M. RIETHMULLER for his collaboration in developing the computer program.

TABLE OF CONTENTS

SUMMARY

The integral method of Lees and Reeves-Klineberg has been used to study the effect of changes of wall temperature ratio upon wall pressure and heat transfer distributions, of a shock wave - laminar boundary layer interaction generated by a two-dimensional deflected surface.

Klineberg extended the integral method of Lees and Reeves to the non-adiabatic case (isothermal wall) but his numerical results deal only with a highly cooled surface (S_w=-0.8). The present study consists in an extension of Klineberg's method to intermediate values of wall to stagnation temperature ratio, from adiabatic (S_w=0) to highly cooled wall (S_w=-0.8).

A parametric study has then been carried out to determine the effect of progressive changes in the wall cooling ratio. In particular, a linear reduction of the separation length with the surface cooling ratio has been demonstrated.

LIST OF FIGURES

LIST OF NOTATIONS

a	Speed of sound, also velocity profile parameter
b	Total enthalpy profile parameter
C	Constant in viscosity law $\frac{\mu}{\mu_\infty} \Big/ \frac{T}{T_\infty}$
C_F	Skin friction coefficient $\tau_w/(\rho_\infty u_\infty^2/2)$
C_H	Non-dimensional heat transfer coefficient defined by $q_w/\left[\rho_\infty u_\infty(h_{0_e} - h_{0_w})\right]$
D	Determinant of equations 32
E	$-\frac{1}{\delta_i^*}\int_0^{\delta_i} S\,dY$
f	Function defined in equation 13, also function used in Cohen-Reshotko equations
F	$\mathscr{X} + \frac{1 + m_e}{m_e}(1 - E)$
g	Total enthalpy ratio h_0/h_{0e}
G	$\int_0^\delta \rho u^3 dy$
h	Static enthalpy, also function defined in equation 27
h_0	Total enthalpy
$\mathscr{X}$	θ_i/δ_i^*
I	Momentum flux $\int_0^\delta \rho u^2 dy$
J	θ_i^*/δ_i^*
k	Thermal conductivity of air
K	$\int_0^\delta u\,dy$ also function defined in equations B9 and B14
L	Length of flat plate

m	$\frac{\gamma-1}{2} M^2$
$\dot{m}$	Mass flux $\int_0^\delta \rho u dy$
M	Mach number
N_1, N_2, N_3, N_4	Numerators of equations 32
p	Static pressure
P	$\frac{\delta_i^*}{U_e} \left(\frac{\partial U}{\partial Y}\right)_{Y=0}$
Pr	Prandtl number $\mu c_p/k$
q	Heat flux $-k\partial T/\partial y$
Q	$\delta_i^* \left(\frac{\partial S}{\partial Y}\right)_{Y=0}$
$\overline{Q}$	Q/Pr_w
R	$\frac{2\delta_i^*}{U_e^2} \int_0^{\delta_i} \left(\frac{\partial U}{\partial Y}\right)^2 dY$
Re_u	Unit Reynolds number of free stream $\frac{\rho_\infty u_\infty}{\mu_\infty}$ × unit length
$Re_{\delta_i^*}$	$\frac{\rho_\infty u_\infty}{\mu_\infty} \delta_i^*$
Re_x	$\frac{\rho_\infty u_\infty}{\mu_\infty} x$
S	Total enthalpy function $(h_0/h_{0_e} - 1)$
T	Static temperature, also $T(a,b) = -\int_0^{\eta.99} \frac{U}{U_e} S dY$

T^*	$- \frac{1}{\delta_i^*} \int_0^{\delta_i} \frac{U}{U_e} S dY$
u,v	Velocity components respectively parallel and normal to the wall
U,V	Transformed velocity components
x,y	Coordinates respectively parallel and normal to the wall
x_0	Abscissa of beginning of interaction
X,Y	Transformed coordinates
Z	$\frac{1}{\delta_i^*} \int_0^{\delta_i} \frac{U}{U_e} dY$
α	$\frac{1}{\eta} \frac{Y}{\delta_i^*}$ scaling factor
α_w	Inclination of local wall tangent with respect to free stream direction
β	Pressure gradient parameter (similar solutions) also $p_e a_e / p_\infty a_\infty$
γ	c_p/c_v ratio of specific heats of air
δ	Boundary layer thickness
δ_i	Transformed boundary layer thickness
δ_u	$\int_0^{\delta} (1 - \frac{u}{u_e}) dy$
δ^*	Boundary layer displacement thickness $\int_0^{\delta} (1 - \frac{\rho u}{\rho_e u_e}) dy$
δ_i^*	Transformed boundary layer displacement thickness $\int_0^{\delta_i} (1 - \frac{U}{U_e}) dY$

ε Perturbation parameter

η Non-dimensional normal coordinate (similar solutions)

θ Boundary layer momentum thickness $\int_0^{\delta} \frac{\rho u}{\rho_e u_e} (1 - \frac{u}{u_e}) dy$

θ_i Transformed boundary layer momentum thickness

$$\int_0^{\delta_i} \frac{U}{U_e} (1 - \frac{U}{U_e}) dY$$

θ^* $\int_0^{\delta} \frac{\rho u}{\rho_e u_e} (1 - \frac{u^2}{u_e^2}) dy$

θ_i^* $\int_0^{\delta_i} \frac{U}{U_e} (1 - \frac{U^2}{U_e^2}) dY$

θ^{**} $\int_0^{\delta} \frac{\rho u}{\rho_e u_e} (\frac{h_0}{h_{0_e}} - 1) dy$ boundary layer energy thickness

Θ Local external flow streamline inclination with respect to x coordinate

μ Dynamic viscosity coefficient of air

ν Prandtl-Meyer angle, also kinematic viscosity coefficient of air

ρ Density

σ $-\int_0^{\eta_{.99}} S d\eta$

τ Shear stress, also coefficients defined in equation 39

$\overline{\chi}$ Viscous hypersonic similarity parameter

Subscripts

c	Corner
CR	Critical point
e	Outer inviscid flow
i	Transformed
r	Ratio quantities in jump equations, also reattachment point
s	Separation point
sh	Shock impingement
t	Total or stagnation conditions
w	At the wall
WI	In the weak interaction region
0	At the beginning of interaction
1	Just upstream the jump
2	Just downstream the jump
∞, ∞_-	Free stream conditions upstream of interaction
∞_+	Free stream conditions far downstream of interaction

1. INTRODUCTION

The problem of boundary layer separation induced by a strong external perturbation, such as a shock wave impinging on the boundary layer has received the careful attention of numerous investigators during the past 15 years, mainly because of its unfavourable effects on the performances of control surfaces and air inlets of supersonic vehicles. More recently, the advances in hypersonic flight have emphasized the associated thermal heating problems. Separation has a marked effect upon the thermal parameters of the flow, and it is desirable to be able to theoretically predict the location and strength of heat flux peaks on hypersonic vehicles in the presence of separation.

Numerous methods have been developed in the past for the prediction of boundary layer - shock wave interactions and satisfactory numerical solutions have been found for cases when the boundary layer is wholly laminar.

Though finite differences methods have been successfully applied (Rheyner-Flugge-Lotz) (13) the so-called integral methods are simpler and constitute the majority of the existing methods. The coupling between the inner viscous and the outer essentially non-viscous flow fields was first introduced by Crocco-Lees (1) (1952). From this basic idea other investigators (2), (3) refined the method with the aid of empirical datas. Later (1963) Lees and Reeves (4), (6) developed an integral method excluding empirical data by using the first moment of momentum equation. This method was first applied to the adiabatic wall case, and was later extended by Klineberg (8), (9) (1968) to the non-adiabatic isothermal wall by adding the energy equation. A basically similar method was also applied to axisymmetric bodies (7). Simultaneously with Klineberg, Holden developed a rather similar integral method (10), (11); furthermore he included the effect of non-zero normal pressure gradient in hypersonic flows (12).

A critical evaluation of recent available methods has been published by Murphy (1969) (13), pointing out the weaknesses of each of the methods studied.

Although Klineberg's basic theory is valid for any wall temperature ratio, the polynomial functions required in the theory were given only for the adiabatic and highly cooled wall cases and only two complete calculations were presented. For this reason Klineberg's theory has been extended in the present study to arbitrary wall cooling ratios and the effect of variation of the latter parameter upon the overall features of the interaction has been examined. For this purpose additional "similar solutions" of the boundary layer equations have been calculated in order to provide a set of polynomial functions describing relations between integral properties for each value of wall cooling parameter. Into the main framework of the method an interpolation procedure was found to satisfy the required downstream boundary conditions.

2. ANALYSIS

2.1 Governing equations

This section summarizes Klineberg's development leading to the final form of the differential equations. The partial differential equations describing two-dimensional compressible boundary layer flow are :

$$\frac{\partial}{\partial x}(\rho u) + \frac{\partial}{\partial y}(\rho v) = 0 \quad , \tag{1}$$

$$\rho u \frac{\partial u}{\partial x} + \rho v \frac{\partial u}{\partial y} = - \frac{dp}{dx} + \frac{\partial}{\partial y}\left(\mu \frac{\partial u}{\partial y}\right) \quad , \tag{2}$$

$$\rho u \frac{\partial h_0}{\partial x} + \rho v \frac{\partial h_0}{\partial y} = \frac{\partial}{\partial y}\left(\frac{\mu}{Pr}\frac{\partial h_0}{\partial y}\right) - \frac{\partial}{\partial y}\left[\mu\left(\frac{1 - Pr}{Pr}\right) u \frac{\partial u}{\partial y}\right] \quad , \tag{3}$$

The first moment of momentum equation is obtained by multiplying Eq. (2) by u, giving :

$$\rho u^2 \frac{\partial u}{\partial x} + \rho u v \frac{\partial u}{\partial y} = - u \frac{dp}{dx} + u \frac{\partial}{\partial y} (\mu \frac{\partial u}{\partial y}) \quad . \tag{4}$$

Following the Karman integral approach, these equations are integrated across the boundary layer to yield a system of four ordinary differential equations. Then, after assuming the linear temperature - viscosity law,

$$\frac{\mu}{\mu_\infty} = C \frac{T}{T_\infty} \tag{5}$$

and that the outer inviscid flow is isentropic (i.e. h_{0_e} = const.), we may apply a Stewartson transformation of the form :

$$dX = C \frac{p_e a_e}{p_\infty a_\infty} dx \quad ,$$

$$dY = \frac{\rho a_e}{\rho_\infty a_\infty} dy \quad , \tag{6}$$

to reduce the equations to an equivalent "incompressible" form. The integral properties appearing in these transformed equations do not depend upon the fluid properties, and may be related to the usual compressible integral quantities, δ, δ^*, θ, θ^*, δ_u, θ^{**} by means of equations (6).

The resulting equations can be written in the following form :

$$F \frac{d\delta_i^*}{dx} + \delta_i^* \left[\frac{d\mathcal{X}}{dx} - (\frac{1+m_e}{m_e}) \frac{dE}{dx} \right] + \delta_i^* f \frac{d \text{ Log } M_e}{dx} = \beta \frac{1+m_e}{m_e(1+m_\infty)} \text{tg } \Theta \quad , \tag{7}$$

$$\mathcal{X} \frac{d\delta_i^*}{dx} + \delta_i^* \frac{d\mathcal{X}}{dx} + \delta_i^* (2\mathcal{X}+1-E) \frac{d \text{ Log } M_e}{dx} = \beta C \frac{M_\infty}{M_e} \frac{P}{Re_{\delta_i^*}} \quad , \tag{8}$$

$$J \frac{d\delta_i^*}{dx} + \delta_i^* \frac{dJ}{dx} + \delta_i^*(3J - 2T^*) d \frac{\text{Log } M_e}{dx} = \beta C \frac{M_\infty}{M_e} \frac{R}{Re_{\delta_i^*}} , \qquad (9)$$

$$T^* \frac{d\delta_i^*}{dx} + \delta_i^* \frac{dT^*}{dx} + \delta_i^* T^* \frac{d \text{ Log } M_e}{dx} = \beta C \frac{M_\infty}{M_e} \frac{Q}{Pr_w Re_{\delta_i^*}} , \qquad (10)$$

where $\text{tg } \Theta = \dfrac{v_e}{u_e}$,

$$m_e = \frac{\gamma - 1}{2} M_e^2 ,$$

$$\beta = \frac{p_e a_e}{p_\infty a_\infty} , \qquad (11)$$

and $Re_{\delta_i^*} = \dfrac{\rho_\infty a_\infty M_\infty \delta_i^*}{\mu_\infty}$.

The transformed integral quantities in equations 7 to 10 are defined as follows :

$$\delta_i = \int_0^{\delta_i} dY \qquad\qquad Z = \frac{1}{\delta_i^*} \int_0^{\delta_i} \frac{U}{U_e} dY$$

$$\delta_i^* = \int_0^{\delta_i} (1 - \frac{U}{U_e}) dY \qquad\qquad R = 2\delta_i^* \int_0^{\delta_i} \left[\frac{\partial}{\partial Y} (\frac{U}{U_e}) \right]^2 dY$$

$$\theta_i = \int_0^{\delta_i} \frac{U}{U_e} (1 - \frac{U}{U_e}) dY \qquad\qquad P = \delta_i^* \left[\frac{\partial}{\partial Y} (\frac{U}{U_e}) \right]_{Y=0}$$

$$(12)$$

$$\theta_i^* = \int_0^{\delta_i} \frac{U}{U_e}\left(1 - \frac{U^2}{U_e^{\,2}}\right) dY \qquad Q = \delta_i^* \left(\frac{\partial S}{\partial Y}\right)_{Y=0}$$

$$\mathcal{X} = \frac{\theta_i}{\delta_i^*} \qquad E = -\frac{1}{\delta_i^*}\int_0^{\delta_i} S\,dY$$

$$J = \frac{\theta_i^*}{\delta_i^*} \qquad T^* = -\frac{1}{\delta_i^*}\int_0^{\delta_i} \frac{U}{U_e} S\,dY$$

(12 cont'd)

The functions F and f are defined as :

$$F = \mathcal{X} + \frac{1 + m_e}{m_e}(1 - E) \quad ,$$

$$f = \left[2 + \frac{\gamma+1}{\gamma-1}\,\frac{m_e}{1 + m_e}\right]\mathcal{X} + \frac{3\gamma - 1}{\gamma - 1}(1 - E) + \frac{(M_e^{\,2} - 1)\,Z}{m_e\,(1 + m_e)}$$

(13)

Numerical integration of equations 7 to 10 can be performed providing we reduce the number of unknowns by choosing suitable families of velocity and total enthalpy profiles. The integral quantities (Eq. 12) must be expressed in terms of at least two parameters a and b defining respectively a velocity and a total enthalpy profile. Nevertheless it is not necessary to precisely define the detailed shape of each profile, since only relations between each of the integral quantities and the two profile parameters are needed. Relations of the following type must be obtained.

$\mathcal{X} = \mathcal{X}(a)$

$J = J(a)$

(14)

$E = E(a,b)$

$T^* = T^*(a,b)$ etc...

Note that the integrals containing U/U_e only are functions of a alone. Using the similar solutions concept, Cohen and Reshotko obtained velocity and total enthalpy profile families with streamwise pressure gradient and constant wall temperature, i.e., assuming :

$$U_e \sim X^m \quad , \tag{15}$$

$$S_w = \text{const.} \quad .$$

For given values of β (pressure gradient parameter $\beta = 2m/(m+1)$) and S_w (wall enthalpy), one can relate each of the integral quantities to any other. The fundamental assumption made by Lees-Reeves-Klineberg is that the relationships between integral quantities obtained from similar solutions are also valid for non-similar flows, for example separated flows. As outlined by Klineberg, this procedure is different from local similarity technique since only relations between integral parameters are assumed to be universal, and the velocity and total enthalpy profiles are not specified by the local pressure gradient parameter as in the method first applied by Thwaites.

2.2 Velocity and total enthalpy profile calculations :

Assuming the linear viscosity law (Eq. 5) for a perfect gas and using the Stewartson transformation, we reduce the compressible boundary layer equations to their equivalent incompressible form. Then assuming S_w = const. (isothermal wall) and Prandtl number equal 1, similar solutions are those for which $U_e \sim X^m$, in which case the shape of the non-dimensional velocity and enthalpy profiles does not depend upon X.

The similarity variable is :

$$\eta = Y \left[\frac{m+1}{2} \; \frac{U_e}{\partial_\infty X} \right]^{\frac{1}{2}} \quad . \tag{16}$$

Thus the system of three partial differential equations is reduced to a system of two ordinary differential equations :

$$f'''(\eta) + f(\eta)\, f''(\eta) + \beta(1 + S - f'^2(\eta)) = 0 \quad ,$$
$$S''(\eta) + f(\eta)\, S'(\eta) = 0 \quad , \qquad (17)$$

with $\beta = \dfrac{2m}{m+1}$.

The boundary conditions are :

$$f(0) = f'(0) = 0 \qquad\qquad f'(\infty) = 1$$
$$S(0) = S_w \qquad\qquad S(\infty) = 0 \qquad (18)$$

The system of equations (17) is numerically integrated as a two-point boundary value problem for fixed values of β and S_w, using $f''(0)$ and $g'(0)$ as iteration parameters.

The upper limit of the boundary layer is arbitrarily taken as :

$$u_\delta = 0.99 u_e \quad , \quad \text{i.e. :}$$
$$\eta_{\delta_i} = \eta_{\frac{U}{U_e} = 0.99} = \eta_{.99} \qquad (19)$$

All the integral quantities (Eq. 12) can be integrated simultaneously with the parameters selected for defining both velocity and total enthalpy profiles.

Attached flow velocity profile

$$a = \eta_{.99}\, f''(0) = \left[\frac{\partial(\frac{U}{U_e})}{\partial(\frac{Y}{\delta_i})}\right]_{Y=0} \qquad (20)$$

Separated flow velocity profile

$$a = \frac{\eta_{f'=0}}{\eta_{.99}} = \left[\frac{Y}{\delta_i}\right]_{\frac{U}{U_e}=0} \tag{21}$$

All total enthalpy profiles

$$b = S'(0) = \alpha(a) \left[\frac{\partial S}{\partial(\frac{Y}{\delta_i^*})}\right]_{Y=0} \tag{22}$$

where $\alpha(a)$ is a scaling factor :

$$\alpha(a) = \frac{1}{\delta_i^*} \frac{Y}{\eta}$$

Note : The velocity profile parameter a must be single-valued for all profiles, that explains the change in the definition of a when the flow separates.

2.3 Relationships between integral quantities of boundary layer profiles

For a given profile, each of the integral quantities (Eq. 12) must be related to a, b, or a and b. As a result, the number of unknowns in equations 7 to 10 is reduced to 5 : M_e, δ_i^*, a, b, Θ. A more convenient form of the system may be rewritten as follows :

$$F \frac{d\delta_i^*}{dx} + \delta_i^*\left(\frac{\partial F}{\partial a}\frac{da}{dx} + \frac{\partial F}{\partial b}\frac{db}{dx}\right) + f \frac{\delta_i^*}{M_e}\frac{dM_e}{dx} = \beta C \frac{M_\infty}{M_e} \frac{h}{Re\,\delta_i^*} , \tag{23}$$

$$\mathcal{X} \frac{d\delta_i^*}{dx} + \delta_i^* \frac{d\mathcal{X}}{da}\frac{da}{dx} + (2\mathcal{X} + 1 - E)\frac{\delta_i^*}{M_e}\frac{dM_e}{dx} = \beta C \frac{M_\infty}{M_e}\frac{P}{Re_{\delta_i^*}} , \quad (24)$$

$$J \frac{d\delta_i^*}{dx} + \delta_i^* \frac{dJ}{d\mathcal{X}}\frac{d\mathcal{X}}{da}\frac{da}{dx} + (3J - 2T^*)\frac{\delta_i^*}{M_e}\frac{dM_e}{dx} = \beta C \frac{M_\infty}{M_e}\frac{R}{Re_{\delta_i^*}} , \quad (25)$$

$$T^* \frac{d\delta_i^*}{dx} + \delta_i^* \left(\frac{\partial T^*}{\partial a}\frac{da}{dx} + \frac{\partial T^*}{\partial b}\frac{db}{dx}\right) + T^* \frac{\delta_i^*}{M_e}\frac{dM_e}{dx} = \beta C \frac{M_\infty}{M_e}\frac{\overline{Q}}{Re_{\delta_i^*}}, \quad (26)$$

with : $\frac{\partial F}{\partial a} = \frac{d\mathcal{X}}{da} - \frac{1 + m_e}{m_e}\frac{\partial E}{\partial a}$,

$$\frac{\partial F}{\partial b} = - \left(\frac{1 + m_e}{m_e}\right)\frac{\partial E}{\partial b} , \quad (27)$$

$$\overline{Q} = \frac{Q}{Pr_w}$$

and $h = \frac{M_e}{M_\infty}\frac{1 + m_e}{m_e(1 + m_\infty)} Re_{\delta_i^*} \frac{tg\ \Theta}{C}$.

According to Klineberg's treatment of the equations, one can introduce the variables $\alpha(a)$ and $\sigma(b)$ in order to reduce to one only the functions depending upon both a and b.

$$\frac{dY}{d\eta} = \alpha\delta_i^* = \frac{Y}{\eta} ,$$

$$\alpha = \frac{1}{\int_0^{\eta_{.99}} (1 - \frac{U}{U_e})d\eta} , \quad (28)$$

$$\sigma = - \int_0^{\eta_{.99}} S d\eta$$

Thus : $Q = \frac{b}{\alpha(a)}$,

$$E = \alpha(a)\ \sigma(b) \quad , \tag{29}$$

$T^* = \alpha(a)\ T(a,b)$,

with $T(a,b) = - \int_0^{\eta_{.99}} \frac{U}{U_e} S d\eta$.

To summarize, the profile-dependent integral quantities we need are the following ones :

Velocity profile functions :

$\mathcal{X}(a)$, $J(a)$, $Z(a)$, $R(a)$, $P(a)$, $\frac{d\mathcal{X}}{da}(a)$, $\frac{dJ}{d\mathcal{X}}(a)$, $\alpha(a)$, $\frac{d\alpha}{da}(a)$

Total enthalpy profile functions :

$$\sigma(b),\ \frac{d\sigma}{db}(b) \tag{30}$$

Both velocity and total enthalpy profile functions :

$T(a,b)$, $\frac{\partial T}{\partial a}(a,b)$, $\frac{\partial T}{\partial b}(a,b)$

2.4 Final form of basic differential equations

The last remaining unknown Θ, the local inclination of streamlines at the outer edge of the boundary layer with respect to the wall is related to the local outer flow Mach number M_e, through the Prandtl-Meyer relationship;

$$\Theta = \alpha_w(x) + \nu(M_{\underline{\infty}}) - \nu(M_e) \quad , \tag{31}$$

assuming a supersonic, isentropic outer inviscid flow field and Θ being small.

A convenient final form of the differential equations is given by Klineberg (8) :

$$\frac{\delta_i^*}{M_e}\frac{dM_e}{dx} = \frac{\beta C}{Re\,\delta_i^*}\frac{M_\infty}{M_e}\frac{N_1}{D} ,$$

$$\frac{d\delta_i^*}{dx} = \frac{\beta C}{Re\,\delta_i^*}\frac{M_\infty}{M_e}\frac{N_2}{D} ,$$

$$\delta_i^*\frac{da}{dx} = \frac{\beta C}{Re\,\delta_i^*}\frac{M_\infty}{M_e}\frac{N_3}{D} , \qquad (32)$$

$$\delta_i^*\frac{db}{dx} = \frac{\beta C}{Re\,\delta_i^*}\frac{M_\infty}{M_e}\frac{N_4}{D} .$$

where : $D = B_1\frac{\partial T^*}{\partial b} - B_2\frac{\partial F}{\partial b}$,

$$N_1 = B_3\frac{\partial T^*}{\partial b} - B_4\frac{\partial F}{\partial b} ,$$

$$N_2 = B_5\frac{\partial T^*}{\partial b} - B_6\frac{\partial F}{\partial b} , \qquad (33)$$

$$N_3 = B_7\frac{\partial T^*}{\partial b} - B_8\frac{\partial F}{\partial b} ,$$

$$N_4 = B_4 f + B_6 F + B_8\frac{\partial F}{\partial a} - B_2 h .$$

with :

$$B_1 = A_6 \frac{\partial F}{\partial a} + (A_3 f - A_8 F) \frac{d\chi}{da} \quad ,$$

$$B_2 = A_6 \frac{\partial T^*}{\partial a} + (A_3 - A_8)\, T^* \frac{d\chi}{da} \quad ,$$

$$B_3 = A_2 \frac{\partial F}{\partial a} + (A_3 h - A_4 F) \frac{d\chi}{da} \quad ,$$

$$B_4 = A_2 \frac{\partial T^*}{\partial a} + (A_3 \overline{Q} - A_4 T^*) \frac{d\chi}{da} \quad , \tag{34}$$

$$B_5 = A_7 \frac{\partial F}{\partial a} + (A_4 f - A_8 h) \frac{d\chi}{da} \quad ,$$

$$B_6 = A_7 \frac{\partial T^*}{\partial a} + (A_4 T^* - A_8 \overline{Q}) \frac{d\chi}{da} \quad ,$$

$$B_7 = A_6 h - (A_2 f + A_7 F) \quad ,$$

$$B_8 = A_6 \overline{Q} - (A_2 + A_7)\, T^* \quad ,$$

and

$$A_1 = 2\chi + 1 - E$$

$$A_2 = PJ - \chi R$$

$$A_3 = \chi \frac{dJ}{d\chi} - J \tag{35}$$

$$A_4 = P \frac{dJ}{d\chi} - R$$

$$A_5 = 3J - 2T^*$$

$$A_6 = A_1 J - A_5 \chi$$

$$A_7 = A_1 R - A_5 P$$

$$A_8 = A_1 \frac{dJ}{d\mathcal{X}} - A_5 \, . \qquad (35 \text{ cont'd})$$

2.5 Numerical procedure for obtaining polynomial representation of integral functions

For a given value of S_w a complete family of similar profiles and their associated integral quantities is computed and then tabulated including both the regimes of reverse flow ($\beta < 0$ and $f''(0) < 0$) and attached flow ($f''(0) > 0$) with adverse ($\beta < 0$) and favourable ($\beta > 0$) pressure gradient. When a sufficient number of similar solutions has been computed (here in $\sim$ 30 separated and $\sim$50 attached similar solutions) these discrete points are curve-fitted by polynomial expressions in a, b or a and b, taking for example the following form of polynomial :

$$\mathcal{X}(a) = \sum_{i=0}^{N} C_{\mathcal{X}_i} \, a^i \; . \qquad (36)$$

The polynomial coefficients $C_{\mathcal{X}_i}$ are determined using the least square rule in conjunction with a best fit procedure, that is the chosen degree of polynomial is that which provides the minimum error (this error is taken as the sum of square deviations for each point). The maximum number of coefficients is 9.

Functions depending directly of one profile only are the following : $\mathcal{X}(a)$, $J(a)$, $Z(a)$, $R(a)$, $P(a)$, $\alpha(a)$ and $\sigma(b)$. The first order derivatives of these functions are determined by taking the slope of the segment joining two adjacent points as the derivative value at the middle point of this segment, for example :

$$\frac{d\mathcal{X}}{da}(\bar{a}) = \frac{\mathcal{X}_{i+1} - \mathcal{X}_i}{a_{i+1} - a_i} \; , \qquad (37)$$

with $\bar{a} = \frac{a_i + a_{i+1}}{2}$.

Hence we obtain :

$$\frac{d\mathcal{X}}{da}(a), \quad \frac{dJ}{da}(a), \quad \frac{d\alpha}{da}(a) \quad \text{and} \quad \frac{d\sigma}{db}(b) \quad .$$

Functions depending on both velocity and enthalpy profiles are represented by a double summation on a and b :

$$T(a,b) = \sum_{k=0}^{M} \left[\sum_{\ell=0}^{N} D_{k,\ell} \, b^{\ell} \right] a^k \quad , \tag{38}$$

but, prior to this curve fitting, the function T(a,b) is determined point by point in the following manner :
Each total enthalpy profile is multiplied point by point (i.e. for each value of η) successively by all the velocity profiles (for both reversed and attached flow). This procedure provides a complete dehooking of the enthalpy and velocity profiles.

From the tabulated values of T, a first curve-fit gives, for each value of b, a polynomial function of a, i.e. :

$b = b_1$

$$T(b_1,a) = \sum_{k=0}^{M} \zeta_k(b_1) a^k \quad . \tag{39}$$

A second curve-fit of ζ_k coefficients (for each value of k) gives a polynomial function of b :

$$\zeta_k(b) = \sum_{\ell=0}^{N} D_{k,\ell} \, b^{\ell} \quad . \tag{40}$$

Hence the complete set of T(a,b) coefficients can be calculated. Both partial derivatives $\frac{\partial T}{\partial a}(a,b)$ and $\frac{\partial T}{\partial b}(a,b)$ are now determined using a slightly different procedure to that of Klineberg (In fact, direct differentiation of the T(a,b) polynomial provides

$\partial T/\partial a$ and $\partial T/\partial b$ in Klineberg's framework).

Here we use a procedure similar to that employed for the T(a,b) curve fitting, from a discrete distribution of derivative points. The first partial derivative is obtained from five adjacent points of T(a,b) functions using a Taylor's formula :

$$f'(x) = f(x,x_1) - (x-x_1)\, f(x,x_1,x_2) + (x-x_1)(x-x_2)\, f(x,x_1,x_2,x_3)$$
$$+ \ldots (-1)^{n-1} (x-x_1)(x-x_2) \ldots (x-x_{n-1})\, f(x,x_1,x_2,x_3 \ldots x_n), \tag{41}$$

with $$f(x,x_1) = \frac{f(x) - f(x_1)}{x - x_1} ,$$

$$f(x,x_1,x_2) = \frac{f(x,x_1) - f(x\ ,x_2)}{x_1 - x_2}$$

$$f(x,x_1,x_2 \ldots x_r) = \frac{f(x,x_1,x_2 \ldots x_{r-1}) - f(x_1,x_2 \ldots x_r)}{x - x_r}$$

Finally, the polynomial expressions for $\partial T/\partial a$ and $\partial T/\partial b$ are :

$$\frac{\partial T}{\partial a}(a,b) = \sum_{k=0}^{M} \mathcal{E}_k(b)\, a^k ,$$

$$\text{with} \quad \mathcal{E}_k(b) = \sum_{\ell=0}^{N} F_{k,\ell}\, b^\ell , \tag{42}$$

$$\text{and} \quad \frac{\partial T}{\partial b}(a,b) = \sum_{k=0}^{M} \phi_k(a)\, b^k ,$$

$$\phi_k(a) = \sum_{\ell=0}^{N} G_{k,\ell}\, a^\ell . \tag{43}$$

Polynomial expressions for T, $\partial T/\partial a$, $\partial T/\partial b$ are limited to the fifth degree in a and b.

The result of these curve fits is a table of 29 polynomials giving functional dependence of the integral quantities to profile parameters a and b. A table of these coefficients has been computed for the following values of S_w (S_w=-0.8, -0.6, -0.4, -0.2) - Appendix A.

Most of the velocity dependent integral functions are quite independent of S_w except P(a) in the separated region but the remaining functions $\sigma(b)$, $d\sigma/db(b)$, T(a,b), $\partial T/\partial a(a,b)$ and $\partial T/\partial b(a,b)$ are directly dependent upon the value of S_w. For example the dependence of T(a,b) and $\partial T/\partial a(a,b)$ on S_w is shown in figures 2 and 3.

Remark : A pair of polynomial expressions are needed for all the parameters depending upon a, respectively for attached and separated flow, due to the change in the definition of a in these two regions.

3. METHOD OF SOLUTION FOR SHOCK-WAVE BOUNDARY LAYER INTERACTION GENERATED BY A FLAT PLATE-RAMP

In order to compare Klineberg theory with the numerous experimental data available the theory has been applied to the simple geometry constituted by a flat plate followed by a deflected flap, θ being the deflection angle. The physical model of flow field developed in such interactions is shown in figure 1.

3.1 Physical flow pattern

3.1.1 Principle of equivalence :

Lees and Reeves used the following simple flow model. A laminar boundary layer developing on a flat plate is subjected to an impinging externally-generated plane oblique shock wave. The impingement point of the shock upon the external boundary of viscous flow field is a given parameter for the interaction (sketch 1).

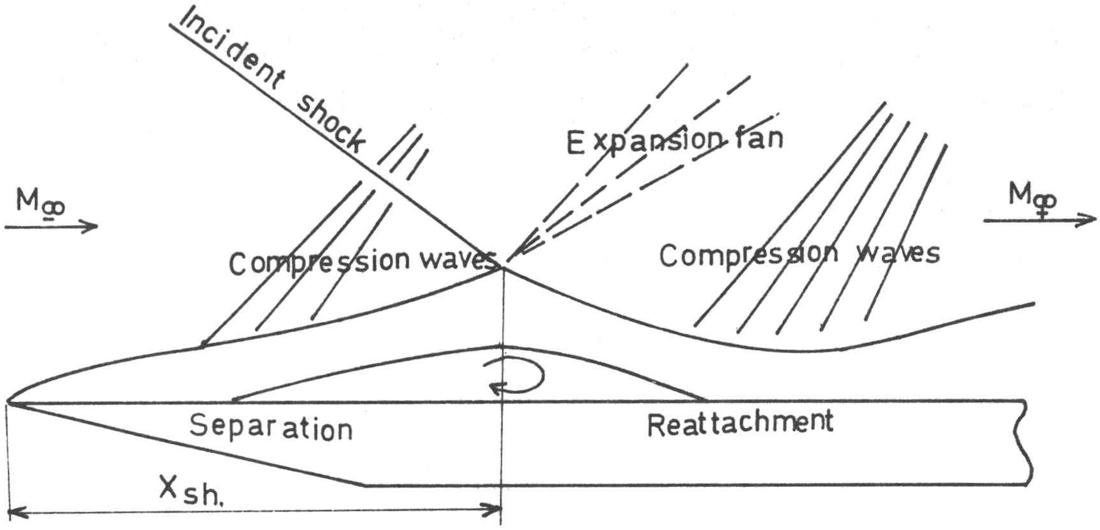

Sketch 1

If we consider only the inviscid flow field, the ramp flow can be considered as equivalent to a flat plate-incident shock with the following assumptions summarized in sketch 2.

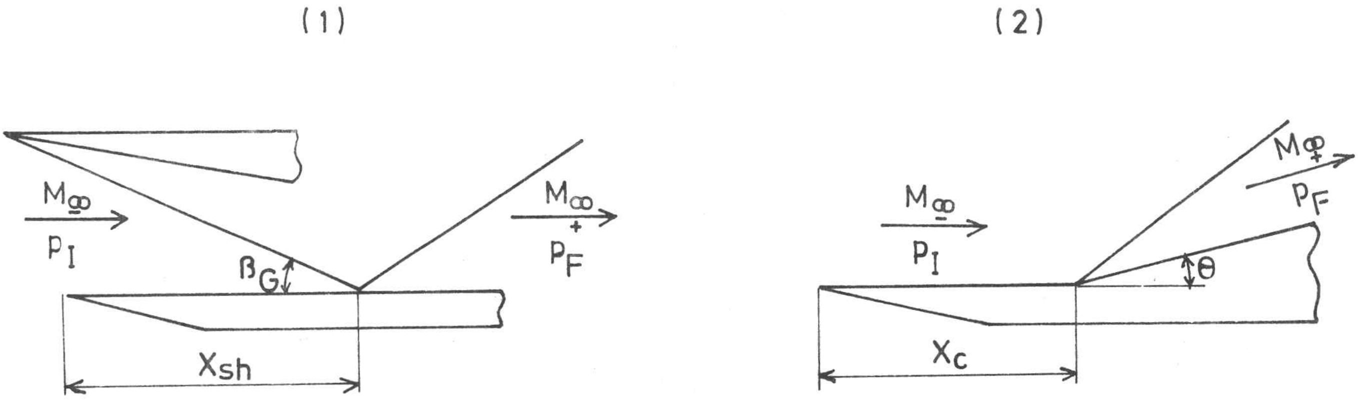

Sketch 2.

$$Re_{x_{SH}} = Re_c \quad , \tag{44}$$

$$\left(\frac{p_F}{p_I}\right)_1 = \left(\frac{p_F}{p_I}\right)_2 \quad .$$

The equivalence is discussed in greater details in ref (22).

3.1.2 Entropy variation through the impinging shock wave :

We consider the static pressure to be continuous across the incident shock and its cancelling expansion fan, i.e. $p_{e_1} = p_{e_2}$ but we allow the Mach number to be discontinuous, i.e. $M_{e_1} \neq M_{e_2}$. To compute M_{e_2} (just behind the incident shock) we assume that streamlines are straight lines between x_{sep} and x_{SH} and parallel to the wall at x_0. Therefore :

$$\Theta_{SH} = \Theta_{sep} = \nu(Me_0) - \nu(Me_{sep}). \qquad (45)$$

More details are also given in reference (22).
Note that subscripts 1 and 2 refer respectively to flow conditions just ahead and just behind of shock impingement point.

3.2 Nature of solution - boundary conditions

The integration of the differential equations system (32) is treated as a two point boundary value problem.

3.2.1 Upstream initial boundary condition :

Klineberg performed a detailed study of solution's nature for any typical viscous interactions. For the particular case of an interaction generated by external shock wave, the initialization procedure of integration must depend on the "state" of boundary layer at the beginning of the interaction.
One can distinguish :

- An initially subcritical flow for which a thickening of the boundary layer produces a pressure rise of the external flow, which in turn thickens the viscous layer, and so on, leading to an unstable system.
- The inverse case of an initially supercritical boundary layer for which a thickening produces a pressure drop, which does not allow upstream propagation of disturbances.

This distinction is based on the integral properties of the viscous layer, more precisely on the relative "areas" of the subsonic and supersonic parts of the Mach number profile. In the framework of Klineberg's theory, the passage from a sub- to supercritical state is reflected by the vanishing of the determinant D in equations (32).

The sub- or supercritical character of a boundary layer developing on a flat plate is strongly dependent upon the surface cooling ratio.

At the same distance x_0 from the leading edge of a flat plate, which was chosen sufficiently large for the self-induced interaction to be in the weak regime, i.e.

$$\bar{\chi} = \frac{M_\infty^3 \sqrt{C}}{\sqrt{Rex_0}} << 1 \quad .$$

We have computed $M_e(x_0)$, $\delta_i^*(x_0)$, $a(x_0)$ and $b(x_0)$ for given free stream conditions and various value of wall cooling ratio. The determinant $D(M_e,a,b)$ is negative for $s_w = -0.8$, -0.6, -0.4, vanishes for $-0.4 < s_w < -0.2$ and then becomes positive for $s_w = -0.2$ and 0 reflecting in the Klineberg's formulation a passage from a supercritical to a subcritical state of the boundary layer at point x_0 as the surface gradually approaches adiabatic conditions. This behaviour necessitates two different starting processes for the integration.

3.2.1.1 Initially supercritical flow : As has been shown in reference (8), a supercritical boundary layer subjected to a strong adverse pressure gradient responds only by means of a rapid but continuous change in the governing parameters of the flow field because the supercritical viscous layer does not allow for upstream propagation of disturbances over larger range than a few boundary layer thicknesses. But in the integral formulation, no upstream propagation is possible in such a case, and to start the calculation a "jump" in flow properties must be introduced at some point, this jump approximating to the physically continuous but very rapid process. Downstream of the jump the flow proceeds smoothly into the subcritical region and under certain conditions of Mach number wall temperature and pressure gradient may experience a second change from sub- to supercritical state prior to attaining the final downstream conditions.

3.2.1.2 Initially subcritical flows : Within a subcritical boundary layer, perturbations are propagated over a considerable distance upstream, the intensity diminishing exponentially, as one moves upstream. We choose a point x_0 as the beginning of the interaction, such that the amplitude of the disturbance becomes less than some arbitrary value - say ε -. As in the case of an initially supercritical boundary layer, the flow field upstream of x_0 is described by viscous weak interaction upon an undisturbed flat plate.

3.2.2 Downstream boundary condition :

According to the sub- or supercritical state of the downstream interacting flow, two types of downstream conditions must be used. However, both types lead to the same condition at downstream infinity, where we assume a self-preserving flat plate flow with a free stream Mach number (M_{+}^{∞}) given by inviscid theory.

3.2.2.1 Boundary layer becomes supercritical downstream of the interaction :

According to ref. (8), a study of the sub- to supercritical "transition" for various types of viscous interaction showed that the boundary layer flowing along a highly cooled compression surface goes through a smooth sub- supercritical transition downstream of the interaction, process entirely different to the shock-like jump at the beginning of the interaction. This "transition" point is marked by the simultaneous vanishing of :

$$N_1,\ N_2,\ N_3,\ N_4 \rightarrow 0 \qquad \text{and} \qquad D \rightarrow 0 \quad .$$

It is a singular point of the basic differential equations (saddle point type). As shown in reference (5), there is one, and only one, integral trajectory among an infinity tending toward the singular point which passes through it; this determines the correct integral solution. Nevertheless a step-by-step numerical integration cannot determine even after numerous iterations the mathematically exact integral path. Though it is possible by applying l'Hospital's rule, in conjunction with a suitable iteration process, to release the indetermination of the differential equations at the critical point, we apply a simple graphical extrapolation in this region as suggested by Klineberg. Downstream of the critical point, the integral solution is stable and asymptotically approaches the downstream final conditions. (Within the accuracy of the plots, the graphical procedure doesn't affect the final result.) Also, it must be pointed out that a marked overshoot of pressure above inviscid downstream value occurs. Sketch 3 describes qualitatively the behaviour of the integral solutions in the vicinity of critical point.

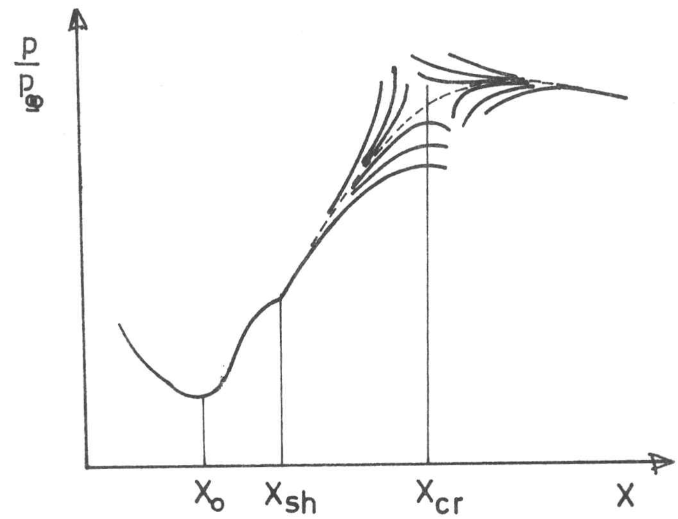

Sketch 3

3.2.2.2 Boundary layer remains subcritical downstream of the interaction :

As will be shown later, in the section 5.1, the assumed location of the critical point moves downstream as we approach the adiabatic condition from highly cooled ones. Thus for a moderate wall cooling ratio ($s_w = -0.4, -0.2$) the critical point lies out of the maximum range of x variation which is of practical interest.

For these conditions, the correct integral path is obtained respectively by iteration on both x_0 and $\mathcal{E}$, the perturbation parameter according to the procedure used by Klineberg for the adiabatic case.

An interpolation procedure (described in section 4) limits the number of iterations, when x_0 and $\mathcal{E}_0$ have been determined with a sufficient accuracy, and achieves to determine the correct downstream curve. This interpolation procedure applies both when smooth sub- supercritical transition exists through a critical point or when the final downstream conditions are obtained directly. In fact the interpolation between diverging solutions of different type leads automatically to $D \to 0$ and $N_i \to 0$ $(i=1,2,3,4)$ and thus to an approach to the critical point.

3.2.2.3 Locations of critical point :

A numerical evaluation of the critical point location has been performed for some particular cases. A plot of a_{CR} as a function of Me_{CR}, corresponding to $D(M_e, a, b) = 0$, for various values of b_{CR} is shown in figure 4 for different values of the wall cooling ratio. The general behaviour of the function D with variation of a at given values of b is shown in figure 5. (The Mach number M_e is fixed at 5.0, fig. 4 showing that a_{CR} is not very sensitive to Mach number above M=3.) As S_w goes from -0.8 to 0, these curves flatten along "a" axis but the general shape remains unchanged. Despite the fact that D=0 is <u>not</u> single value (i.e. three critical points exist in most cases) the limited range of "a" variation for practical cases of shock wave boundary layer interactions $(0 < a < a_{Blasius})$ define the single critical point which must be considered.

4. NUMERICAL METHODS

This section describes the numerical methods used in the different parts of a viscous interaction generated by a two-dimensional flat plate ramp geometry in order to be able to use digital computer.

4.1 The weak interaction region

One considers the viscous interaction developing on an undisturbed flat plate - Kubota (23) showed that a solution can be obtained by coordinate expansions of the basic differential equations in the neighbourhood of the Blasius solution, taking $\bar{\chi}$ (the viscous hypersonic interaction parameter) as the variable, provided that $\bar{\chi} << 1$, i.e. at a point sufficiently far from the leading edge. Klineberg (8) performed such a coordinate expansion of equations (23 to 26) rearranged into a convenient form.

Taking a priori solutions of this form :

$$\begin{aligned}
(M_e)_{WI} &= M_\infty(1 + m_1\bar{\chi} + m_2\bar{\chi}^2 + \ldots) \quad , \\
(\Delta)_{WI} &= \delta_0(1 + \delta_1\bar{\chi} + \ell_2\bar{\chi}^2 \log \bar{\chi} + \delta_2\bar{\chi}^2 + \ldots) \quad , \\
a_{WI} &= a_0 + a_1\bar{\chi} + a_2\bar{\chi}^2 + \ldots \quad , \\
b_{WI} &= b_0 + b_1\bar{\chi} + b_2\bar{\chi}^2 + \ldots \quad ,
\end{aligned} \tag{46}$$

and by introducing these expressions into the basic differential equations, one identifies the coefficients for each power in $\bar{\chi}$. This provides the series of coefficients (m_1, m_2, δ_0, δ_1, δ_2, ℓ_2, a_0, a_1, a_2, b_0, b_1, b_2).

Note that the integral functions appearing in these expressions ($\mathscr{X}(a)$, $T(a,b)$,...) are found from Taylor expansions of these functions in the neighbourhood of the Blasius values of a and b.

The complete expressions of series coefficients are given in Appendix B and numerical values for each value of S_w investigated are given in Appendix A.

Typical trajectories for $p/p_\infty(x)$, $\delta_i^*(x)$, $a(x)$ and $b(x)$ are given in figure 6 for $M_\infty = 6.06$ and $Re_u = 0.239 \times 10^7$ per meter, and various values of the wall cooling ratio.

4.2 Iteration procedure

From the undisturbed flat plate solution assumed to be existing upstream of the interaction, the required departure conditions are applied according to the "state" of the boundary layer at the assumed beginning of interaction, as discussed in section 3.2.1.

4.2.1 Subcritical flow at the beginning of the interaction

According to an analysis of Kubota (19) using a linearization of the hypersonic form of moment equations in the neighbourhood of Blasius solution, the following form of perturbation must be applied at any point of the weak interaction solution in order to properly initiate shock-wave boundary layer interaction computation.

$$
\begin{aligned}
M_e &= M_{e_0} (1 + P_1 \varepsilon) , \\
\delta_i^* &= \delta_{i_0}^* (1 + P_2 \varepsilon) , \\
a &= a_0 (1 + P_3 \varepsilon) , \\
b &= b_0 (1 + P_4 \varepsilon) ,
\end{aligned}
\qquad (47)
$$

with $\varepsilon \ll 1$

$$\text{and} \quad P_1 = \left[\mathcal{X} \frac{dJ}{d\mathcal{X}} - J\right] ,$$

$$P_2 = \left[3J - 2T^* - (2\mathcal{X} + 1 - E) \frac{dJ}{d\mathcal{X}}\right] ,$$

$$P_3 = \left[(2\mathcal{X} + 1 - E)J - (3J - 2T^*)\mathcal{X}\right] / (\frac{d\mathcal{X}}{da}) , \tag{48}$$

$$P_4 = \left[(P_1 + P_2)T^* + P_3(\frac{\partial T^*}{\partial a})\right] / (\frac{\partial T^*}{\partial b}) .$$

The following numerical procedure is then used. Taking arbitrary chosen values of x_0 (beginning of the interaction) and $\mathcal{E}$ (perturbation parameter), x_0 is iterated using a fixed value of $\mathcal{E}$ ($\sim 10^{-3}$) until the integral trajectory approximately satisfies the downstream boundary condition . When x_0 has been localized with a sufficient accuracy (taken arbitrarily), $\mathcal{E}$ is then iterated for this fixed value of x_0 until the correct integral path is determined by approaching the correct downstream conditions, i.e. the Blasius solution.

4.2.2 Supercritical flow at the beginning of interaction

In reality perturbations are communicated upstream over a short distance, the interaction being then initiated with a rapid change in the flow quantities. This process is mathematically simulated by a shock-like jump at the beginning of the interaction.

Writing suitable conservation equations across the jump, Klineberg obtained relations between flow quantities upstream and downstream of the discontinuity. This was done by writing conservation equations of mass and momentum flux. A third equation which describes the variation of mechanical energy across the jump is obtained in the limit : the size of the control volume (sketch 4) tends toward zero (i.e. ΔX_1, $\Delta X_2 \to 0$).

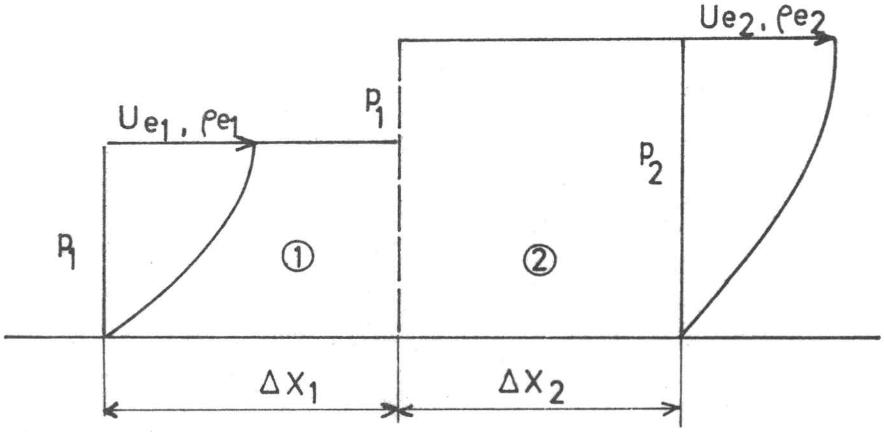

Sketch 4

These conservation equations are the following :

mass flux : $\dot{m}_2 - \dot{m}_1 = (\rho_e u_e)_1 \, (\delta_2 - \delta_1)$,

momentum flux : $I_2 - I_1 = (\rho_e u_e^2)_1 \, (\delta_2 - \delta_1) - \delta_2 \, (p_2 - p_1)$,

total enthalpy : $(M_e \, \delta_1^* T^*)_2 = (M_e \, \delta_1^* T^*)_1$, (49)

and mechanical energy (moment of momentum) :

$$G_2 - G_1 = (\rho_e u_e)_1^3 \, (\delta_2 - \delta_1) - 2K_2(p_2 - p_1) \, , \tag{50}$$

when ΔX_1 and $\Delta X_2 \to 0$,

with $\dot{m} = \int_0^\delta \rho u \, dy$,

$$I = \int_0^\delta \rho u^2 dy \, ,$$

(51)

$$G = \int_0^\delta \rho u^3 dy \, ,$$

$$K = \int_0^\delta u \, dy \quad . \qquad (51 \text{ cont'd})$$

At the jump location the external flow is assumed to experience a plane oblique shock wave. The "strength" of this shock is fixed by the above relations between upstream and downstream flow quantities. Finally we get three simultaneous algebraic equations which give, together with the shock equations, the relations between upstream and downstream unknowns, respectively M_{e_1}, $\delta^*_{i_1}$, a_1, b_1 and M_{e_2}, $\delta^*_{i_2}$, a_2, b_2.

$$m_{e_2} F_2 \left[\frac{\mathcal{K}_1}{m_{e_1} F_1} - \frac{\mathcal{K}_2}{m_{e_2} F_2} \right] + \frac{1}{\gamma M_{e_1}^2} \left(\frac{p_2}{p_1} - 1 \right) \left[m_{e_2} F_2 + Z_2 \right] \ldots$$

$$- (1 - \rho_r u_r^2)(Z_2 - \mathcal{K}_2) + (1 - \rho_r u_r)\left(1 - \frac{\mathcal{K}_1}{m_{e_1} F_1}\right) Z_2 = 0 \quad ,$$

(52)

$$m_{e_2} F_2 \left[\frac{J_1}{m_{e_1} F_1} - \frac{J_2}{m_{e_2} F_2} \right] + \frac{2u_r}{\gamma M_{e_1}^2} \left(\frac{p_2}{p_1} - 1 \right) \left[m_{e_2} J_2 + Z_2 - (1 + m_{e_2}) T_2^* \right] \ldots$$

$$- (1 - \rho_r u_r^3)(Z_2 - J_2) + (1 - \rho_r u_r)\left(1 + \frac{J_1}{m_{e_1} F_1}\right) Z_2 = 0 \quad ,$$

(53)

$$m_{e_2} F_2 \left[\frac{T_1^*}{m_{e_1} F_1} - \frac{T_2^*}{m_{e_2} F_2} \right] + (1 - \rho_r u_r)\left(T_2^* + \frac{T_1^*}{m_{e_1} F_1} Z_2\right) = 0 \quad . \qquad (54)$$

(Subscript r refers to ratio quantities across a plane oblique shock wave, i.e. :

$$u_r = \frac{u_2}{u_1} \quad , \quad \rho_r = \frac{\rho_2}{\rho_1} \quad).$$

Then with an initially supercritical boundary layer the interaction parameter is x_0, and for each trial value, equations 52, 53, 54 must be solved simultaneously, to provide initial values (M_{e_2}, $\delta^*_{i_2}$, a_2, b_2) for starting the integration. x_0 is iterated until the integral path satisfies the downstream boundary conditions with a sufficient accuracy.

Remark : Convergence of equations 52 to 54 is relatively fast for high wall cooling ratios (S_w = -0.8, -0.6) but becomes difficult to achieve (within accuracy of numerical computations) for intermediate values (S_w = -0.4) where the jump intensity is very small.

4.3 Numerical integration of basic differential equations

Starting with initial conditions as described in the previous section, the four basic differential equations (eq. 32) are integrated simultaneously using a Runge Kutta numerical procedure (4th order). A computer program has been written for an IBM 1130 digital computer.

The integration variable is x (physical abscissa along the wall) for attached flow, but it is convenient to use the velocity profile parameter "a" as the independent variable in the separated region, due to the steep gradients in "a" after separation and before reattachment, particularly in the case of a highly cooled wall.

Also, the set of polynomial coefficients must be changed from attached to separated flow values as one goes through the separation and vice versa at the reattachment point, since the definition of the velocity profile parameter is different for attached and separated flows.

4.4 Interpolation procedure

In order to limit the number of iterations upon both x_0 and ξ, a linear interpolation procedure is used between two solutions of different type downstream of reattachment (see sketch 5).

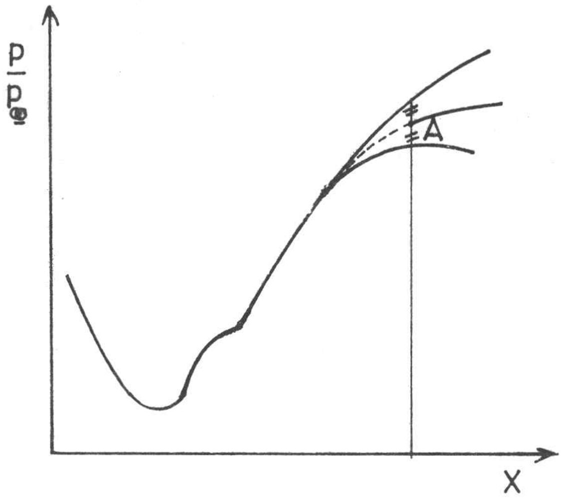

Sketch 5

When a sufficient number of iterations has been performed the divergence between solutions of different type (one goes to a new separation and the other to an expansion) becomes apparent some distance downstream of reattachment, the upstream part of the integral curves being quite undistinguishable from each other, a new starting point is defined by linearly interpolating between two diverging solutions (point A sketch 5) and the integration is continued downstream. This provides a new set of two diverging integral curves and the process is repeated moving downstream from the divergence point. On highly cooled wall the boundary layer experiences a sub- to supercritical change downstream of reattachment. In this vicinity the above interpolation procedure does not allow for an exact determination of this critical point (D=0), the divergence of solutions becoming very rapid here. A graphical extrapolation is used, as suggested by Klineberg (8), and the numerical integration is restarted at one point lying downstream of the critical point. The equations are now stable and converge to the downstream final conditions.

Note that in all cases investigated, the pressure reached a peak value above the inviscid final pressure (p_+^∞) and then levels off downstream. This pressure overshoot is ≈5% of the inviscid pressure rise for numerical computations carried out in the present study but increases as the free stream Mach number of the interaction increases. Practically, the extent of graphical extrapolation required is small for highly cooling rate and increases as adiabatic conditions are approached. For $S_w = -0.4$ (with free stream conditions investigated here) the downstream critical point lies beyond the maximum value of the abscissa x reached. For moderate ratios of cooling ($-0.4<S_w<0$) the interpolation procedure applies in the same way as for the adiabatic case, and final downstream conditions can be reached by this means. (A detailed description of the so-called interpolation procedure is given in reference 22.)

5. NUMERICAL RESULTS

5.1 Parametric study of surface cooling effects

The experimental conditions used by Lewis (ref. 17) apart from the wall cooling ratio, have been used for a theoretical analysis of the effect of step-by-step variation of wall cooling ratio ($0.2 < T_w/T_t < 1$) upon the main features of shock wave boundary layer interactions generated by a deflected surface.

The calculated pressure distributions are shown in figure 7a, we observe that a progressive cooling of the surface starting with adiabatic conditions produces :

- an increase of pressure at the beginning of interaction (p_0/p_-^∞) (weak interaction region),
- a strong decrease of upstream influence ($x_0 - x_{sh}$),
- an increase of pressure gradient in the neighbourhood of reattachment.

The effect of cooling the surface upon distributions of M_e, δ_i^*, a and b is also shown in figures 7b and 7c.

The skin friction distributions are shown in figure 7d. It is found that, as expected, an increase of skin friction is produced by surface cooling. The heat transfer coefficient distributions are shown in figure 7e. This coefficient C_H is defined in a manner homogeneous to a Stanton number where the reference quantities are related to stagnation conditions (due to assumption $P_r=1$).

$$C_H = \frac{-q_w}{\rho_\infty u_\infty (h_{0_e} - h_{0_w})} \qquad (55)$$

In order to study the effect of wall temperature variation upon the x scaling of an interaction, the non-dimensionalized form of pressure distribution, as defined by Lewis (ref. 17, 18), has been used.

One plots $\frac{p - p_0}{p_+^\infty - p_0}$ against $\frac{x - x_c}{\delta_c^*}$ (figure 8),

where δ_c^* is the displacement thickness of an undisturbed flat plate flow at the point x_c calculated using the free stream and wall temperature conditions of the interaction studied. The qualitative behaviour is in agreement with Lewis' experiments but the decrease in upstream influence due to wall cooling is magnified by the unrealisitc jump assumption.

5.1.1 Effect of surface cooling upon characteristic lengths of the interaction :

Figure 9a shows the variations of the following characteristic lengths of an interaction with change of wall cooling ratio.

- x_0/L beginning of the interaction.
- x_s/L separation point.
- x_R/L reattachment point
- L_{sep}/L or $(x_r - x_s)/L$ length of separated flow.

In addition the effect of free stream Reynolds number is also shown. All these lengths vary almost linearly with the ratio of wall-to-stagnation temperature ratio. In particular, the length of the separated region (L_{sep}) is very nearly proportional to T_w/T_t over the whole range considered. Also, $(L - x_0)/L$ which may be considered to be a measure of the extent of upstream influence, is again almost proportional to T_w/T_t. The latter result is in accordance with the free interaction scaling of Curle, but is more general in that it applies to the extent of upstream influence in a complete interaction.

5.1.2 Effect of surface cooling upon characteristic features of the pressure distribution :

Figure 9b shows the variations of the following pressure ratios as a function of wall-to-stagnation temperature ratio for two free stream Reynolds number values :

- p_0/p_∞ beginning of the interaction (undisturbed flat plate flow),
- p_{SH}/p_∞ impingement point of incident shock wave (or "plateau" pressure),
- p_r/p_∞ reattachment pressure rise.

Also plotted are these pressures referred to p_0. It will be seen that the results must be interpreted in different ways according to which non-dimensionalized representation is used.

Figures 9c and 9d show the effect of wall temperature variations upon the extremes of the skin friction coefficient and heat transfer coefficient (C_H), these being respectively the minimum value reached at corner and peak value in the neighbourhood of reattachment. The latter moves downstream as adiabatic conditions are approached (see figure 7e).

Figures 10 show the effect of variation of the Reynolds number upon the pressure and heat transfer distribution respectively.

<u>Remark</u> : From the definition of C_H the actual heat flux is :

$$q_w(x) = \rho_\infty u_\infty C_p T_t S_w C_H(x) \quad , \qquad (56)$$

In order to obtain directly the effects of both unit Reynolds number and wall temperature ratio changes on the heat flux distribution, one must bear in mind that $C_H(x)$ must be multiplied by factors proportional to these two parameters.

5.2 Comparison with experimental results

5.2.1 Limitations of the Lees-Reeves-Klineberg laminar theory

Despite the fact that numerous experimental data are available for boundary layer shock wave interactions, only a few results are suitable for testing the laminar theory.

The assumptions used in the theoretical development are not valid for certain cases. For example :

The external inviscid flow is assumed to be isentropic, and the compression waves generated by the flow deflection coalesce far from the boundary layer edge. This condition is required in order to apply the Prandtl-Meyer relationship relating the local external flow Mach number to the inclination of streamlines at the boundary layer edge. Needham (ref. 16) developed a physical model of shock wave boundary layer interaction in hypersonic flow showing that compression waves starting at the sonic line in the boundary layer coalesce into a shock near the boundary layer edge. Thus Klineberg's theory, in the present formulation, is not applicable for very high Mach numbers. Klineberg suggests the use of the tangent-wedge formula in place of that of Prandtl-Meyer in such cases, but this does not fully take account of the entropy discontinuities of the shock waves. Another question arises when we consider the validity of the boundary layer equations, particularly the assumption that $dp/dy = 0$. When the separated boundary layer thickness has the same order of magnitude as the separated length (at high Mach numbers and strong deflection angles) the streamline curvature at the boundary layer edge differs considerably from the wall curvature and generates a pressure gradient normal to the wall.

Holden (12) has developed an integral theory which includes this normal pressure gradient. He was able to demonstrate that the inclusion of this effect eliminated the necessity for a super- to subcritical jump and concluded that such jump is a mathematical approximation without physical meaning. Unfortunately the addition of the normal momentum equation increases considerably the complexity of the integral method, and the improvement in agreement with experimental data is small except at very high Mach numbers.

The linearized viscosity law $\mu \sim T$ is not a good assumption for hypersonic flow, where large temperature differences occur within the boundary layer.

These arguments limit the application of Lees-Reeves-Klineberg theory to moderately hypersonic flows.

5.2.2 Selection of experimental data for comparison with theory :

Most of the experimental results fall into two groups, according to the facility used during tests :

- Low Mach number, adiabatic wall data (refs. 14,15,20)
- High Mach number, cold wall data (refs. 11,12,16).

Also available are a few data at moderately low hypersonic speeds with a controlled wall temperature, usually achieved by internal circulation of coolant (refs. 17, 18, 24, 25, 26).

The most severe limitation arises when transition appears in the boundary layer near the reattachment point. The concept of "entirely laminar interaction" is understood in different ways by experimentators. As an example, Johnson (refs. 25, 26) considers an interaction to be laminar as long as the transition (detected by flow visualization, heat transfer measurements or velocity profile surveys) occurs behind the reattachment point. A theoretical analysis of the effect of transition is excluded in the framework of laminar theory, so we consider here only those interactions for which the transition is located "far" downstream of the reattachment region following the conclusions carried out by Lewis-Kubota-Lees (18,19).

A criterion for detecting transition has been defined in reference (20)-(21). It is based upon the observation that upstream influence increases with increasing unit Reynolds number in purely laminar flow, but decreases in transitional flow. Thus, if the measured pressure at a suitably chosen point (p_N) in the separation pressure rise region is plotted against unit Reynolds number, it is found that the pressure rises in the laminar regime as Re_u increases, in agreement with laminar theory but then reaches a peak and starts to fall in the turbulent regime. The flow is inferred to be <u>certainly</u> transitional at Reynolds number higher than that at which the pressure peak occurs (sketch 6).

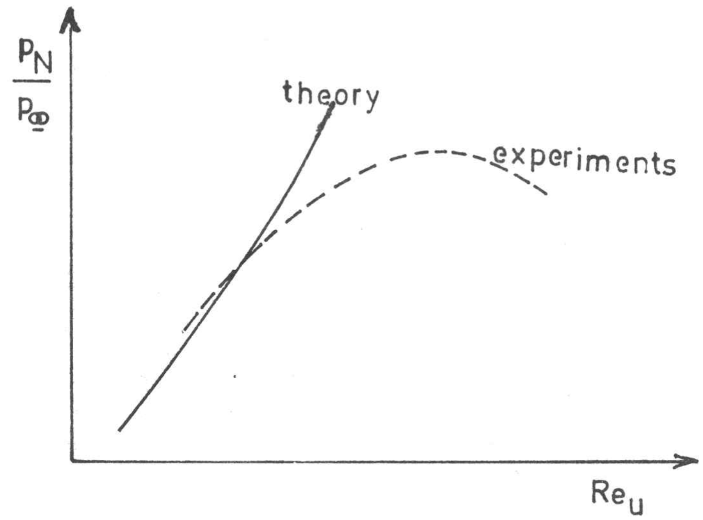

Sketch 6

5.2.3 Summary of the major limitations of Lees-Reeves-Klineberg theory :

- The external flow must be supersonic or moderately low hypersonic.
- The whole extent of the shock wave boundary layer interaction considered must be laminar (i.e. the transition point must be located "far" downstream of reattachment).
- The theory is valid for a short extent of separated region and the maximum thickness of the separation bubble must be small with respect to the separated length.

5.2.4 Direct comparison with experiment :

Klineberg has already made a comparison between his theory and the measurements of Lewis (17) which shows good agreement. To provide further comparisons, we have considered the experimental results of Needham (16), despite the fact that they must be considered as limiting cases for the application of the present theory.

Non-dimensionalized pressure and heat transfer distributions are presented by Needham, but the method of data reduction used to convert the data obtained in conical flow into an equivalent two-dimensional form makes a direct comparison against theory difficult. Here we match the theoretical values of M_{e_0} and Re_0 at the beginning of the interaction with experimental values, but allowing x_0 to be free to be determined by iteration.

Figure 11a shows experimental and theoretical pressure and heat transfer distributions on a flat plate, the interaction being generated externally by an oblique plane shock wave impinging on the boundary layer at 6 inches behind the plate leading edge. Free stream conditions are $M_{e_0} = 7.4$ and $Re_{xSH} = 2.2 \times 10^6$.

Figure 11b shows similar distributions for an interaction generated by a flat plate ramp configuration. The deflection angle and free stream conditions are : $\theta = 10°$, $M_{e_0} = 9.7$, $Re\ x_c = 0.95 \times 10^5$.

Figure 11c shows pressure distribution on a flat plate ramp with deflection angle $\theta = 6°$ and free stream conditions are $M_{e_0} = 7.4$, $Re\ x_c = 2.2 \times 10^6$.

All these experimental results have been obtained in a gun tunnel so that surface model is kept cold ($s_w \simeq -0.8$).

The length of separation is magnified by the theory, whilst the predicted heating is too low. Nevertheless the agreement between theory and experiment is reasonable.

In figure 12, theoretical results obtained both in this section and from the parametric study (section 5.1) have been used to check the experimental plateau pressure correlation presented by Needham (16) and derived from the "free interaction" concept. The theoretical points lie within the scatter of the experimental data.

Finally a comparison of the Lees-Reeves-Klineberg theory with experimental results obtained by the author on an adiabatic wall model with a short flat plate ramp is presented in figure 13. Good agreement for both unit Reynolds numbers of 1.03 and 2.32×10^7 per meter is achieved, and theoretical trend when Reynolds number is increased is clearly demonstrated by the experimental results.

6. CONCLUDING REMARKS

Shock wave laminar boundary layer interactions generated by a flat plate ramp geometry with a non-adiabatic isothermal surface have been studied using the Lees-Reeves-Klineberg theory. The method has been extended to a wide range of wall-to-stagnation temperature ratios from adiabatic to highly cooled conditions.

A parametric study of the effect of surface cooling upon the main overall features of pressure and heat transfer distributions has been carried out which showed that the length of separation and the "upstream influence" decrease quasi linearly with the wall-to-stagnation temperature ratio. Within the basic limitations of the theory, i.e. considering a purely laminar interaction at moderate hypersonic speed over a model geometry generating a short length of separation, good agreement with experimental results has been found for both pressure and heat transfer distributions.

REFERENCES

1. CROCCO, L. and LEES, L. : A mixing theory for the interaction between dissipative flows and nearly isentropic stream. J.A.S. Vol.19 n°10, pp. 649-676, October 1952.

2. CROCCO, L. : Considerations on shock-boundary layer interaction. Proceedings of the Conference on high speed aerodynamics held at the Polytechnic Institute of Brooklyn, Jan. 20-22, 1955.

3. GLICK, H.S. : Modified CROCCO-LEES mixing theory for supersonic separated and reattaching flows G.A.L.C.I.T. Cal. Inst. of Tech. Hypersonic research project Memo 52 May 2, 1960.

4. LEES, L. and REEVES, L.B. : Supersonic separated and reattaching laminar flows : I General theory and application to adiabatic boundary layer-shock wave interactions, AIAA Jl. Vol.2 N°11, Nov. 1964, pp. 1907-1920.

5. WEBB, W.H., GOLIK, R.L., VOGENITZ, F.W. and LEES,L. : A multi-moment integral theory for laminar supersonic near wake. Proceedings of the 1965 heat transfer and fluid mechanics conference . Cal. Inst. of Tech. University of Cal. Los Angeles, June 21-22-23, 1965.

6. GRANGE, J.H., KLINEBERG, J.M. and LEES,L. : Laminar boundary layer separation and near wake flow for smooth blunt body at supersonic and hypersonic speeds, AIAA 3th Aerospace Sciences Meeting, N.Y., Jan. 23-26 1967, pp. 67-62

7. NIELSEN, J.N., LYNES, L.L. and GOODWIN, F.K.:Calculations of laminar separation with free interaction by the method of integral relations. Part II Two dimensional non adiabatic flow and axisymmetric supersonic adiabatic and non adiabatic flows, A.F.F.D.L., TR 65-107 Part II(1966).

8. KLINEBERG, J.M. : Theory of laminar viscous-inviscid interactions in supersonic flow. Ph.D. Thesis June 68, Cal. Inst. of Tech. Pasadena Cal.

9. KLINEBERG, J.M. and LEES, L. : Theory of laminar viscous inviscid interactions in supersonic flow. AIAA Jl. Vol.7 N°12, pp. 2211-2221, Dec. 1969.

10. HOLDEN, M.S. : Theoretical and experimental studies of separated flows induced by shock wave boundary layer interaction. Proceedings of the 4th A.G.A.R.D. Meeting, Rhode-Saint-Genèse, 10-13 May 1966. Separated flows part I, Pp. 147-180.

11. HOLDEN, M.S. : Theoretical and experimental studies of laminar flow separation on a flat plate-wedge compression surface in hypersonic strong interaction regime. Cornell-Aero. Lab. Rep. N°AF 1894 A2, Final Report May 1967.

12. HOLDEN, M.S. : Theoretical and experimental studies of the shock wave boundary layer interaction as curved compression surfaces. Proceedings of the Symposium on viscous interaction phenomena in supersonic and hypersonic flow, May 7-8, 1969.

REFERENCES (Cont'd)

13. MURPHY, J.D. : A critical evaluation of analytic methods for predicting laminar boundary layer shock wave interaction. N.A.S.A. Symposium on analytic methods in aircraft aerodynamics. A.M.E.S. Research Center, October 28-30, 1969, N.A.S.A. SP 228, pp. 515-539.

14. CHAPMAN, D.R., KUEHN, D.M. and LARSON, H. : Investigation of separated flows in supersonic and subsonic streams with emphasis of the effect of transition. N.A.C.A. Rep. 1356, 1958.

15. HAKKINEN, R.S., GREGER, I., TRILLING, L. and ABARBANEL, S.S. : The interaction of an oblique shock wave with a laminar boundary layer. N.A.S.A. Memo 2-18-59 W, March 1959.

16. NEEDHAM, O.A. : Laminar separation in hypersonic flow. Ph.D. Thesis, Faculty of Engineering of the University of London, Aug. 1965.

17. LEWIS, J.E. : Experimental investigation of supersonic laminar, two-dimensional boundary layer separation in a compression corner with and without cooling. Cal. Inst. of Tech., Ph.D. Thesis, 1967.

18. LEWIS, J.E., KUBOTA, T., and LEES, L. : Experimental investigation of supersonic laminar two dimensional boundary layer separation in a compression corner with and without cooling. AIAA Jl. Vol.6 N°1, Jan. 68, pp. 7-14.

19. KO, D.R.S. and KUBOTA, T. : Supersonic laminar boundary layer along a two dimensional adiabatic curved ramp. AIAA Jl. Vol.7 N°2, Feb.69, pp. 298-304.

20. GINOUX, J.J. : Supersonic separated flows over wedges and flares with emphasis on a method of detecting transition. von Karman Institute, Rhode-Saint-Genèse, TN47 1968.

21. GAUTIER, B. : Calcul de l'interaction onde de choc - couche limite laminaire incluant le décollement provoqué par une rampe à l'aide des méthodes intégrales de CROCCO-LEES mod. par GLICK et de LEES-REEVES. NT23A, 1969. Université Libre de Bruxelles

22. RIETHMULLER, M.L. and GINOUX, J.J. : A parametric study of adiabatic laminar boundary layer shock wave interaction by the method of LEES-REEVES-KLINEBERG. von Karman Institute, Rhode-Saint-Genèse, TN60-1970.

23. KUBOTA, T. and KO, D.R.S. : A second order weak interaction expansion for moderately hypersonic flow past a flat plate. AIAA Jl., Vol.5 N°10, Oct. 1967, pp. 1915-1917.

24. JOHNSON, C.B. : Pressure and flow field study at M=8 of flow separation on a flat plate with deflected trailing edge flap. NASA TND 4308(1968).

25. JOHNSON, C.B. : Heat transfer measurements at M=8 on a flat plate with deflected trailing edge flap with effect of transition included. N.A.S.A. TND 5899 (1970)

26. Don GRAY, J. : Wall cooling effects on an axisymmetric laminar reattaching flow at hypersonic speed. A.E.D.C. TR. 68-1935, Nov. 1968.

APPENDIX A

1. Notations used for weak interaction coefficients

CC(MJ,LJ)	CC(MJ,1)	CC(MJ,2)	CC(MJ,3)
CC(1,LJ)	d_0	a_0	b_0
CC(2,LJ)	m_{11}	m_{12}	m_{21}
CC(3,LJ)	d_{11}	d_{21}	d_{22}
CC(4,LJ)	a_{11}	a_{21}	a_{22}
CC(5,LJ)	b_{11}	b_{21}	b_{22}

2. Notations used for profiles dependent integral functions

2.1 Single profile dependent functions

$$F(a) = \sum_{NK=1}^{NK=9} CD(NJ,NK)\ a^{NK-1}$$

where F is the integral function considered
NJ is the subscript of definition of function F
NK is the subscript of summation
a is the parameter of summation.

Example :

$$\mathcal{H}(a) = \sum_{NK=1}^{NK=9} CD(6,NK)\ a^{NK-1}$$

2.2 Functions depending on both velocity and total enthalpy profiles

$$T(a,b) = \sum_{k=0}^{5} \tau_k(b)\ a^k$$

with $\tau_k(b) = \sum_{NK=1}^{6} CD(NJ,NK)\ b^{NK-1}$

$$\frac{\partial T}{\partial a}(a,b) = \sum_{k=0}^{5} \xi_k(b)\ a^k$$

$$\text{with} \quad \xi_k(b) = \sum_{NK=1}^{6} CD(NJ,NK)\ b^{NK-1}$$

$$\frac{\partial T}{\partial b}(a,b) = \sum_{k=0}^{5} \phi_k\ b^k$$

$$\text{with} \quad \phi_k(b) = \sum_{NK=1}^{6} CD(NJ,NK)\ a^{NK-1}$$

where NJ is the subscript of definition of $\mathcal{T}_k$, ξ_k, ϕ_k
and NK is the subscript of summation

Integral function	Subscript of definition (NJ)	Summation parameter
$\mathcal{T}_0$	1	b
σ	2	b
$d\sigma/db$	3	b
ξ_0	4	b
ϕ_0	5	a
$\mathcal{H}$	6	a
J	7	a
Z	8	a
R	9	a
P	10	a
$d\mathcal{H}/da$	11	a
$dJ/d\mathcal{H}$	12	a
α	13	a
$d\alpha/da$	14	a

Integral functions	Subscript of definition (NJ)	Summation parameter
τ_1	15	b
τ_2	16	b
τ_3	17	b
τ_4	18	b
τ_5	19	b
ξ_1	20	b
ξ_2	21	b
ξ_3	22	b
ξ_4	23	b
ξ_5	24	b
ϕ_1	25	a
ϕ_2	26	a
ϕ_3	27	a
ϕ_4	28	a
ϕ_5	29	a

SW -0.200

WEAK INTERACTION COEFFICIENTS

	CC(MJ,1)	CC(MJ,2)	CC(MJ,3)
CC(1,LJ)	0.17240469E 01	0.16340014E 01	0.93572139E-01
CC(2,LJ)	0.66186177E 00	0.13781654E 01	0.16065371E 01
CC(3,LJ)	0.18419537E 01	-0.48865032E 01	0.34234957E 01
CC(4,LJ)	-0.30817132E 01	-0.10742689E 02	0.35315408E 01
CC(5,LJ)	0.50650164E-01	-0.25904259E 01	0.13036112E 01

PROFILES COEFFICIENTS

ATTACHED FLOW

	CD(NJ,1)	CD(NJ,2)	CD(NJ,3)	CD(NJ,4)	CD(NJ,5)	CD(NJ,6)	CD(NJ,7)	CD(NJ,8)	CD(NJ,9)
CD(1,NK)	0.1012041E 01	-0.5047927E 02	0.1153801E 04	-0.1387696E 05	0.8424815E 05	-0.2026955E 06	0.0000000E 00	0.0000000E 00	0.0000000E 00
CD(2,NK)	0.8795088E 00	-0.1368297E 02	0.9960583E 02	-0.2780326E 03	0.0000000E 00	0.0000000E 00	0.0000000E 00	0.0000000E 00	0.0000000E 00
CD(3,NK)	0.2007842E 01	-0.5436568E 03	0.1216447E 05	-0.9961009E 05	0.2820441E 06	0.0000000E 00	0.0000000E 00	0.0000000E 00	0.0000000E 00
CD(4,NK)	0.2281252E 00	-0.3539281E 01	0.1177166E 02	0.1472182E 03	-0.1299488E 04	0.2842161E 04	0.0000000E 00	0.0000000E 00	0.0000000E 00
CD(5,NK)	-0.7186277E 02	-0.1518796E 01	-0.1680972E 01	0.2113904E 01	-0.7680599E 00	0.8863358E-01	0.0000000E 00	0.0000000E 00	0.0000000E 00
CD(6,NK)	0.2432078E 00	0.1142097E 00	-0.2133638E-01	0.3446024E-02	-0.6690906E-03	0.6692868E-04	-0.1683542E-06	0.0000000E 00	0.0000000E 00
CD(7,NK)	0.3676652E 00	0.1693942E 00	-0.1353361E-01	-0.1695096E-02	0.2649824E-03	0.0000000E 00	0.0000000E 00	0.0000000E 00	0.0000000E 00
CD(8,NK)	0.1012450E 01	0.4594261E 00	0.3377379E-01	0.3237293E-02	-0.5287739E-03	0.0000000E 00	0.0000000E 00	0.0000000E 00	0.0000000E 00
CD(9,NK)	0.1276809E 01	-0.5942157E 00	0.3563117E 00	-0.1135015E 00	0.2301015E-01	-0.2861258E-02	0.1659720E-03	0.0000000E 00	0.0000000E 00
CD(10,NK)	0.1391656E-03	0.4952537E 00	-0.1086566E 00	0.1188776E-01	0.3939403E-03	-0.3543800E-03	0.3791654E-04	0.0000000E 00	0.0000000E 00
CD(11,NK)	0.1136275E 00	-0.3572020E-01	-0.1834999E-01	0.5089926E-01	-0.5147828E-01	0.2770314E-01	-0.8265964E-02	0.1289575E-02	-0.8201556E-04
CD(12,NK)	0.1511220E 01	0.2244828E 00	0.2845154E-01	-0.4192491E-01	0.1401205E-01	-0.1466130E-02	0.0000000E 00	0.0000000E 00	0.0000000E 00
CD(13,NK)	0.4170089E 00	0.1549519E 00	0.1150744E 00	-0.9130536E-01	0.4738381E-01	-0.8776338E-02	0.4865755E-03	0.0000000E 00	0.0000000E 00
CD(14,NK)	0.2016546E 00	-0.4722840E-01	0.2645002E 00	-0.2817051E 00	0.1611833E 00	-0.4036320E-01	0.3530115E-02	0.0000000E 00	0.0000000E 00
CD(15,NK)	0.2204281E 00	-0.2194535E 01	-0.4280882E 02	0.1142487E 04	-0.9593486E 04	0.2838957E 05	0.0000000E 00	0.0000000E 00	0.0000000E 00
CD(16,NK)	-0.6593967E-01	-0.2174748E 00	0.7720492E 02	-0.1716420E 04	0.1491038E 05	-0.4623654E 05	0.0000000E 00	0.0000000E 00	0.0000000E 00
CD(17,NK)	0.1875200E-01	0.5760566E 00	-0.4947714E 02	0.1057011E 04	-0.9329457E 04	0.2960383E 05	0.0000000E 00	0.0000000E 00	0.0000000E 00
CD(18,NK)	-0.3699270E-02	-0.1548264E 00	0.1194590E 02	-0.2565513E 03	0.2305351E 04	-0.7462201E 04	0.0000000E 00	0.0000000E 00	0.0000000E 00
CD(19,NK)	0.3067735E-03	0.1118205E-01	-0.9376580E 00	0.2071095E 02	-0.1904819E 03	0.6299467E 03	0.0000000E 00	0.0000000E 00	0.0000000E 00
CD(20,NK)	-0.1682139E 00	0.6047677E 01	-0.1095075E 03	0.1378137E 04	-0.1019487E 05	0.3046426E 05	0.0000000E 00	0.0000000E 00	0.0000000E 00
CD(21,NK)	0.1106624E 00	-0.8034078E 01	0.2494444E 03	-0.4077232E 04	0.3220142E 05	-0.9571915E 05	0.0000000E 00	0.0000000E 00	0.0000000E 00
CD(22,NK)	-0.4944029E-01	0.5577351E 01	-0.2048198E 03	0.3572309E 04	-0.2891132E 05	0.8685406E 05	0.0000000E 00	0.0000000E 00	0.0000000E 00
CD(23,NK)	0.1129086E-01	-0.1677208E 01	0.6594230E 02	-0.1181328E 04	0.9689585E 04	-0.2937162E 05	0.0000000E 00	0.0000000E 00	0.0000000E 00
CD(24,NK)	-0.9987279E-03	0.1759699E 00	-0.7167904E 01	0.1303086E 03	-0.1078170E 04	0.3290778E 04	0.0000000E 00	0.0000000E 00	0.0000000E 00
CD(25,NK)	0.4390039E 04	-0.1989711E 03	0.3978322E 03	-0.3287593E 03	0.1090818E 03	-0.1217095E 02	0.0000000E 00	0.0000000E 00	0.0000000E 00
CD(26,NK)	-0.1138261E 06	0.9122404E 04	-0.1731730E 05	0.1408695E 05	-0.4659340E 04	0.5201066E 03	0.0000000E 00	0.0000000E 00	0.0000000E 00
CD(27,NK)	0.1481395E 07	-0.1571627E 06	0.3122597E 06	-0.2572816E 06	0.8570825E 05	-0.9616470E 04	0.0000000E 00	0.0000000E 00	0.0000000E 00
CD(28,NK)	-0.9465590E 07	0.1228785E 07	-0.2531726E 07	0.2111752E 07	-0.7088488E 06	0.7997489E 05	0.0000000E 00	0.0000000E 00	0.0000000E 00
CD(29,NK)	0.2358122E 08	-0.3600359E 07	0.7588980E 07	-0.6386908E 07	0.2158036E 07	-0.2447505E 06	0.0000000E 00	0.0000000E 00	0.0000000E 00

SEPARATED FLOW

	CD(NJ,1)	CD(NJ,2)	CD(NJ,3)	CD(NJ,4)	CD(NJ,5)	CD(NJ,6)	CD(NJ,7)	CD(NJ,8)	CD(NJ,9)
CD(1,NK)	0.1010356E 01	-0.4992520E 02	0.1131355E 04	-0.1350616E 05	0.8147603E 05	-0.1949407E 06	0.0000000E 00	0.0000000E 00	0.0000000E 00
CD(2,NK)	0.1711652E 01	-0.8822534E 02	0.3197853E 04	-0.7509432E 05	0.1078225E 07	-0.8612346E 07	0.2938358E 08	0.0000000E 00	0.0000000E 00
CD(3,NK)	-0.1184227E 03	0.1158314E 05	-0.5770347E 06	0.1646610E 08	-0.2705836E 09	0.2380160E 10	-0.8678436E 10	0.0000000E 00	0.0000000E 00
CD(4,NK)	-0.2601510E 00	-0.8901453E 01	0.4021512E 03	-0.5698633E 04	0.3603473E 05	-0.8664879E 05	0.0000000E 00	0.0000000E 00	0.0000000E 00
CD(5,NK)	-0.7169670E 02	0.1059423E 02	-0.8727325E 02	0.9608088E 03	-0.3541714E 04	0.5386795E 04	0.0000000E 00	0.0000000E 00	0.0000000E 00
CD(6,NK)	0.2430146E 00	-0.2348471E 00	-0.6332638E 00	0.2702778E 01	-0.1313284E 02	0.2076036E 02	-0.1128720E 01	-0.1106946E 02	0.0000000E 00
CD(7,NK)	0.3669505E 00	-0.3620679E 00	-0.6890594E 00	0.2589437E 01	-0.1466418E 02	0.3109081E 02	-0.2001859E 02	0.0000000E 00	0.0000000E 00
CD(8,NK)	0.1009939E 01	-0.1010514E 01	-0.1169582E 01	0.3497865E 01	-0.2086277E 02	0.4540653E 02	-0.2926388E 02	0.0000000E 00	0.0000000E 00
CD(9,NK)	0.1276387E 01	0.1341297E 01	0.4721058E 01	-0.2893853E 02	0.1954983E 03	-0.3773260E 03	0.2479320E 03	0.0000000E 00	0.0000000E 00
CD(10,NK)	-0.2866114E-03	-0.1018305E 01	-0.3709193E 01	0.2687367E 02	-0.1454293E 03	0.3126624E 03	-0.2105257E 03	0.0000000E 00	0.0000000E 00
CD(11,NK)	-0.2612833E 00	0.7434800E-01	-0.1252811E 02	0.9311746E 02	-0.4387744E 03	0.1097330E 04	-0.1237780E 04	0.4923961E 03	0.0000000E 00
CD(12,NK)	0.1506058E 01	-0.4660438E 00	-0.9389562E 00	-0.4567602E 01	0.3986344E 02	-0.1146492E 03	0.1300661E 03	0.0000000E 00	0.0000000E 00
CD(13,NK)	0.4127476E 00	-0.4048745E 00	-0.4769246E 00	0.1539471E 01	-0.7454624E 01	0.1478646E 02	-0.9046825E 01	0.0000000E 00	0.0000000E 00
CD(14,NK)	-0.4359281E 00	0.3084968E 00	-0.1032689E 02	0.4737627E 02	-0.1220907E 03	0.1863487E 03	-0.1141363E 03	0.0000000E 00	0.0000000E 00
CD(15,NK)	-0.3138301E 00	-0.3858612E 02	0.1734677E 04	-0.2765317E 05	0.1951122E 06	-0.5137912E 06	0.0000000E 00	0.0000000E 00	0.0000000E 00
CD(16,NK)	-0.5451201E 01	0.8426081E 03	-0.2970861E 05	0.4464240E 06	-0.3081020E 07	0.8029295E 07	0.0000000E 00	0.0000000E 00	0.0000000E 00
CD(17,NK)	0.3489904E 02	-0.5096239E 04	0.1748877E 06	-0.2584974E 07	0.1764671E 08	-0.4564025E 08	0.0000000E 00	0.0000000E 00	0.0000000E 00
CD(18,NK)	-0.1115597E 03	0.1280081E 05	-0.4125087E 06	0.5917823E 07	-0.3970661E 08	0.1015575E 09	0.0000000E 00	0.0000000E 00	0.0000000E 00
CD(19,NK)	0.1018879E 03	-0.1006172E 05	0.3096586E 06	-0.4343267E 07	0.2875901E 08	-0.7292795E 08	0.0000000E 00	0.0000000E 00	0.0000000E 00
CD(20,NK)	-0.2236704E 02	0.1293393E 04	-0.2960689E 05	0.3376425E 06	-0.1911262E 07	0.4282562E 07	0.0000000E 00	0.0000000E 00	0.0000000E 00
CD(21,NK)	0.2919593E 03	-0.1644304E 05	0.3613880E 06	-0.3937849E 07	0.2127414E 08	-0.4552502E 08	0.0000000E 00	0.0000000E 00	0.0000000E 00
CD(22,NK)	-0.1434123E 04	0.7180287E 05	-0.1410560E 07	0.1362827E 08	-0.6437761E 08	0.1181893E 09	0.0000000E 00	0.0000000E 00	0.0000000E 00
CD(23,NK)	0.2579852E 04	-0.1096177E 06	0.1738421E 07	-0.1190596E 08	0.2671202E 08	0.2277867E 08	0.0000000E 00	0.0000000E 00	0.0000000E 00
CD(24,NK)	-0.1496832E 04	0.5032238E 05	-0.4569868E 06	-0.1900187E 07	0.4726599E 08	-0.1800811E 09	0.0000000E 00	0.0000000E 00	0.0000000E 00
CD(25,NK)	0.4374763E 04	-0.8595760E 03	0.2052351E 05	-0.1627131E 06	0.5497548E 06	-0.6808765E 06	0.0000000E 00	0.0000000E 00	0.0000000E 00
CD(26,NK)	-0.1132137E 06	0.3429344E 05	-0.8497768E 06	0.6417504E 07	-0.2095292E 08	0.2432540E 08	0.0000000E 00	0.0000000E 00	0.0000000E 00
CD(27,NK)	0.1469797E 07	-0.5896708E 06	0.1404771E 08	-0.1042375E 09	0.3337893E 09	-0.3751930E 09	0.0000000E 00	0.0000000E 00	0.0000000E 00
CD(28,NK)	-0.9365388E 07	0.4488342E 07	-0.1032996E 09	0.7598323E 09	-0.2402994E 10	0.2649459E 10	0.0000000E 00	0.0000000E 00	0.0000000E 00
CD(29,NK)	0.2326390E 08	-0.1254525E 08	0.2815454E 09	-0.2060415E 10	0.6460408E 10	-0.7032983E 10	0.0000000E 00	0.0000000E 00	0.0000000E 00

SW -0.400

WEAK INTERACTION COEFFICIENTS

	CC(MJ,1)	CC(MJ,2)	CC(MJ,3)
CC(1,LJ)	0.17241990E 01	0.16341772E 01	0.18798846E 00
CC(2,LJ)	0.66196978E 00	0.10341641E 01	0.16064856E 01
CC(3,LJ)	0.15666942E 01	-0.43954992E 01	0.30966854E 01
CC(4,LJ)	-0.24827699E 01	-0.79538545E 01	0.28607301E 01
CC(5,LJ)	0.88014036E-01	-0.33026561E 01	0.16812727E 01

PROFILES COEFFICIENTS

ATTACHED FLOW

	CD(NJ,1)	CD(NJ,2)	CD(NJ,3)	CD(NJ,4)	CD(NJ,5)	CD(NJ,6)	CD(NJ,7)	CD(NJ,8)	CD(NJ,9)
CD(1,NK)	0.1890959E 01	-0.4539928E 02	0.4979707E 03	-0.2896391E 04	0.8587521E 04	-0.1017739E 05	0.0000000E 00	0.0000000E 00	0.0000000E 00
CD(2,NK)	0.1722617E 01	-0.1293621E 02	0.4496427E 02	-0.5944349E 02	0.0000000E 00	0.0000000E 00	0.0000000E 00	0.0000000E 00	0.0000000E 00
CD(3,NK)	-0.1002562E 02	-0.3195771E 02	0.1309435E 04	-0.7169710E 04	0.1204925E 05	0.0000000E 00	0.0000000E 00	0.0000000E 00	0.0000000E 00
CD(4,NK)	0.5041592E 00	-0.3680449E 01	-0.1735736E 01	0.1288671E 03	-0.5689027E 03	0.8121652E 03	0.0000000E 00	0.0000000E 00	0.0000000E 00
CD(5,NK)	-0.5441587E 02	-0.2095991E 01	-0.2522788E 01	0.3614362E 01	-0.1379924E 01	0.1623575E 00	0.0000000E 00	0.0000000E 00	0.0000000E 00
CD(6,NK)	0.2377678E 00	0.1192232E 00	-0.2050001E-01	0.1343508E-02	0.2974451E-04	0.0000000E 00	0.0000000E 00	0.0000000E 00	0.0000000E 00
CD(7,NK)	0.3582686E 00	0.1783417E 00	-0.1401867E-01	-0.3378159E-02	0.8037465E-03	-0.4002901E-04	0.0000000E 00	0.0000000E 00	0.0000000E 00
CD(8,NK)	0.9794896E 00	0.4794356E 00	0.3276316E-01	0.5475098E-02	-0.1559927E-02	0.1899216E-04	0.0000000E 00	0.0000000E 00	0.0000000E 00
CD(9,NK)	0.1306113E 01	-0.6488384E 00	0.3868538E 00	-0.1132663E 00	0.1743565E-01	-0.1109170E-02	0.0000000E 00	0.0000000E 00	0.0000000E 00
CD(10,NK)	0.1108829E-03	0.5039683E 00	-0.1188545E 00	0.1676002E-01	-0.1326236E-02	0.6181496E-04	0.0000000E 00	0.0000000E 00	0.0000000E 00
CD(11,NK)	0.1213817E 00	-0.5129218E-01	0.2020438E-01	-0.1137002E-01	0.4041757E-02	-0.6831059E-03	0.4391901E-04	0.0000000E 00	0.0000000E 00
CD(12,NK)	0.1498178E 01	0.2735725E 00	-0.3589206E-01	0.1055891E-02	0.1083242E-02	-0.2261844E-03	0.4548707E-05	0.0000000E 00	0.0000000E 00
CD(13,NK)	0.3948658E 00	0.2103243E 00	0.1196742E-01	-0.1169746E-01	0.2773902E-01	-0.9345412E-02	0.8921603E-03	0.0000000E 00	0.0000000E 00
CD(14,NK)	0.2023109E 00	-0.2588326E-01	0.2810809E 00	-0.4119822E 00	0.3391295E 00	-0.1376135E 00	0.2600099E-01	-0.1846924E-02	0.0000000E 00
CD(15,NK)	0.4653913E 00	-0.1871937E 01	-0.3257975E 02	0.3811770E 03	-0.1534942E 04	0.2196385E 04	0.0000000E 00	0.0000000E 00	0.0000000E 00
CD(16,NK)	-0.1143591E 00	-0.1568937E 01	0.6370317E 02	-0.6287818E 03	0.2576037E 04	-0.3822955E 04	0.0000000E 00	0.0000000E 00	0.0000000E 00
CD(17,NK)	0.2075782E-01	0.1646902E 01	-0.4342230E 02	0.4121735E 03	-0.1702281E 04	0.2569708E 04	0.0000000E 00	0.0000000E 00	0.0000000E 00
CD(18,NK)	-0.3533739E-02	-0.4716078E 00	0.1153567E 02	-0.1086161E 03	0.4518616E 03	-0.6899420E 03	0.0000000E 00	0.0000000E 00	0.0000000E 00
CD(19,NK)	0.3253840E-03	0.4345988E-01	-0.1047340E 01	0.9869983E 01	-0.4134529E 02	0.6369726E 02	0.0000000E 00	0.0000000E 00	0.0000000E 00
CD(20,NK)	-0.3879510E 00	0.4230008E 01	0.1773375E 01	-0.2316159E 03	0.1239675E 04	-0.2071842E 04	0.0000000E 00	0.0000000E 00	0.0000000E 00
CD(21,NK)	0.2705689E 00	-0.4605089E 01	0.3236896E 02	-0.8896258E 02	-0.7320907E 02	0.5795192E 03	0.0000000E 00	0.0000000E 00	0.0000000E 00
CD(22,NK)	-0.1307030E 00	0.3389947E 01	-0.4360804E 02	0.2952515E 03	-0.9511889E 03	0.1123021E 04	0.0000000E 00	0.0000000E 00	0.0000000E 00
CD(23,NK)	0.3078758E-01	-0.1084396E 01	0.1686007E 02	-0.1298380E 03	0.4674689E 03	-0.6241909E 03	0.0000000E 00	0.0000000E 00	0.0000000E 00
CD(24,NK)	-0.2681780E-02	0.1179943E 00	-0.1998619E 01	0.1616374E 02	-0.6052213E 02	0.8404975E 02	0.0000000E 00	0.0000000E 00	0.0000000E 00
CD(25,NK)	0.1433484E 04	-0.6572239E 02	0.1958544E 03	-0.1971815E 03	0.7116502E 02	-0.8241472E 01	0.0000000E 00	0.0000000E 00	0.0000000E 00
CD(26,NK)	-0.1635783E 05	0.1352357E 04	-0.3494562E 04	0.3464075E 04	-0.1253529E 04	0.1457753E 03	0.0000000E 00	0.0000000E 00	0.0000000E 00
CD(27,NK)	0.9628857E 05	-0.9379966E 04	0.2654369E 05	-0.2719438E 05	0.1000605E 05	-0.1175125E 04	0.0000000E 00	0.0000000E 00	0.0000000E 00
CD(28,NK)	-0.2850275E 06	0.2883569E 05	-0.9226965E 05	0.9864676E 05	-0.3703998E 05	0.4400469E 04	0.0000000E 00	0.0000000E 00	0.0000000E 00
CD(29,NK)	0.3352595E 06	-0.3307363E 05	0.1205212E 06	-0.1346120E 06	0.5160823E 05	-0.6204315E 04	0.0000000E 00	0.0000000E 00	0.0000000E 00

SEPARATED FLOW

	CD(NJ,1)	CD(NJ,2)	CD(NJ,3)	CD(NJ,4)	CD(NJ,5)	CD(NJ,6)	CD(NJ,7)	CD(NJ,8)	CD(NJ,9)
CD(1,NK)	0.1897599E 01	-0.4524365E 02	0.4924844E 03	-0.2842915E 04	0.8370841E 04	-0.9860314E 04	0.0000000E 00	0.0000000E 00	0.0000000E 00
CD(2,NK)	0.3323193E 01	-0.7789360E 02	0.1218054E 04	-0.1154834E 05	0.5913657E 05	-0.1247853E 06	0.0000000E 00	0.0000000E 00	0.0000000E 00
CD(3,NK)	-0.9219592E 02	0.3525784E 04	-0.6646462E 05	0.6823332E 06	-0.3628416E 07	0.7817852E 07	0.0000000E 00	0.0000000E 00	0.0000000E 00
CD(4,NK)	-0.4791203E 00	-0.1339344E 02	0.2854365E 03	-0.2074368E 04	0.6787196E 04	-0.8448218E 04	0.0000000E 00	0.0000000E 00	0.0000000E 00
CD(5,NK)	-0.5420684E 02	0.2185803E-01	0.1449370E 03	-0.7150365E 03	0.1381561E 04	0.5007945E 03	0.0000000E 00	0.0000000E 00	0.0000000E 00
CD(6,NK)	0.2374196E 00	-0.2527624E 00	0.2596845E 00	-0.5330518E 01	0.2199028E 02	-0.5807538E 02	0.8554100E 02	-0.4802383E 02	0.0000000E 00
CD(7,NK)	0.3573910E 00	-0.3340032E 00	-0.6353008E 00	0.2171027E 01	-0.1290759E 02	0.2739552E 02	-0.1736563E 02	0.0000000E 00	0.0000000E 00
CD(8,NK)	0.9766272E 00	-0.9157787E 00	-0.9998776E 00	0.1727310E 01	-0.1431357E 02	0.3406317E 02	-0.2216424E 02	0.0000000E 00	0.0000000E 00
CD(9,NK)	0.1307616E 01	0.1303407E 01	0.4994744E 01	-0.3311500E 02	0.2059565E 03	-0.3848120E 03	0.2483550E 03	0.0000000E 00	0.0000000E 00
CD(10,NK)	-0.6320771E-03	-0.9183089E 00	-0.3229979E 01	0.2372135E 02	-0.1294306E 03	0.2736879E 03	-0.1802585E 03	0.0000000E 00	0.0000000E 00
CD(11,NK)	-0.2792692E 00	0.2336680E 01	-0.5196495E 02	0.3970874E 03	-0.1636322E 04	0.3617685E 04	-0.3948061E 04	0.1666447E 04	0.0000000E 00
CD(12,NK)	0.1501420E 01	-0.6862806E 00	0.3760630E 01	-0.3786911E 02	0.1499297E 03	-0.2848862E 03	0.2270798E 03	0.0000000E 00	0.0000000E 00
CD(13,NK)	0.3968561E 00	-0.3624773E 00	-0.4448359E 00	0.1134214E 01	-0.5894144E 01	0.1193435E 02	-0.7204075E 01	0.0000000E 00	0.0000000E 00
CD(14,NK)	-0.4395904E 00	0.2988233E 01	-0.5528253E 02	0.3788677E 03	-0.1387051E 04	0.2787650E 04	-0.2857043E 04	0.1164956E 04	0.0000000E 00
CD(15,NK)	-0.1899182E 01	0.6247581E 01	0.2579342E 03	-0.2888373E 04	0.1152338E 05	-0.1620546E 05	0.0000000E 00	0.0000000E 00	0.0000000E 00
CD(16,NK)	0.7324728E 01	0.2047805E 03	-0.6090050E 04	0.5320903E 05	-0.1973872E 06	0.2688913E 06	0.0000000E 00	0.0000000E 00	0.0000000E 00
CD(17,NK)	-0.1980480E 02	-0.1890759E 04	0.4298461E 05	-0.3487530E 06	0.1247920E 07	-0.1663984E 07	0.0000000E 00	0.0000000E 00	0.0000000E 00
CD(18,NK)	-0.4500490E 02	0.6368727E 04	-0.1168204E 06	0.8808625E 06	-0.3037547E 07	0.3961850E 07	0.0000000E 00	0.0000000E 00	0.0000000E 00
CD(19,NK)	0.8263504E 02	-0.5693217E 04	0.9426964E 05	-0.6816561E 06	0.2298194E 07	-0.2956092E 07	0.0000000E 00	0.0000000E 00	0.0000000E 00
CD(20,NK)	-0.5813166E 02	0.1977445E 04	-0.2549803E 05	0.1605861E 06	-0.4954733E 06	0.5992000E 06	0.0000000E 00	0.0000000E 00	0.0000000E 00
CD(21,NK)	0.7871003E 03	-0.2628780E 05	0.3343718E 06	-0.2083237E 07	0.6373055E 07	-0.7655499E 07	0.0000000E 00	0.0000000E 00	0.0000000E 00
CD(22,NK)	-0.3897785E 04	0.1215494E 06	-0.1487074E 07	0.9026096E 07	-0.2709794E 08	0.3209328E 08	0.0000000E 00	0.0000000E 00	0.0000000E 00
CD(23,NK)	0.7280035E 04	-0.2124850E 06	0.2494641E 07	-0.1469919E 08	0.4314467E 08	-0.5020004E 08	0.0000000E 00	0.0000000E 00	0.0000000E 00
CD(24,NK)	-0.4498984E 04	0.1236664E 06	-0.1391669E 07	0.7931024E 07	-0.2265406E 08	0.2577065E 08	0.0000000E 00	0.0000000E 00	0.0000000E 00
CD(25,NK)	0.1427330E 04	0.1564376E 03	-0.2229566E 04	0.7756496E 04	0.1654325E 05	-0.8671532E 05	0.0000000E 00	0.0000000E 00	0.0000000E 00
CD(26,NK)	-0.1628311E 05	-0.1833480E 04	0.5534350E 04	0.5786240E 05	-0.7871328E 06	0.1735227E 07	0.0000000E 00	0.0000000E 00	0.0000000E 00
CD(27,NK)	0.9585217E 05	0.7363718E 04	0.7160635E 05	-0.1119410E 07	0.7602373E 07	-0.1371340E 08	0.0000000E 00	0.0000000E 00	0.0000000E 00
CD(28,NK)	-0.2838471E 06	-0.8926894E 04	-0.4660560E 06	0.5229819E 07	-0.2952993E 08	0.4860147E 08	0.0000000E 00	0.0000000E 00	0.0000000E 00
CD(29,NK)	0.3341166E 06	-0.4315517E 04	0.7884026E 06	-0.7977646E 07	0.4127352E 08	-0.6446034E 08	0.0000000E 00	0.0000000E 00	0.0000000E 00

SW -0.600

WEAK INTERACTION COEFFICIENTS

	CC(MJ,1)	CC(MJ,2)	CC(MJ,3)
CC(1,LJ)	0.17241549E 01	0.16336767E 01	0.28211760E 00
CC(2,LJ)	0.66183984E 00	0.68881285E 00	0.16060264E 01
CC(3,LJ)	0.12964274E 01	-0.38444666E 01	0.27738795E 01
CC(4,LJ)	-0.19024384E 01	-0.56515150E 01	0.22147183E 01
CC(5,LJ)	0.11233793E 00	-0.40482835E 01	0.20676102E 01

PROFILES COEFFICIENTS

ATTACHED FLOW

	CD(NJ,1)	CD(NJ,2)	CD(NJ,3)	CD(NJ,4)	CD(NJ,5)	CD(NJ,6)	CD(NJ,7)	CD(NJ,8)	CD(NJ,9)
CD(1,NK)	0.2912912E 01	-0.4926310E 02	0.3786752E 03	-0.1538372E 04	0.3178047E 04	-0.2619741E 04	0.0000000E 00	0.0000000E 00	0.0000000E 00
CD(2,NK)	0.3273021E 01	-0.2329704E 02	0.8807365E 02	-0.1702461E 03	0.1325679E 03	0.0000000E 00	0.0000000E 00	0.0000000E 00	0.0000000E 00
CD(3,NK)	-0.2156118E 02	0.1467479E 03	-0.3234761E 03	0.1153358E 01	0.5568568E 03	0.0000000E 00	0.0000000E 00	0.0000000E 00	0.0000000E 00
CD(4,NK)	0.8781807E 00	-0.4438156E 01	-0.2950157E 01	0.8575444E 02	-0.2576340E 03	0.2521464E 03	0.0000000E 00	0.0000000E 00	0.0000000E 00
CD(5,NK)	-0.5922720E 02	-0.4145298E 01	0.8924835E 00	0.1384278E 01	-0.8245806E 00	0.1202995E 00	0.0000000E 00	0.0000000E 00	0.0000000E 00
CD(6,NK)	0.2287921E 00	0.1301224E 00	-0.2461319E-01	0.1770436E-02	0.6514634E-04	0.0000000E 00	0.0000000E 00	0.0000000E 00	0.0000000E 00
CD(7,NK)	0.3435018E 00	0.1940737E 00	-0.1894793E-01	-0.2723700E-02	0.6378561E-03	0.0000000E 00	0.0000000E 00	0.0000000E 00	0.0000000E 00
CD(8,NK)	0.9289087E 00	0.5195834E 00	0.3390965E-02	0.3412923E-01	-0.1199552E-01	0.1101652E-02	0.0000000E 00	0.0000000E 00	0.0000000E 00
CD(9,NK)	0.1359245E 01	-0.7727751E 00	0.5148797E 00	-0.1901181E 00	0.4522400E-01	-0.6614011E-02	0.4516236E-03	0.0000000E 00	0.0000000E 00
CD(10,NK)	0.4504812E-04	0.5167260E 00	-0.1304416E 00	0.1861089E-01	-0.9351079E-03	0.0000000E 00	0.0000000E 00	0.0000000E 00	0.0000000E 00
CD(11,NK)	0.1320599E 00	-0.6178326E-01	0.3008609E-01	-0.2082683E-01	0.8576700E-02	-0.1622709E-02	0.1126484E-03	0.0000000E 00	0.0000000E 00
CD(12,NK)	0.1485940E 01	0.2899080E 00	-0.3139439E-01	-0.2605892E-02	0.3986596E-03	0.0000000E 00	0.0000000E 00	0.0000000E 00	0.0000000E 00
CD(13,NK)	0.3749805E 00	0.1988605E 00	0.5265136E-01	-0.5793720E-01	0.6256018E-01	-0.2171938E-01	0.2360651E-02	0.0000000E 00	0.0000000E 00
CD(14,NK)	0.2026946E 00	0.2772013E-01	0.1615620E 00	-0.3319475E 00	0.3865422E 00	-0.2046661E 00	0.4815844E-01	-0.4163511E-02	0.0000000E 00
CD(15,NK)	0.8386147E 00	-0.3218976E 01	-0.1687463E 02	0.1641024E 03	-0.4651708E 03	0.4576787E 03	0.0000000E 00	0.0000000E 00	0.0000000E 00
CD(16,NK)	-0.2907772E 00	-0.1106967E-01	0.3464562E 02	-0.2657899E 03	0.7754127E 03	-0.8014759E 03	0.0000000E 00	0.0000000E 00	0.0000000E 00
CD(17,NK)	0.9671567E-01	0.9828481E 00	-0.2736865E 02	0.1946148E 03	-0.5712381E 03	0.6024168E 03	0.0000000E 00	0.0000000E 00	0.0000000E 00
CD(18,NK)	-0.2451961E-01	-0.3644711E 00	0.8308698E 01	-0.5787398E 02	0.1708120E 03	-0.1822878E 03	0.0000000E 00	0.0000000E 00	0.0000000E 00
CD(19,NK)	0.2592060E-02	0.3896356E-01	-0.8552632E 00	0.5936780E 01	-0.1762838E 02	0.1898196E 02	0.0000000E 00	0.0000000E 00	0.0000000E 00
CD(20,NK)	-0.8068393E 00	0.6082048E 01	0.1817016E 01	-0.1585094E 03	0.5768040E 03	-0.6518139E 03	0.0000000E 00	0.0000000E 00	0.0000000E 00
CD(21,NK)	0.6740213E 00	-0.6474544E 01	0.1907022E 02	0.3329749E 02	-0.2952040E 03	0.4398936E 03	0.0000000E 00	0.0000000E 00	0.0000000E 00
CD(22,NK)	-0.3692193E 00	0.4688066E 01	-0.3105003E 02	0.1131745E 03	-0.1938941E 03	0.1059963E 03	0.0000000E 00	0.0000000E 00	0.0000000E 00
CD(23,NK)	0.9674753E-01	-0.1581751E 01	0.1386276E 02	-0.6620826E 02	0.1529667E 03	-0.1318497E 03	0.0000000E 00	0.0000000E 00	0.0000000E 00
CD(24,NK)	-0.9367635E-02	0.1876195E 00	-0.1873053E 01	0.9768003E 01	-0.2426922E 02	0.2254204E 02	0.0000000E 00	0.0000000E 00	0.0000000E 00
CD(25,NK)	0.1096584E 04	-0.8045093E 01	0.5126657E 02	-0.7884082E 02	0.3563249E 02	-0.4847029E 01	0.0000000E 00	0.0000000E 00	0.0000000E 00
CD(26,NK)	-0.8769525E 04	0.2421282E 03	-0.7263963E 03	0.1009388E 04	-0.4504390E 03	0.6123190E 02	0.0000000E 00	0.0000000E 00	0.0000000E 00
CD(27,NK)	0.3608967E 05	-0.7815559E 03	0.3478544E 04	-0.5371450E 04	0.2478582E 04	-0.3423312E 03	0.0000000E 00	0.0000000E 00	0.0000000E 00
CD(28,NK)	-0.7454214E 05	0.2344541E 03	-0.6849587E 04	0.1279094E 05	-0.6207325E 04	0.8764991E 03	0.0000000E 00	0.0000000E 00	0.0000000E 00
CD(29,NK)	0.6108326E 05	0.1337067E 04	0.4491345E 04	-0.1122879E 05	0.5789452E 04	-0.8383043E 03	0.0000000E 00	0.0000000E 00	0.0000000E 00

SEPARATED FLOW

	CD(NJ,1)	CD(NJ,2)	CD(NJ,3)	CD(NJ,4)	CD(NJ,5)	CD(NJ,6)	CD(NJ,7)	CD(NJ,8)	CD(NJ,9)
CD(1,NK)	0.2909518E 01	-0.4886837E 02	0.3732008E 03	-0.1507484E 04	0.3099419E 04	-0.2545003E 04	0.0000000E 00	0.0000000E 00	0.0000000E 00
CD(2,NK)	0.5141833E 01	-0.8298115E 02	0.8889820E 03	-0.5740300E 04	0.1993020E 05	-0.2843864E 05	0.0000000E 00	0.0000000E 00	0.0000000E 00
CD(3,NK)	-0.1245110E 03	0.4230522E 04	-0.7457459E 05	0.7629208E 06	-0.4536592E 07	0.1453778E 08	-0.1940401E 08	0.0000000E 00	0.0000000E 00
CD(4,NK)	-0.8496940E 00	-0.7339845E 01	0.1349612E 03	-0.6970823E 03	0.1580489E 04	-0.1355198E 04	0.0000000E 00	0.0000000E 00	0.0000000E 00
CD(5,NK)	-0.5916951E 02	-0.1020833E 01	0.1422166E 03	-0.6091092E 03	0.8730449E 03	0.1119307E 04	0.0000000E 00	0.0000000E 00	0.0000000E 00
CD(6,NK)	0.2284925E 00	-0.2009035E 00	-0.2089189E 00	-0.1598114E 01	0.8232807E 01	-0.3188295E 02	0.5967343E 02	-0.3752324E 02	0.0000000E 00
CD(7,NK)	0.3430975E 00	-0.2905073E 00	-0.4727668E 00	-0.7567150E-01	0.1766312E 00	-0.9095745E 01	0.2978683E 02	-0.2294712E 02	0.0000000E 00
CD(8,NK)	0.9289307E 00	-0.7613208E 00	-0.1135972E 01	0.3969454E 00	0.9600368E 00	-0.2038090E 02	0.5775402E 02	-0.4223102E 02	0.0000000E 00
CD(9,NK)	0.1354212E 01	0.2088778E 01	-0.1437306E 02	0.1291994E 03	-0.4618336E 03	0.1031769E 04	-0.1235459E 04	0.6075875E 03	0.0000000E 00
CD(10,NK)	0.4996032E-03	-0.9259158E 00	0.1463316E 01	-0.2091992E 02	0.8041362E 02	-0.2270987E 03	0.3925155E 03	-0.2503818E 03	0.0000000E 00
CD(11,NK)	-0.2465702E 00	0.2111875E 01	-0.4722626E 02	0.3566528E 03	-0.1454021E 04	0.3169413E 04	-0.3399746E 04	0.1407967E 04	0.0000000E 00
CD(12,NK)	0.1478838E 01	0.5804386E-01	-0.8503183E 01	0.5561031E 02	-0.2109996E 03	0.4587796E 03	-0.5548839E 03	0.3247883E 03	0.0000000E 00
CD(13,NK)	0.3749648E 00	-0.3245716E 00	-0.9513976E-02	-0.1888377E 01	0.3256014E 01	-0.1269779E 01	0.0000000E 00	0.0000000E 00	0.0000000E 00
CD(14,NK)	-0.3676629E 00	0.2578781E 01	-0.5045329E 02	0.3522822E 03	-0.1321927E 04	0.2724077E 04	-0.2863049E 04	0.1199299E 04	0.0000000E 00
CD(15,NK)	-0.9161282E 00	-0.3599497E 02	0.5733518E 03	-0.3196122E 04	0.7874599E 04	-0.7247282E 04	0.0000000E 00	0.0000000E 00	0.0000000E 00
CD(16,NK)	-0.1548636E 02	0.8185512E 03	-0.9944634E 04	0.5170174E 05	-0.1238868E 06	0.1124335E 06	0.0000000E 00	0.0000000E 00	0.0000000E 00
CD(17,NK)	0.1027102E 03	-0.4963265E 04	0.5829898E 05	-0.2972322E 06	0.7032547E 06	-0.6326867E 06	0.0000000E 00	0.0000000E 00	0.0000000E 00
CD(18,NK)	-0.3317432E 03	0.1250726E 05	-0.1373556E 06	0.6780007E 06	-0.1574131E 07	0.1398946E 07	0.0000000E 00	0.0000000E 00	0.0000000E 00
CD(19,NK)	0.3040754E 03	-0.9872160E 04	0.1033065E 06	-0.4977598E 06	0.1139199E 07	-0.1002952E 07	0.0000000E 00	0.0000000E 00	0.0000000E 00
CD(20,NK)	-0.7214920E 02	0.1529336E 04	-0.1258521E 05	0.5128922E 05	-0.1035331E 06	0.8266353E 05	0.0000000E 00	0.0000000E 00	0.0000000E 00
CD(21,NK)	0.9483078E 03	-0.1926623E 05	0.1522028E 06	-0.5965242E 06	0.1161088E 07	-0.8966303E 06	0.0000000E 00	0.0000000E 00	0.0000000E 00
CD(22,NK)	-0.4561980E 04	0.8305068E 05	-0.5986695E 06	0.2150248E 07	-0.3839439E 07	0.2720323E 07	0.0000000E 00	0.0000000E 00	0.0000000E 00
CD(23,NK)	0.8084584E 04	-0.1281226E 06	0.7932605E 06	-0.2352134E 07	0.3232138E 07	-0.1538590E 07	0.0000000E 00	0.0000000E 00	0.0000000E 00
CD(24,NK)	-0.4630762E 04	0.6085132E 05	-0.2747559E 06	0.3549774E 06	0.6032597E 06	-0.1390782E 07	0.0000000E 00	0.0000000E 00	0.0000000E 00
CD(25,NK)	0.1096595E 04	0.1006430E 03	-0.6735957E 03	-0.2850148E 04	0.3914419E 05	-0.8862825E 05	0.0000000E 00	0.0000000E 00	0.0000000E 00
CD(26,NK)	-0.8781634E 04	-0.6067462E 03	-0.1115663E 05	0.1455155E 06	-0.7473870E 06	0.1198158E 07	0.0000000E 00	0.0000000E 00	0.0000000E 00
CD(27,NK)	0.3620337E 05	0.5393227E 03	0.1061284E 06	-0.1049407E 07	0.4590832E 07	-0.6559986E 07	0.0000000E 00	0.0000000E 00	0.0000000E 00
CD(28,NK)	-0.7493679E 05	0.3286809E 04	-0.3222858E 06	0.2941699E 07	-0.1200562E 08	0.1618463E 08	0.0000000E 00	0.0000000E 00	0.0000000E 00
CD(29,NK)	0.6155607E 05	-0.6041636E 04	0.3327236E 06	-0.2927467E 07	0.1148841E 08	-0.1495228E 08	0.0000000E 00	0.0000000E 00	0.0000000E 00

SW -0.800

WEAK INTERACTION COEFFICIENTS

	CC(MJ,1)	CC(MJ,2)	CC(MJ,3)
CC(1,LJ)	0.17240300E 01	0.16328401E 01	0.37953001E 00
CC(2,LJ)	0.66210007E 00	0.34260004E 00	0.16127500E 01
CC(3,LJ)	0.10223600E 01	-0.31487402E 01	0.24413504E 01
CC(4,LJ)	-0.13357601E 01	-0.38105902E 01	0.15732300E 01
CC(5,LJ)	0.12736001E 00	-0.49017400E 01	0.28740501E 01

PROFILES COEFFICIENTS

ATTACHED FLOW

	CD(NJ,1)	CD(NJ,2)	CD(NJ,3)	CD(NJ,4)	CD(NJ,5)	CD(NJ,6)	CD(NJ,7)	CD(NJ,8)	CD(NJ,9)
CD(1,NK)	0.4267743E 01	-0.6157092E 02	0.3985996E 03	-0.1343925E 04	0.2273664E 04	-0.1518686E 04	0.0000000E 00	0.0000000E 00	0.0000000E 00
CD(2,NK)	0.3678075E 01	-0.1468022E 02	0.2683578E 02	-0.1844423E 02	0.0000000E 00	0.0000000E 00	0.0000000E 00	0.0000000E 00	0.0000000E 00
CD(3,NK)	-0.2560494E 02	0.1530367E 03	-0.3518975E 03	0.2906592E 03	0.0000000E 00	0.0000000E 00	0.0000000E 00	0.0000000E 00	0.0000000E 00
CD(4,NK)	0.1467029E 01	-0.6195428E 01	-0.1534790E 01	0.6636170E 02	-0.1589657E 03	0.1215743E 03	0.0000000E 00	0.0000000E 00	0.0000000E 00
CD(5,NK)	-0.7406826E 02	-0.4025508E 01	-0.8562842E-01	0.2191791E 01	-0.1166896E 01	0.1791068E 00	0.0000000E 00	0.0000000E 00	0.0000000E 00
CD(6,NK)	0.2139569E 00	0.1446306E 00	-0.2676441E-01	-0.4000408E-03	0.5829025E-03	0.0000000E 00	0.0000000E 00	0.0000000E 00	0.0000000E 00
CD(7,NK)	0.3199875E 00	0.2109286E 00	-0.1466506E-01	-0.8910706E-02	0.1796173E-02	0.0000000E 00	0.0000000E 00	0.0000000E 00	0.0000000E 00
CD(8,NK)	0.8606224E 00	0.5360091E 00	0.2517679E-01	0.3501240E-01	-0.1492288E-01	0.1165230E-02	0.0000000E 00	0.0000000E 00	0.0000000E 00
CD(9,NK)	0.1457706E 01	-0.9707156E 00	0.6568454E 00	-0.2256523E 00	0.4103874E-01	-0.3069945E-02	0.0000000E 00	0.0000000E 00	0.0000000E 00
CD(10,NK)	0.1699928E-03	0.5347523E 00	-0.1442540E 00	0.1828404E-01	0.5143890E-03	-0.1396539E-03	0.0000000E 00	0.0000000E 00	0.0000000E 00
CD(11,NK)	0.1491844E 00	-0.7996785E-01	0.4553073E-01	-0.3123530E-01	0.1001542E-01	-0.7780675E-03	-0.8590212E-04	0.0000000E 00	0.0000000E 00
CD(12,NK)	0.1458878E 01	0.3382785E 00	-0.3709781E-01	-0.3751733E-01	0.5194626E-01	-0.2203759E-01	0.2932755E-02	0.0000000E 00	0.0000000E 00
CD(13,NK)	0.3456743E 00	0.1563510E 00	0.2181642E 00	-0.2988359E 00	0.2390384E 00	-0.8096699E-01	0.9510543E-02	0.0000000E 00	0.0000000E 00
CD(14,NK)	0.2202414E 00	-0.1412186E 00	0.9620319E 00	-0.1980170E 01	0.2110243E 01	-0.1124021E 01	0.2845030E 00	-0.2739579E-01	0.0000000E 00
CD(15,NK)	0.1407069E 01	-0.4673536E 01	-0.1446585E 02	0.1234345E 03	-0.2802988E 03	0.2184363E 03	0.0000000E 00	0.0000000E 00	0.0000000E 00
CD(16,NK)	-0.6501719E 00	0.1475198E 01	0.2731601E 02	-0.1884711E 03	0.4504433E 03	-0.3740145E 03	0.0000000E 00	0.0000000E 00	0.0000000E 00
CD(17,NK)	0.3130033E 00	0.1494366E 00	-0.2222988E 02	0.1401812E 03	-0.3394885E 03	0.2894647E 03	0.0000000E 00	0.0000000E 00	0.0000000E 00
CD(18,NK)	-0.9878188E-01	-0.1552839E 00	0.7365338E 01	-0.4504640E 02	0.1098691E 03	-0.9506629E 02	0.0000000E 00	0.0000000E 00	0.0000000E 00
CD(19,NK)	0.1199229E-01	0.1991355E-01	-0.8434880E 00	0.5118777E 01	-0.1256854E 02	0.1099148E 02	0.0000000E 00	0.0000000E 00	0.0000000E 00
CD(20,NK)	-0.1683068E 01	0.1160509E 02	-0.1875526E 02	-0.5216923E 02	0.2128265E 03	-0.2029576E 03	0.0000000E 00	0.0000000E 00	0.0000000E 00
CD(21,NK)	0.1676513E 01	-0.1464785E 02	0.6020643E 02	-0.1403068E 03	0.1643352E 03	-0.6175170E 02	0.0000000E 00	0.0000000E 00	0.0000000E 00
CD(22,NK)	-0.9765148E 00	0.1050139E 02	-0.6316760E 02	0.2279887E 03	-0.4171379E 03	0.2888297E 03	0.0000000E 00	0.0000000E 00	0.0000000E 00
CD(23,NK)	0.2607175E 00	-0.3544685E 01	0.2584793E 02	-0.1064026E 03	0.2128204E 03	-0.1590093E 03	0.0000000E 00	0.0000000E 00	0.0000000E 00
CD(24,NK)	-0.2522801E-01	0.4379843E 00	-0.3579971E 01	0.1565586E 02	-0.3254103E 02	0.2510894E 02	0.0000000E 00	0.0000000E 00	0.0000000E 00
CD(25,NK)	0.1168381E 04	-0.5137349E 02	0.1105750E 03	-0.1139075E 03	0.4793986E 02	-0.6807435E 01	0.0000000E 00	0.0000000E 00	0.0000000E 00
CD(26,NK)	-0.7864746E 04	0.6340898E 03	-0.1241206E 04	0.1233086E 04	-0.5144517E 03	0.7297830E 02	0.0000000E 00	0.0000000E 00	0.0000000E 00
CD(27,NK)	0.2686553E 05	-0.2469258E 04	0.5331488E 04	-0.5525328E 04	0.2355393E 04	-0.3384402E 03	0.0000000E 00	0.0000000E 00	0.0000000E 00
CD(28,NK)	-0.4549103E 05	0.4179989E 04	-0.1009791E 05	0.1106101E 05	-0.4852531E 04	0.7089919E 03	0.0000000E 00	0.0000000E 00	0.0000000E 00
CD(29,NK)	0.3025512E 05	-0.2604653E 04	0.7039856E 04	-0.8172907E 04	0.3696934E 04	-0.5498604E 03	0.0000000E 00	0.0000000E 00	0.0000000E 00

SEPARATED FLOW

	CD(NJ,1)	CD(NJ,2)	CD(NJ,3)	CD(NJ,4)	CD(NJ,5)	CD(NJ,6)	CD(NJ,7)	CD(NJ,8)	CD(NJ,9)
CD(1,NK)	0.4370448E 01	-0.6347748E 02	0.4123527E 03	-0.1391791E 04	0.2354332E 04	-0.1571543E 04	0.0000000E 00	0.0000000E 00	0.0000000E 00
CD(2,NK)	0.7663401E 01	-0.1140055E 03	0.1187404E 04	-0.7749337E 04	0.2938108E 05	-0.5796773E 05	0.4468747E 05	0.0000000E 00	0.0000000E 00
CD(3,NK)	-0.1327965E 03	0.3377002E 04	-0.4345064E 05	0.3163644E 06	-0.1304398E 07	0.2818322E 07	-0.2456204E 07	0.0000000E 00	0.0000000E 00
CD(4,NK)	-0.1904914E 01	-0.1067966E 02	0.2121764E 03	-0.1001222E 04	0.1991677E 04	-0.1459769E 04	0.0000000E 00	0.0000000E 00	0.0000000E 00
CD(5,NK)	-0.7387666E 02	-0.1072111E 02	0.2613652E 03	-0.1094471E 04	0.1428890E 04	0.1102238E 04	0.0000000E 00	0.0000000E 00	0.0000000E 00
CD(6,NK)	0.2135439E 00	-0.2132991E 00	0.1138919E 01	-0.1332634E 02	0.6415286E 02	-0.1905997E 03	0.3275771E 03	-0.2877533E 03	0.9957688E 02
CD(7,NK)	0.3192735E 00	-0.2346050E 00	-0.4170284E 00	0.2279195E 01	-0.1871977E 02	0.4710648E 02	-0.4612138E 02	0.1574676E 02	0.0000000E 00
CD(8,NK)	0.8590445E 00	-0.6518702E 00	0.2339219E 00	-0.4640319E 01	-0.1722493E 01	0.2490831E 02	-0.2803178E 02	0.8816490E 01	0.0000000E 00
CD(9,NK)	0.1458739E 01	0.9495550E 00	0.7940913E 01	-0.5884376E 02	0.2752751E 03	-0.4585149E 03	0.2760114E 03	0.0000000E 00	0.0000000E 00
CD(10,NK)	-0.4281918E-03	-0.2821226E 00	-0.8527181E 01	0.7148799E 02	-0.3206760E 03	0.6826390E 03	-0.6597211E 03	0.2361735E 03	0.0000000E 00
CD(11,NK)	-0.2560153E 00	0.3724676E 01	-0.5782386E 02	0.3630224E 03	-0.1294467E 04	0.2568210E 04	-0.2564739E 04	0.9995854E 03	0.0000000E 00
CD(12,NK)	0.1493762E 01	-0.1767776E 01	0.1669609E 02	-0.7623469E 02	0.8610224E 02	0.2555378E 03	-0.7414084E 03	0.5490654E 03	0.0000000E 00
CD(13,NK)	0.3419051E 00	-0.2557996E 00	0.3926206E 00	-0.4484457E 01	0.1108418E 02	-0.1536933E 02	0.1410988E 02	-0.6026988E 01	0.0000000E 00
CD(14,NK)	-0.3325813E 00	0.3927558E 01	-0.5590923E 02	0.3113539E 03	-0.9633940E 03	0.1685057E 04	-0.1525127E 04	0.5515919E 03	0.0000000E 00
CD(15,NK)	-0.1339615E 02	0.2044382E 03	-0.1321417E 04	0.4329795E 04	-0.7059744E 04	0.4544945E 04	0.0000000E 00	0.0000000E 00	0.0000000E 00
CD(16,NK)	0.1282109E 03	-0.1988905E 04	0.1249225E 05	-0.3935768E 05	0.6169219E 05	-0.3830113E 05	0.0000000E 00	0.0000000E 00	0.0000000E 00
CD(17,NK)	-0.4871962E 03	0.6580105E 04	-0.3659682E 05	0.1026630E 06	-0.1436605E 06	0.7975890E 05	0.0000000E 00	0.0000000E 00	0.0000000E 00
CD(18,NK)	0.6506949E 03	-0.7368958E 04	0.3278942E 05	-0.6661459E 05	0.5368195E 05	-0.5376768E 04	0.0000000E 00	0.0000000E 00	0.0000000E 00
CD(19,NK)	-0.2823281E 03	0.2479061E 04	-0.5955044E 04	-0.7745866E 04	0.4910963E 05	-0.5096571E 05	0.0000000E 00	0.0000000E 00	0.0000000E 00
CD(20,NK)	-0.9480354E 02	0.3153088E 04	-0.2889168E 05	0.1169091E 06	-0.2199936E 06	0.1571397E 06	0.0000000E 00	0.0000000E 00	0.0000000E 00
CD(21,NK)	0.1372878E 04	-0.3996389E 05	0.3520345E 06	-0.1396610E 07	0.2596763E 07	-0.1840010E 07	0.0000000E 00	0.0000000E 00	0.0000000E 00
CD(22,NK)	-0.6633544E 04	0.1697725E 06	-0.1432383E 07	0.5560625E 07	-0.1020634E 08	0.7170955E 07	0.0000000E 00	0.0000000E 00	0.0000000E 00
CD(23,NK)	0.1167855E 05	-0.2751445E 06	0.2250239E 07	-0.8594286E 07	0.1561910E 08	-0.1090203E 08	0.0000000E 00	0.0000000E 00	0.0000000E 00
CD(24,NK)	-0.6705450E 04	0.1495183E 06	-0.1195494E 07	0.4510065E 07	-0.8134053E 07	0.5648293E 07	0.0000000E 00	0.0000000E 00	0.0000000E 00
CD(25,NK)	0.1165101E 04	0.1727296E 03	-0.1031099E 04	-0.5022015E 04	0.5277018E 05	-0.9861953E 05	0.0000000E 00	0.0000000E 00	0.0000000E 00
CD(26,NK)	-0.7841081E 04	-0.4372172E 03	-0.1610338E 05	0.1954570E 06	-0.8476107E 06	0.1151934E 07	0.0000000E 00	0.0000000E 00	0.0000000E 00
CD(27,NK)	0.2678362E 05	-0.1422032E 04	0.1235789E 06	-0.1141430E 07	0.4269094E 07	-0.5237721E 07	0.0000000E 00	0.0000000E 00	0.0000000E 00
CD(28,NK)	-0.4536228E 05	0.6879550E 04	-0.3028460E 06	0.2572666E 07	-0.9029334E 07	0.1052920E 08	0.0000000E 00	0.0000000E 00	0.0000000E 00
CD(29,NK)	0.3018369E 05	-0.7077070E 04	0.2506001E 06	-0.2044715E 07	0.6924970E 07	-0.7834236E 07	0.0000000E 00	0.0000000E 00	0.0000000E 00

APPENDIX B

Weak interaction coefficients computation

The four basic differential equations of moment (eq. 7 to 10) can be rewritten in the following form with the hypersonic viscous interaction parameter $\bar{\chi}$ as the independent variable :

$$F\frac{d\Delta}{d\bar{\chi}} + \Delta\left(\frac{\partial F}{\partial a}\frac{da}{d\bar{\chi}} + \frac{\partial F}{\partial b}\frac{db}{d\bar{\chi}}\right) + f\frac{\Delta}{M_e}\frac{dM_e}{d\bar{\chi}} = \frac{1}{\bar{\chi}}\left[F\Delta - 2\left(\frac{1+m_\infty}{1+m_e}\right)^{\frac{\gamma+1}{2(\gamma-1)}}\frac{M_\infty^3 tg\theta}{m_e\,\bar{\chi}}\right],$$

$$\mathcal{E}\frac{d\Delta}{d\bar{\chi}} + \Delta\frac{d\mathcal{E}}{da}\frac{da}{d\bar{\chi}} + \left(\frac{2\mathcal{E}+1-E}{M_e}\right)\Delta\frac{dM_e}{d\bar{\chi}} = \frac{1}{\bar{\chi}}\left[\mathcal{E}\Delta - 2\left(\frac{1+m_\infty}{1+m_e}\right)^{\frac{3\gamma-1}{2(\gamma-1)}}\frac{M_\infty P}{M_e\Delta}\right],$$

$$(B1)$$

$$J\frac{d\Delta}{d\bar{\chi}} + \Delta\frac{dJ}{d\mathcal{E}}\frac{d\mathcal{E}}{da}\frac{da}{d\bar{\chi}} + \left(\frac{3J-2T^*}{M_e}\right)\Delta\frac{dM_e}{d\bar{\chi}} = \frac{1}{\bar{\chi}}\left[J\Delta - 2\left(\frac{1+m_\infty}{1+m_e}\right)^{\frac{3\gamma-1}{2(\gamma-1)}}\frac{M_\infty R}{M_e\Delta}\right],$$

$$T^*\frac{d\Delta}{d\bar{\chi}} + \Delta\left(\frac{\partial T^*}{\partial a}\frac{da}{d\bar{\chi}} + \frac{\partial T^*}{\partial b}\frac{db}{d\bar{\chi}}\right) + \frac{T^*\Delta}{M_e}\frac{dM_e}{d\bar{\chi}} = \frac{1}{\bar{\chi}}\left[T^*\Delta - 2\left(\frac{1+m_\infty}{1+m_e}\right)^{\frac{3\gamma-1}{2(\gamma-1)}}\frac{M_\infty\bar{Q}}{M_e\Delta}\right].$$

where $$\Delta = \frac{Re\,\delta_1^*\,\bar{\chi}}{M_\infty^3 C}$$

and $$\bar{\chi} = \frac{M_\infty^3\sqrt{C}}{\sqrt{Re\,x}}.$$

Expansions in powers of $\overline{X}$ about the zero pressure gradient Blasius solution are assumed of the form :

$$M_{e_{WI}} = M_\infty(1 + m_1\overline{X} + m_2\overline{X}^2 + \ldots) ,$$

$$\Delta_{WI} = \delta_0(1 + \delta_1\overline{X} + \mathcal{E}_2\overline{X}^2 \text{ Log } \overline{X} + \delta_2\overline{X}^2 + \ldots) ,$$

$$a_{WI} = a_0 + a_1\overline{X} + a_2\overline{X}^2 + \ldots , \qquad \text{(B2)}$$

$$b_{WI} = b_0 + b_1\overline{X} + b_2\overline{X}^2 + \ldots .$$

Here the logarithmic term in the expansion for Δ has been found necessary because of the singular nature of a particular solution of equations B1. It may be shown (ref. 8) that :

$$\delta_2 = \frac{1}{2}\,\delta_1^2 - \mathcal{E}_2 \text{Log } \delta_0 . \qquad \text{(B3)}$$

After introducing these expressions (B2) into equations (B1) the unknown coefficients are determined by equating terms of the same power in $\overline{X}$ up to the second degree in $\overline{X}$.

The integral functions of velocity and total enthalpy profiles are found by Taylor expansions in the neighbourhood of the Blasius point (a_B and b_B). For example :

$$\mathcal{X}(a) = \mathcal{X}_B + (a - a_0)\left(\frac{\partial \mathcal{X}}{\partial a}\right)_B + \left(\frac{a - a_0}{2!}\right)^2 \left(\frac{\partial^2 \mathcal{X}}{\partial a^2}\right)_B + \ldots ,$$

or

$$\mathcal{X}(a) = \mathcal{X}_B + a_1\left(\frac{d\mathcal{X}}{da}\right)_B \overline{X} + a_2\left(\frac{d\mathcal{X}}{da}\right)_B \overline{X}^2 + \frac{a_1^2}{2}\left(\frac{d^2\mathcal{X}}{da^2}\right)_B X^2 + \ldots ,$$

(B4)

and for T(a,b) :

$$T(a,b) = T_B + \left[a_1 \left(\frac{\partial T}{\partial a}\right)_B + b_1 \left(\frac{\partial T}{\partial b}\right)_B \right] \bar{\chi} + \left[a_2 \left(\frac{\partial T}{\partial a}\right)_B + b_2 \left(\frac{\partial T}{\partial b}\right)_B + \ldots \right.$$

$$\left. \ldots + \frac{a_1^2}{2} \left(\frac{\partial^2 T}{\partial a^2}\right)_B + \frac{b_1^2}{2} \left(\frac{\partial^2 T}{\partial b^2}\right)_B + a_1 b_1 \left(\frac{\partial^2 T}{\partial a \partial b}\right)_B \right] \bar{\chi}^2 .$$

(B4 cont'd)

Derivatives of the first order ($\frac{d\mathcal{X}}{da}$, $\frac{\partial T}{\partial a}$, $\frac{\partial T}{\partial b}$, etc.) are directly available using the polynomial expressions resulting from the curve-fits of the similar solutions, (see section 2-5), whilst derivatives of the second order such as $\frac{d^2\mathcal{X}}{da^2}$, $\frac{\partial^2 T}{\partial a^2}$, $\frac{\partial^2 T}{\partial b^2}$ are obtained by differentiation of the polynomial expression of the first order derivatives.

The following expressions for the coefficients in the coordinate expansions of equations (B2) are found :

<u>0^{th} degree in $\bar{\chi}$ coefficients</u> :

$$(\mathcal{X}R)_B = (PJ)_B \quad , \tag{B5}$$

$$\delta_0 = \left(2\frac{P_B}{\mathcal{X}_B}\right)^{1/2} \quad , \tag{B6}$$

$$b_0 = Pr_w \, \alpha_B \frac{P_B}{\mathcal{X}_B} T_B^* \quad . \tag{B7}$$

Since $\mathcal{X}$, R, P, J are polynomial functions of a, the value of a_0 may be found from (B5) using an iteration procedure.

<u>1^{st} degree in $\bar{\chi}$ coefficients</u> :

$$m_1 = \frac{-(\gamma-1)(1+m_\infty)}{4M_\infty\sqrt{M_\infty^2-1}}\left[m_{11} + \left(\frac{1+m_\infty}{m_\infty}\right)m_{12}\right] \quad , \tag{B8}$$

with $\quad m_{11} = \mathcal{K}_B\delta_0 \quad ,$

$$m_{12} = (1 - E)_B\ \delta_0 \ .$$

$$\delta_1 = (d_{11} - K_1)m_1 \ , \tag{B9}$$

with
$$d_{11} = \frac{\left[\left(\frac{dR}{da}\right)_B (\mathcal{K} + 1 - E)_B - 2\left(\frac{dP}{da}\right)_B (J - T^*)_B\right]}{\left[\mathcal{K}_B\left(\frac{dR}{da}\right)_B - J_B\left(\frac{dP}{da}\right)_B\right]} \quad ,$$

$$K_1 = \frac{3\gamma - 1}{\gamma - 1}\left(\frac{m_\infty}{1 + m_\infty}\right) \quad .$$

$$a_1 = a_{11}m_1 \quad , \tag{B10}$$

with
$$a_{11} = \frac{\delta_0^2}{2}\ \frac{\left[J_B(1 - E - \mathcal{K})_B + 2\mathcal{K}_B T^*_B\right]}{\left[\mathcal{K}_B\left(\frac{dR}{da}\right)_B - J_B\left(\frac{dP}{da}\right)_B\right]} \quad .$$

$$b_1 = b_{11}m_1 \quad , \tag{B11}$$

with
$$b_{11} = b_0\left[\frac{\left(\frac{d\alpha}{da}\right)_B}{\alpha_B}\, a_{11} + d_{11}\right] \quad .$$

<u>2^{nd} degree in $\bar{\chi}$ coefficients</u> :

$$m_2 = \left[\frac{\sqrt{M_\infty^2 - 1}}{M_\infty^3}\, m_{21}\right]m_1 + \left[\frac{m_\infty}{1 + m_\infty} - \frac{1}{2(M_\infty^2 - 1)}\right]m_1^2 \quad , \tag{B12}$$

with $m_{21} = \frac{\delta_0 Z_B}{2}$

$$a_2 = (a_{21} + K_1 a_{22}) m_1^2 + (a_{11} - a_{22}) m_2 \qquad \text{(B13)}$$

where a_{21} and a_{22} are given by the following relations :

$$a_{21} = \left[1 - \frac{(2\hat{B} + \hat{C})}{(\hat{B} - \hat{C})}\right] a_{11} d_{11} + \left[\frac{\hat{E}}{(\hat{B} - \hat{C})} + \frac{\hat{D}\, a_{11}}{2(\hat{B} - \hat{C})}\right] a_{11} + \frac{\hat{F}\, b_{11}}{(\hat{B} - \hat{C})}$$

$$a_{22} = - \frac{\hat{A}}{\hat{C}} \frac{(\hat{B} + \hat{C})}{(\hat{B} - \hat{C})}$$

where :

$$\hat{A} = J_B \left[\mathcal{X}_B - (1 - E)_B\right] - 2\mathcal{X}_B T^*_B \quad ,$$

$$\hat{B} = J_B \left(\frac{d\mathcal{X}}{da}\right)_B - \mathcal{X}_B \left(\frac{dJ}{da}\right)_B \quad ,$$

$$\hat{C} = \frac{2}{\delta_0^2} \left[\mathcal{X}_B \left(\frac{dR}{da}\right)_B - J_B \left(\frac{dP}{da}\right)_B\right]$$

$$\hat{D} = \left[\mathcal{X}_B \left(\frac{d^2 J}{da^2}\right)_B - J_B \left(\frac{d^2 \mathcal{X}}{da^2}\right)_B\right] + \frac{2}{\delta_0^2} \left[\mathcal{X}_B \left(\frac{d^2 R}{da^2}\right)_B - J_B \left(\frac{d^2 P}{da^2}\right)_B\right]$$

$$\hat{E} = \mathcal{X}_B \frac{\partial}{\partial a} (3J - 2T^*)_B - J_B \frac{\partial}{\partial a} (2\mathcal{X} + 1 - E)_B$$

$$\hat{F} = J_B \alpha_B \left(\frac{d\sigma}{db}\right)_B - 2\mathcal{X}_B \alpha_B \left(\frac{\partial T}{\partial b}\right)_B$$

$$\mathcal{E}_2 = (d_{21} + K_1 d_{22} + K_2) m_1^2 + (K_1 - d_{22}) m_2 \quad , \tag{B14}$$

with :

$$K_2 = \frac{3\gamma-1}{2(\gamma-1)} \left(\frac{m_\infty}{1+m_\infty}\right) \left[1 - \frac{5\gamma-3}{\gamma-1} \frac{m_\infty}{1+m_\infty}\right] ,$$

$$d_{22} = \frac{1}{\mathcal{X}_B} \left\{ \left[\left(\frac{d\mathcal{X}}{da}\right)_B + \frac{\mathcal{X}_B}{P_B} \left(\frac{dP}{da}\right)_B \right] (a_{11} - a_{22}) + 2(2\mathcal{X}_B + 1 - \alpha_B \sigma_B) \right\} - 1 ,$$

$$d_{21} = -\frac{1}{\mathcal{X}_B} \left[\left(\frac{d\mathcal{X}}{da}\right)_B + \frac{\mathcal{X}_B}{P_B} \left(\frac{dP}{da}\right)_B \right] a_{21} + \left\{ -\frac{1}{\mathcal{X}_B} \left[\left(\frac{d\mathcal{X}}{da}\right)_B a_{11} + 2(2\mathcal{X}_B + 1 - \alpha_B \sigma_B \right] + 1 \right\} d_{11}$$

$$- \frac{1}{\mathcal{X}_B} \left\{ \left[\left(\frac{d^2\mathcal{X}}{da^2}\right)_B + \frac{\mathcal{X}_B}{P_B} \left(\frac{d^2P}{da^2}\right)_B \right] \frac{a_{11}}{2} + \left[2\left(\frac{d\mathcal{X}}{da}\right)_B - \sigma_B \left(\frac{d\alpha}{da}\right)_B \right] \right\} a_{11} + \frac{1}{\mathcal{X}_B} \alpha_B \left(\frac{d\sigma}{db}\right)_B b_{11} .$$

$$\delta_2 = \frac{1}{2} \delta_1^2 - \mathcal{E}_2 \operatorname{Log} \delta_0 \quad . \tag{B15}$$

Finally,

$$b_2 = (b_{21} + K_1 b_{22}) m_1^2 + (b_{11} - b_{22}) m_2 \quad , \tag{B16}$$

with

$$b_{22} = - \left\{ \frac{\alpha_B T_B^*(d_{22} - d_{11} - 1) + \alpha_B \left(\frac{\partial T^*}{\partial a}\right)_B (a_{22} - a_{11}) - \alpha_B \left(\frac{\partial T^*}{\partial b}\right)_B b_{11} - T_B^* \left(\frac{d\alpha}{da}\right)_B a_{22}}{\alpha_B \left(\frac{\partial T^*}{\partial b}\right)_B + \frac{2}{\delta_0^2 \, Pr_w}} \right\} ,$$

$$
\begin{aligned}
b_{21} = T_B^* \Bigg\{ & \alpha_B(d_{21}+d_{11}) - \left(\frac{d\alpha}{da}\right)_B (a_{11}d_{11}+a_{21}) - \left(\frac{d^2\alpha}{da^2}\right)_B \frac{a_{11}^2}{2} \Bigg\} \\
& + \alpha_B \left\{ \left(\frac{\partial T^*}{\partial a}\right)_B a_{21} + \left[\left(\frac{\partial T^*}{\partial a}\right)_B a_{11} + \left(\frac{\partial T^*}{\partial b}\right)_B b_{11} \right] (1+d_{11}) \right\} \\
& + \alpha_B \left\{ \left(\frac{\partial^2 T^*}{\partial a^2}\right)_B \frac{a_{11}^2}{2} + \left(\frac{\partial^2 T^*}{\partial b^2}\right)_B \frac{b_{11}^2}{2} + \left(\frac{\partial^2 T^*}{\partial a \partial b}\right)_B a_{11}b_{11} \right\} \\
& \Big/ - \left[\alpha_B \left(\frac{\partial T^*}{\partial b}\right)_B + \frac{\mathcal{K}_B}{P_B \, Pr_w} \right] .
\end{aligned}
$$

Numerical values of the coefficients given by equations B5 to B16 are given in Appendix A for each value of S_w investigated.

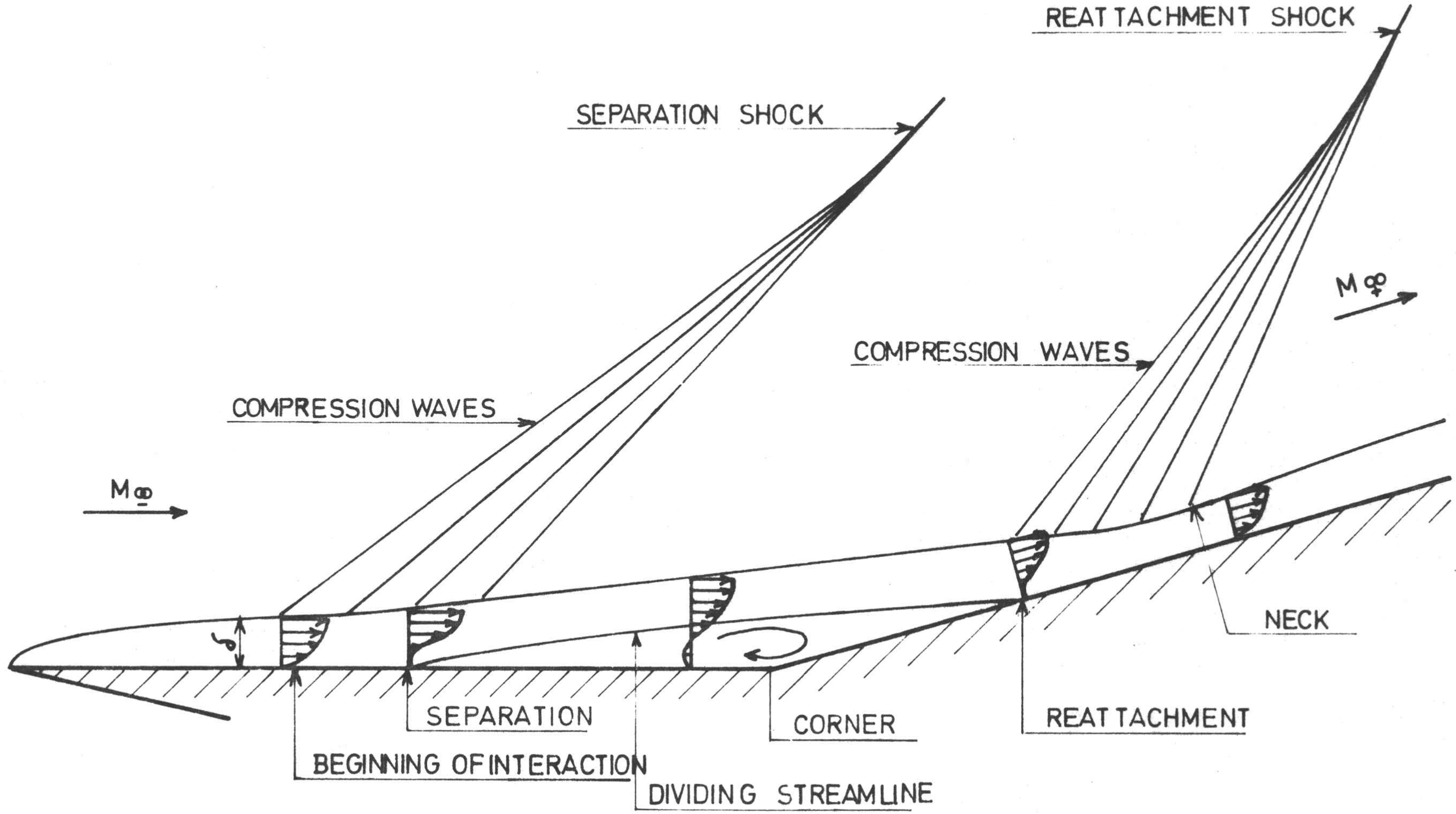

FIG:1 SCHEMATIC REPRESENTATION OF SHOCK-WAVE-LAMINAR BOUNDARY LAYER INTERACTION

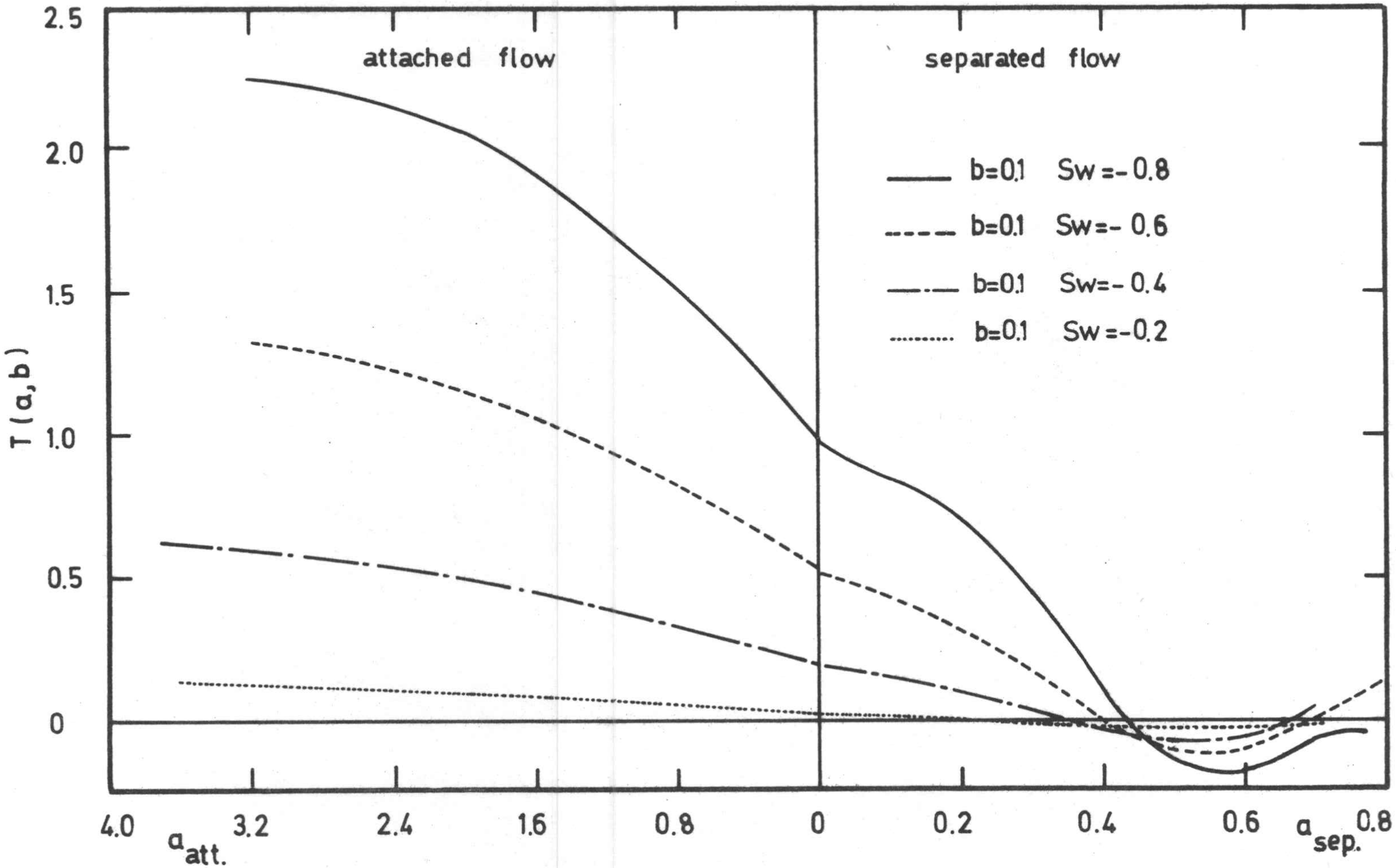

FIG: 2 FUNCTION T(a, b) DISTRIBUTION FOR VARIOUS WALL COOLING RATIOS

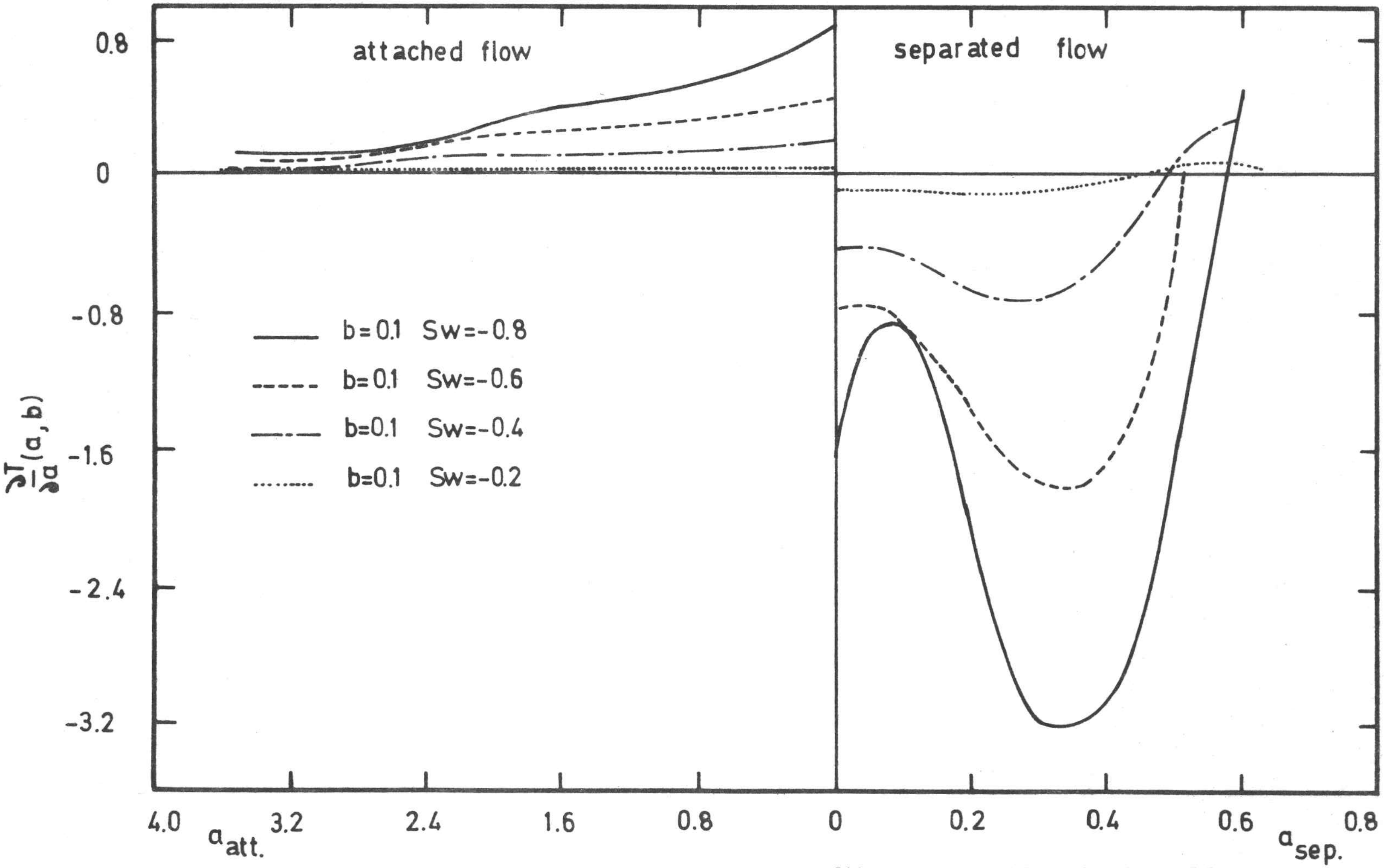

FIG:3 FUNCTION $\partial T/\partial a(a,b)$ DISTRIBUTION FOR VARIOUS WALL COOLING RATIOS

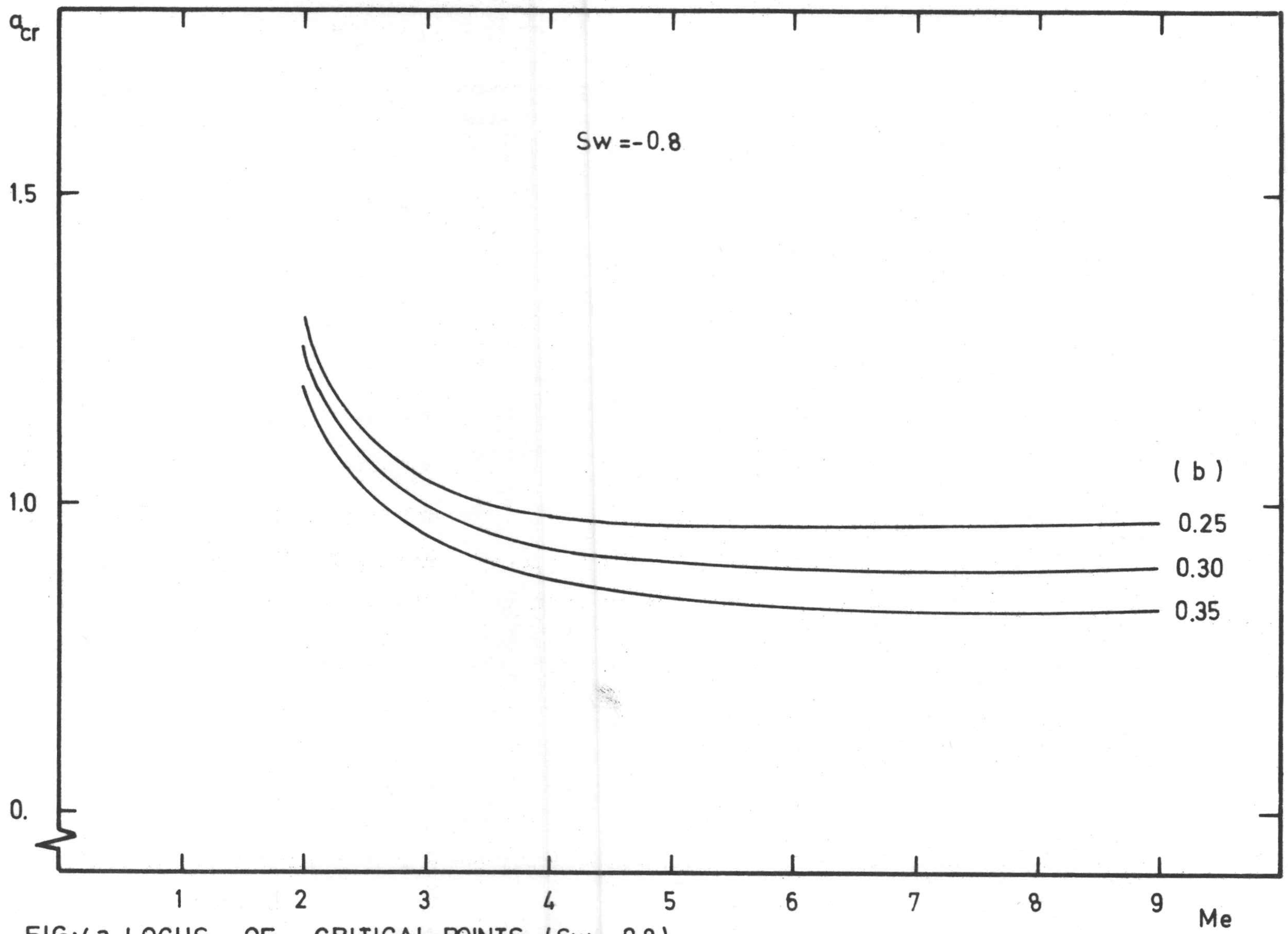

FIG:4a LOCUS OF CRITICAL POINTS (Sw=-0.8)

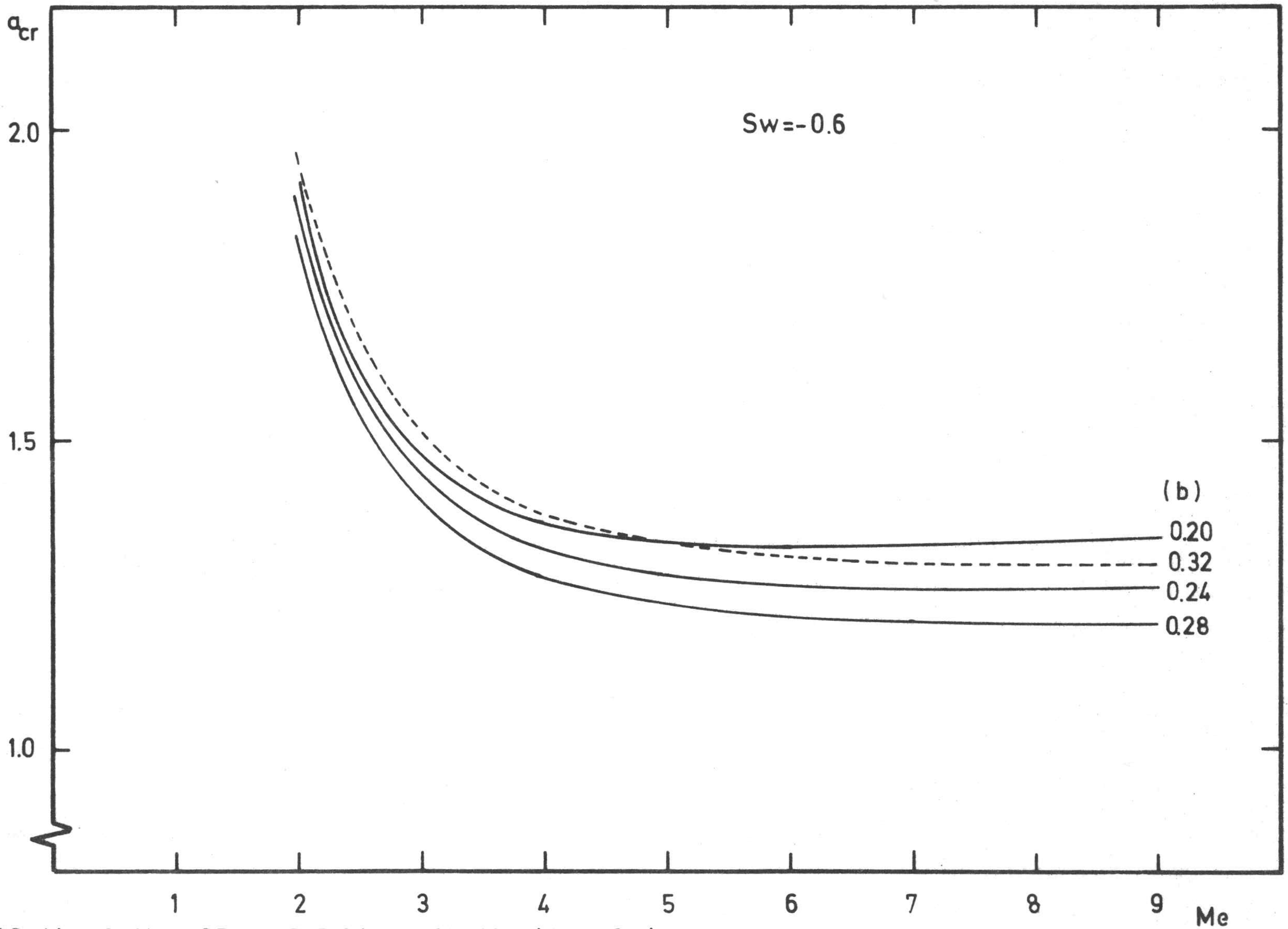

FIG:4b LOCUS OF CRITICAL POINTS (Sw=-0.6)

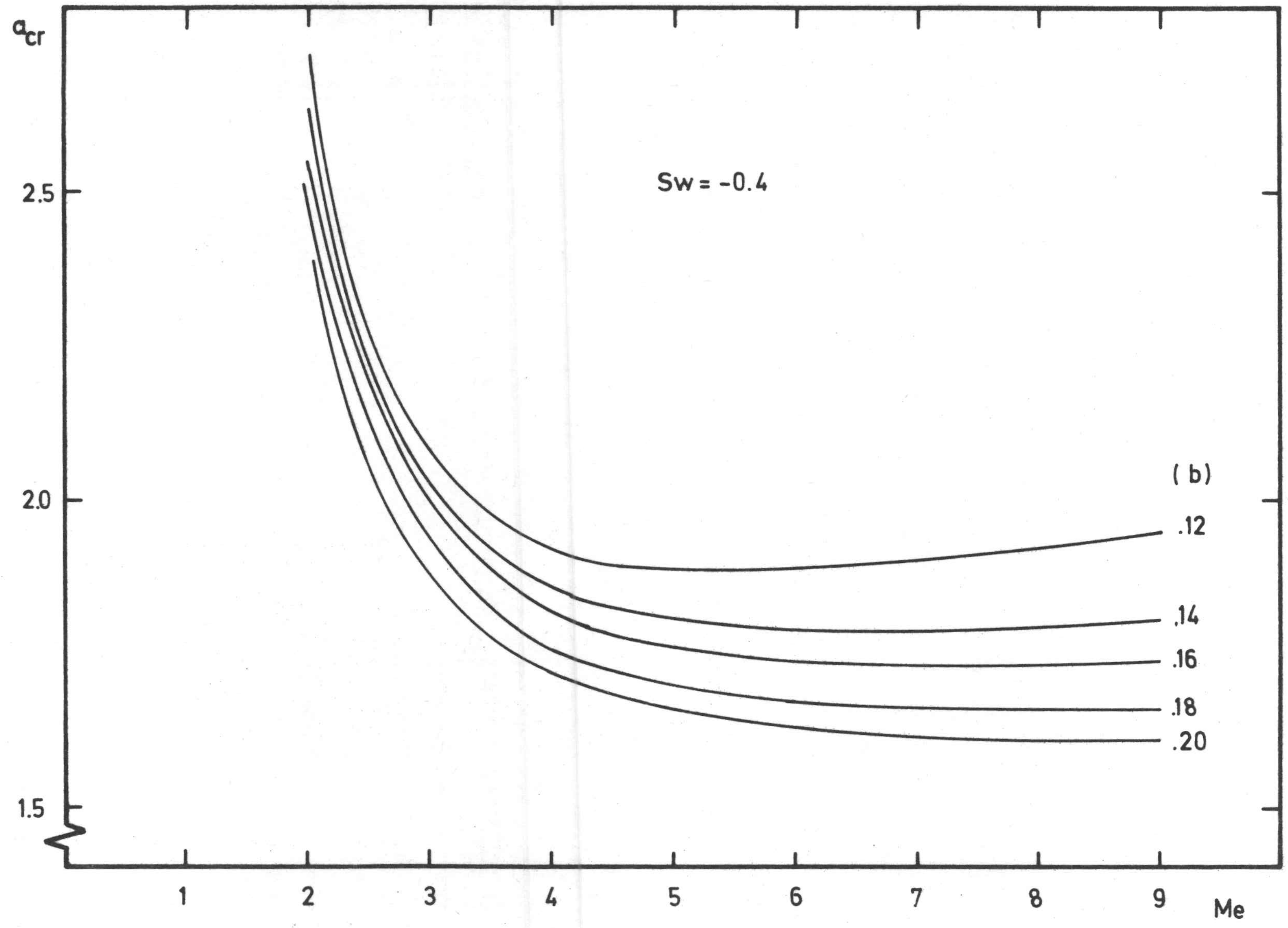

FIG:4c LOCUS OF CRITICAL POINTS (Sw = -0.4)

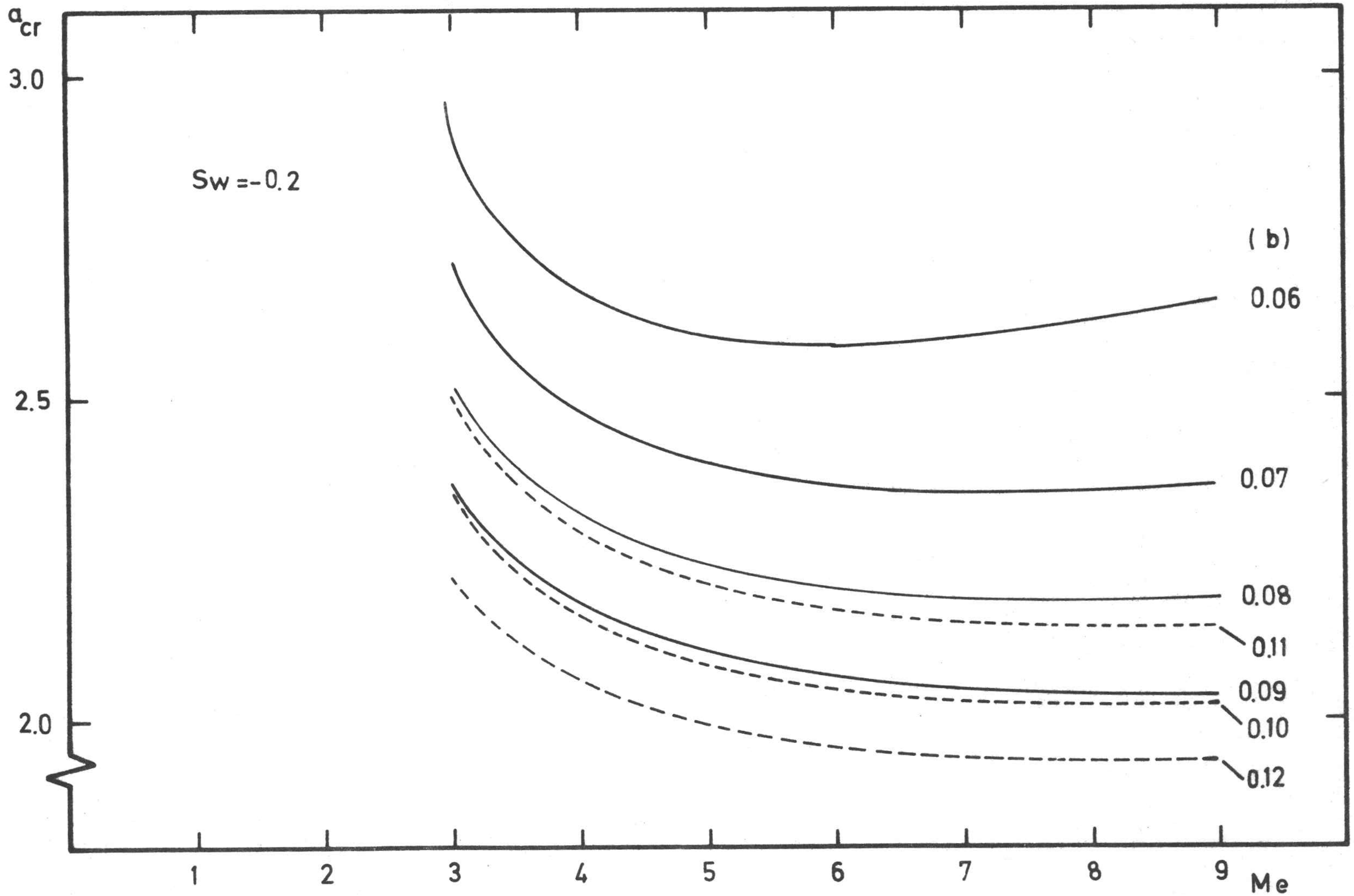

FIG:4d LOCUS OF CRITICAL POINTS (Sw=-0.2)

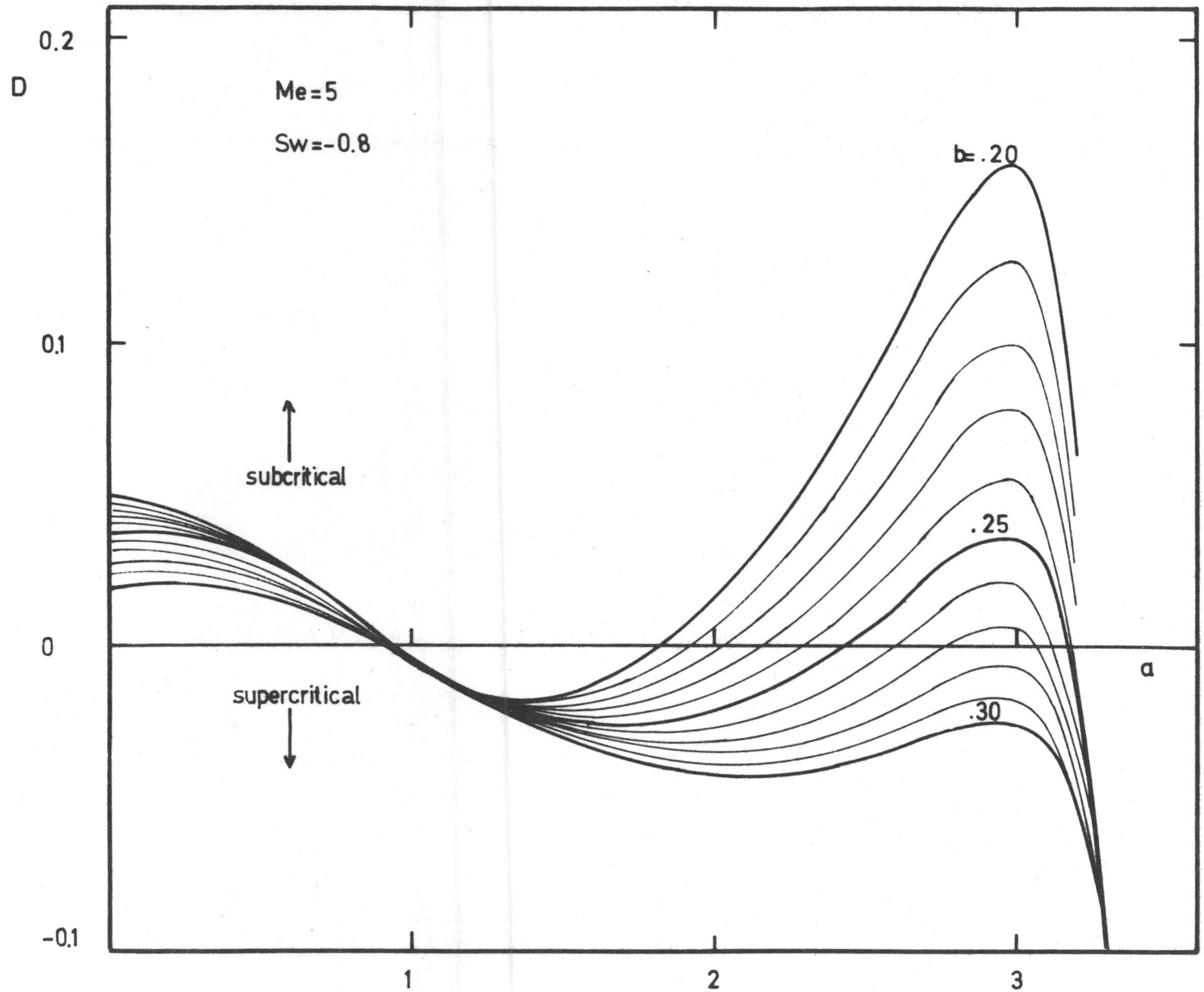

FIG: 5 TYPICAL TRAJECTORIES OF FUNCTION D(Me,a,b)

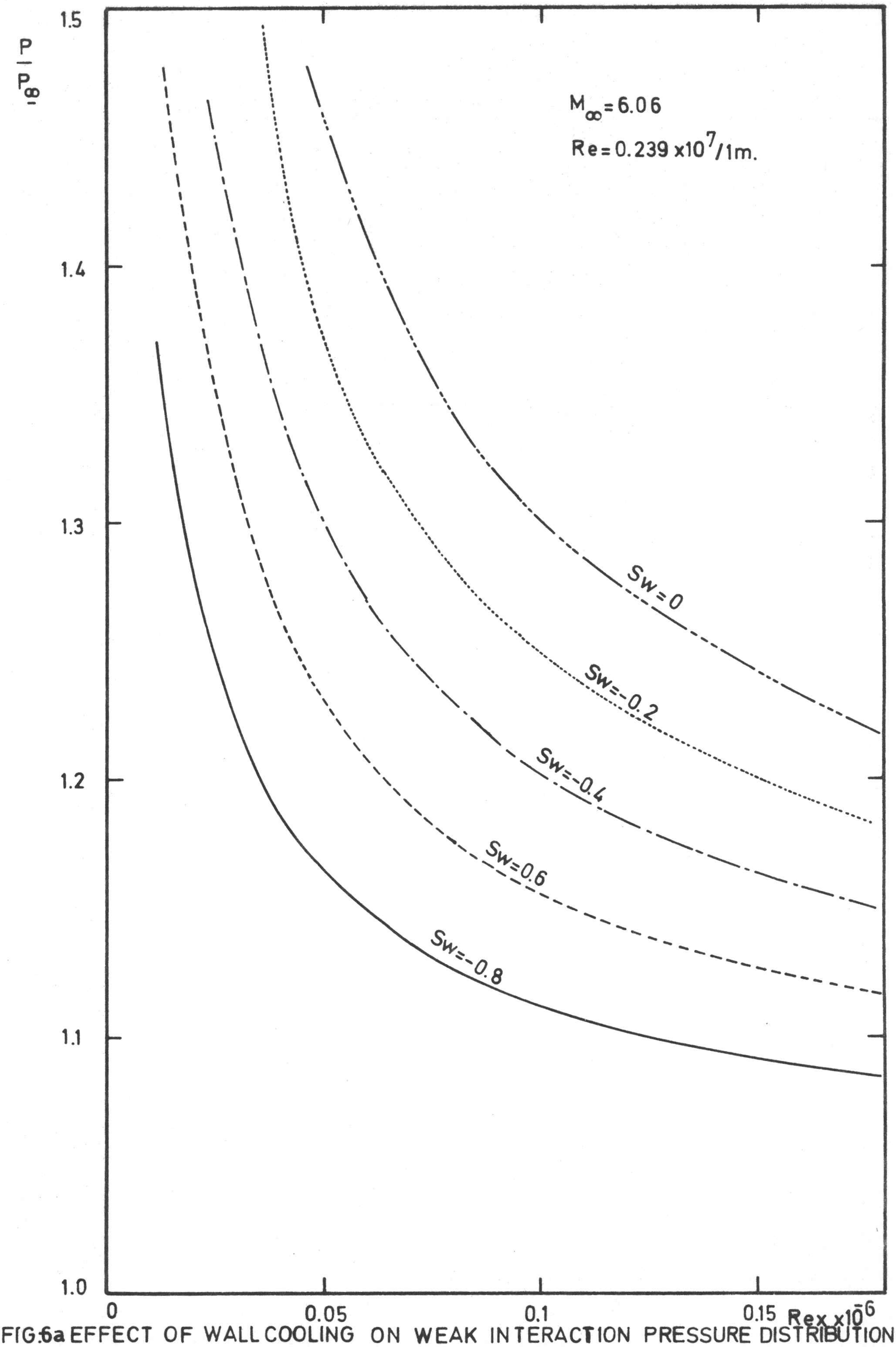

FIG:6a EFFECT OF WALL COOLING ON WEAK INTERACTION PRESSURE DISTRIBUTION

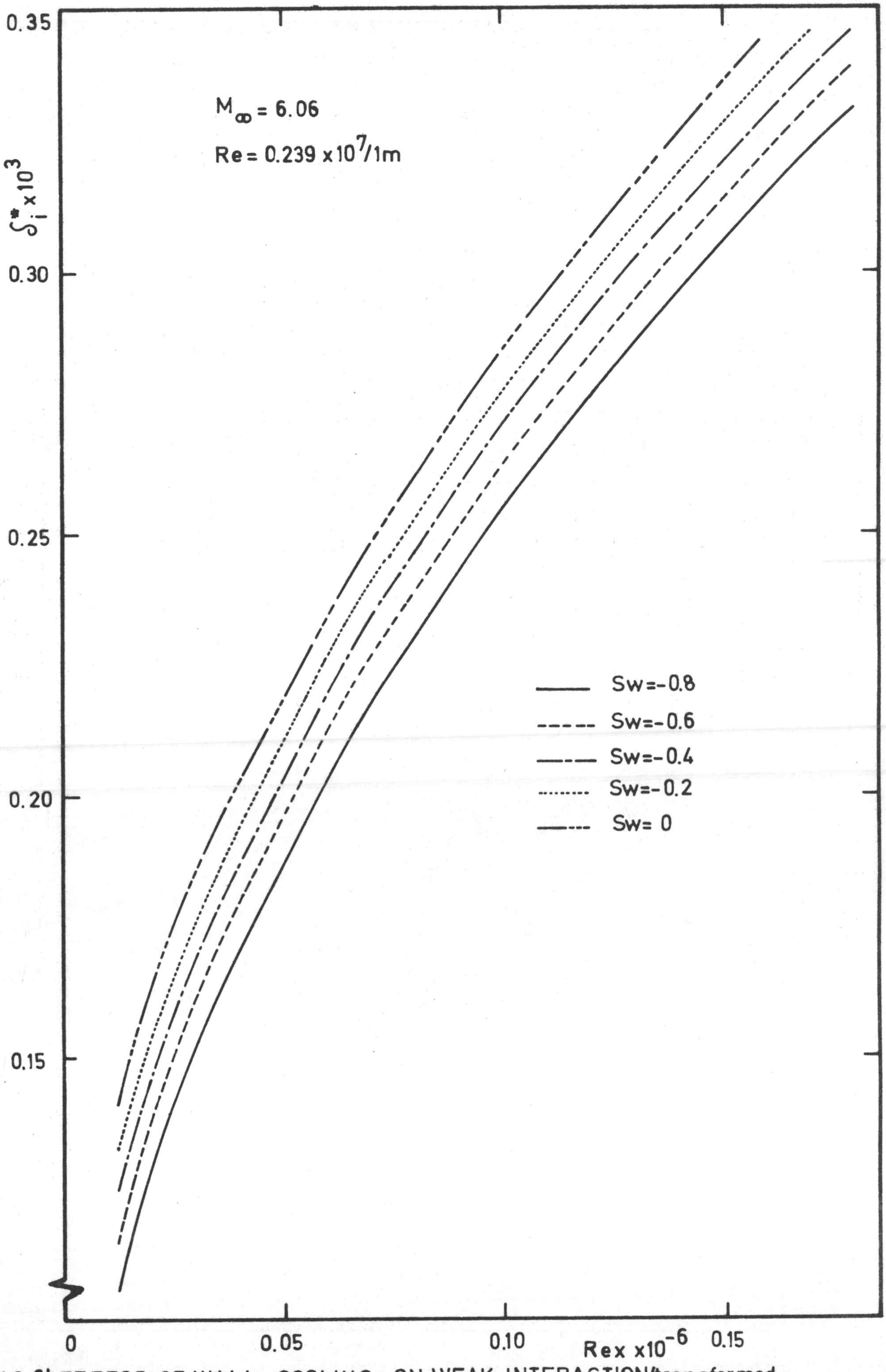

FIG:6b EFFECT OF WALL COOLING ON WEAK INTERACTION(transformed-displacement thickness)

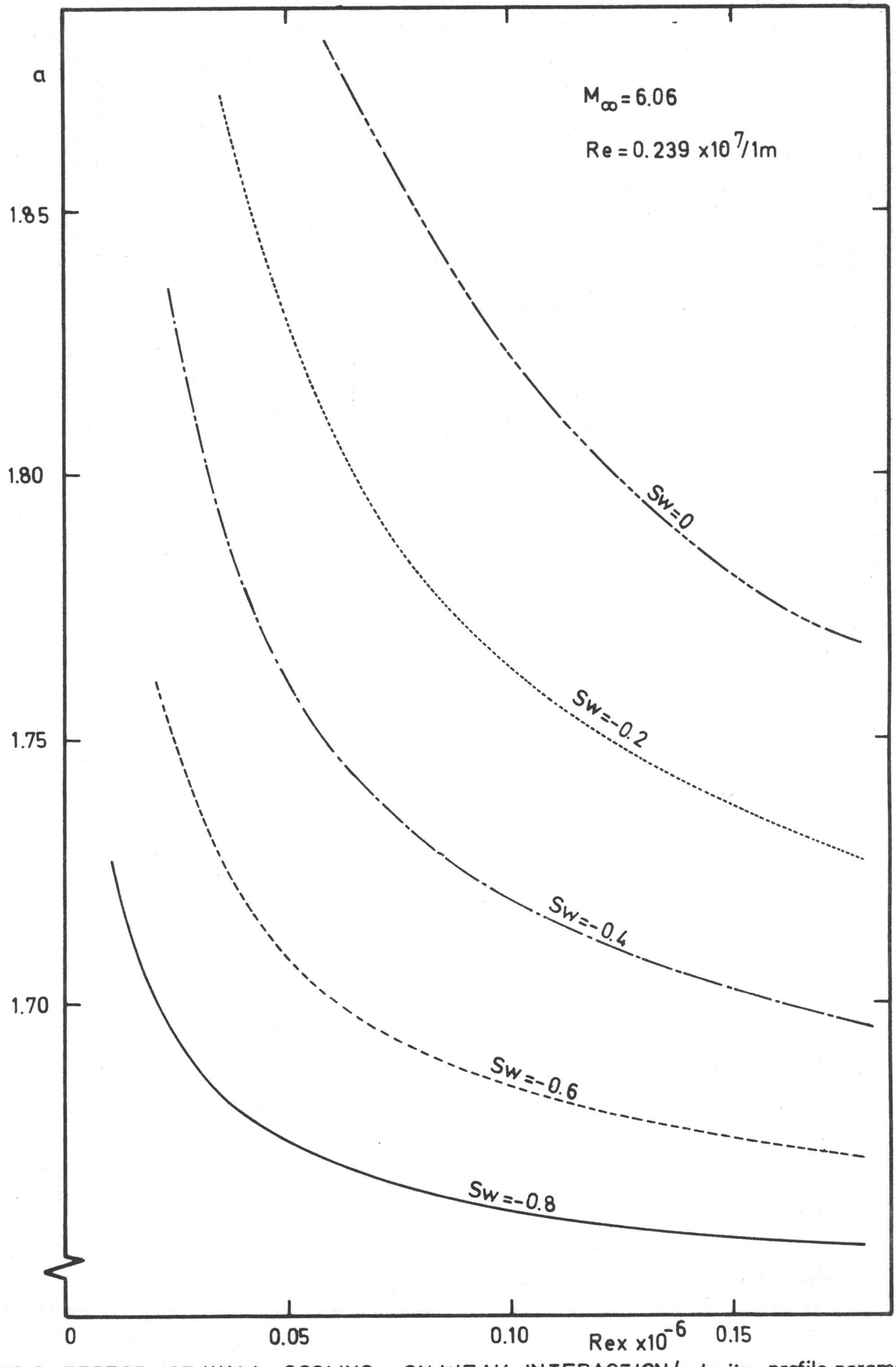

FIG:6c EFFECT OF WALL COOLING ON WEAK INTERACTION (velocity profile parameter)

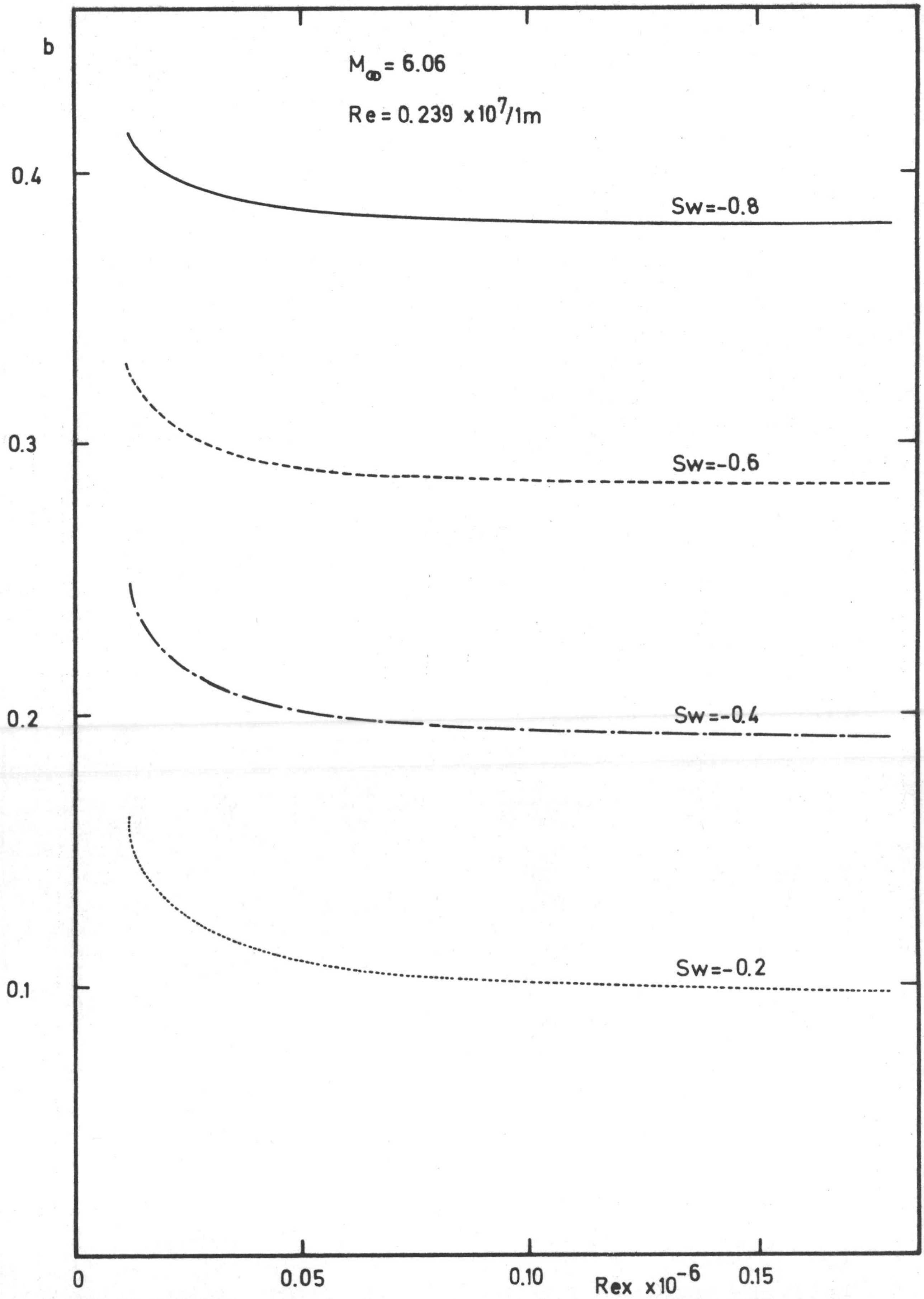

FIG:6d EFFECT OF WALL COOLING ON WEAK INTERACTION (total enthalpy parameter)

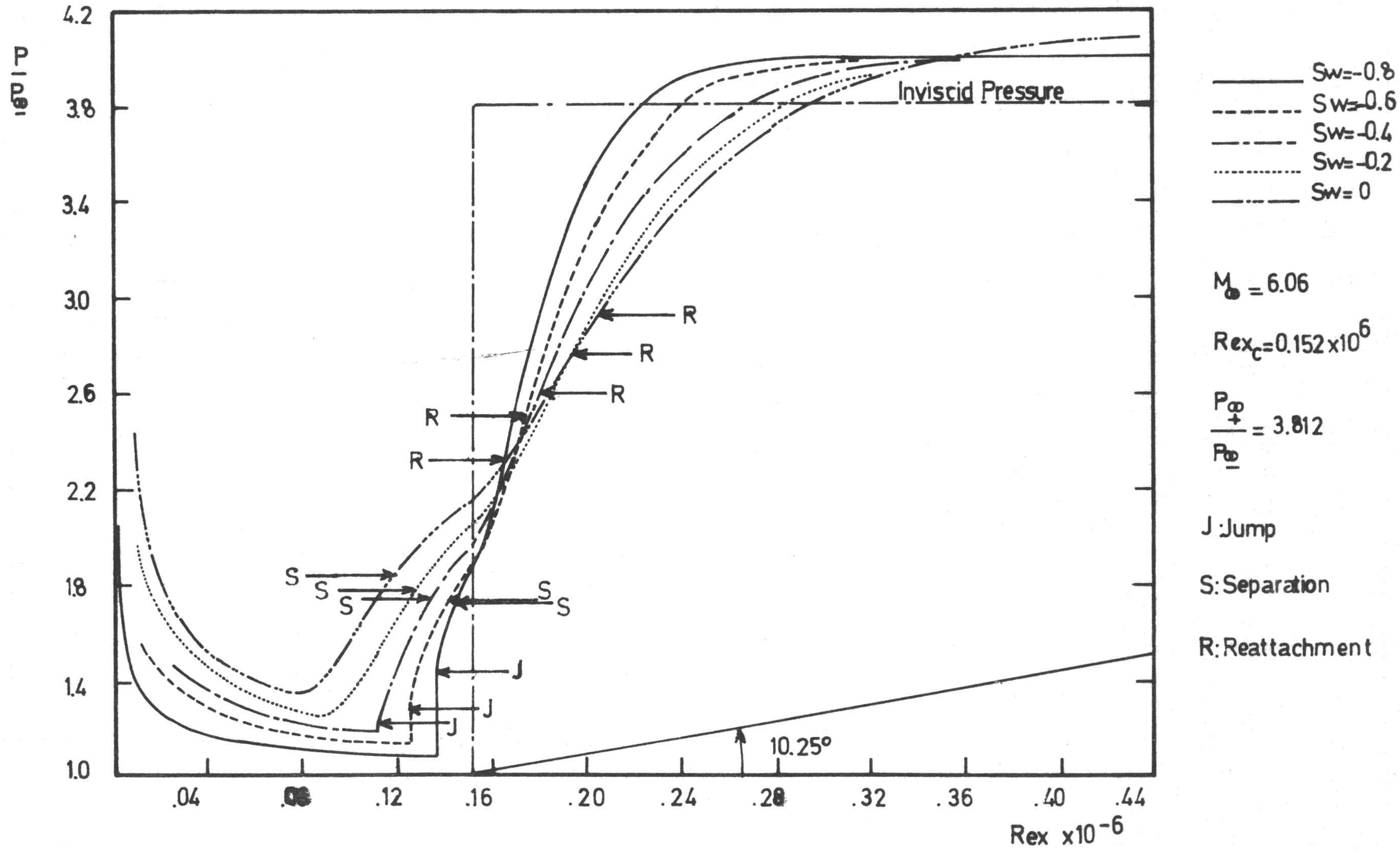

FIG: 7a EFFECT OF SURFACE COOLING ON PRESSURE DISTRIBUTION

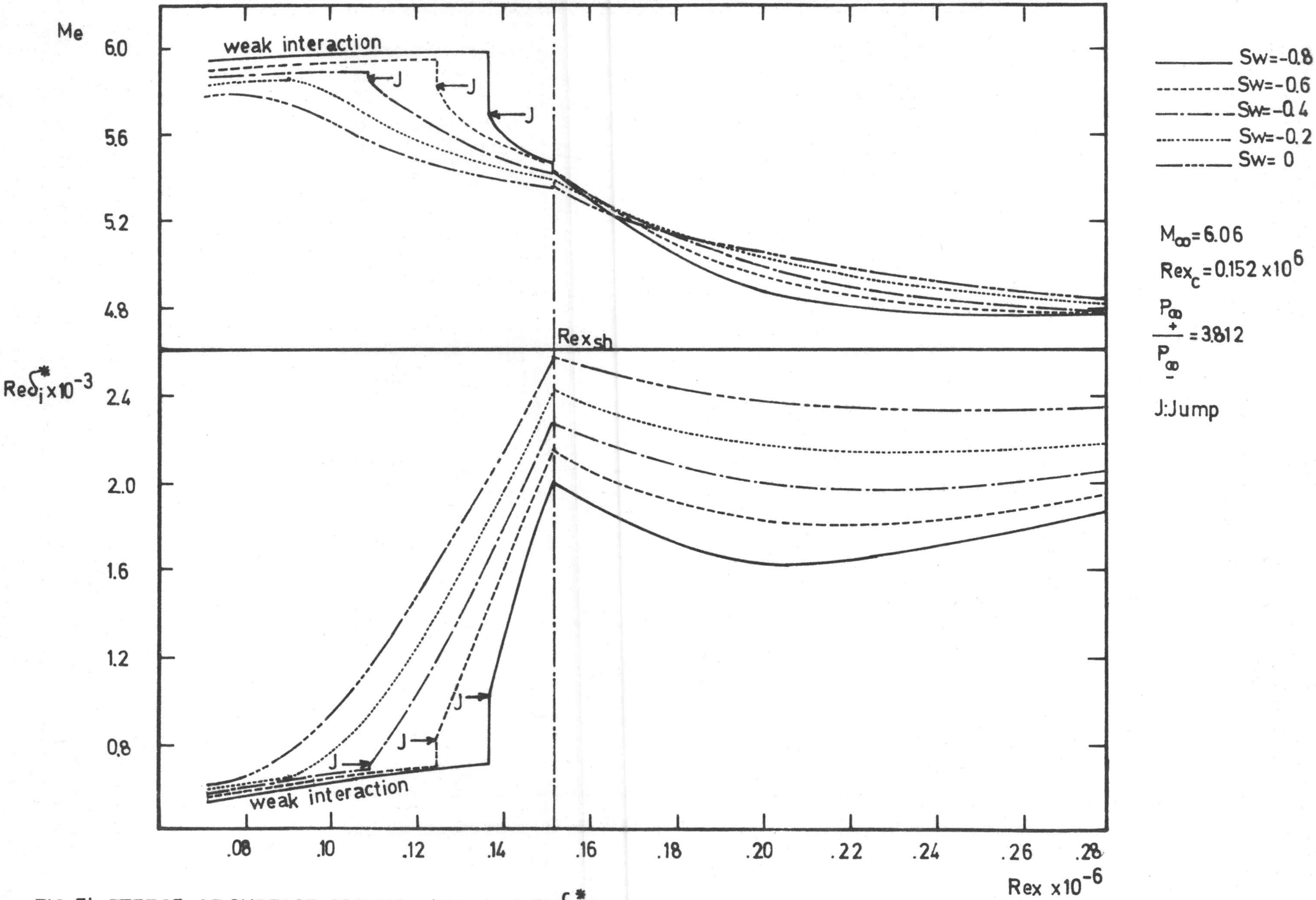

FIG: 7b EFFECT OF SURFACE COOLING (Me and Reδ_i^*)

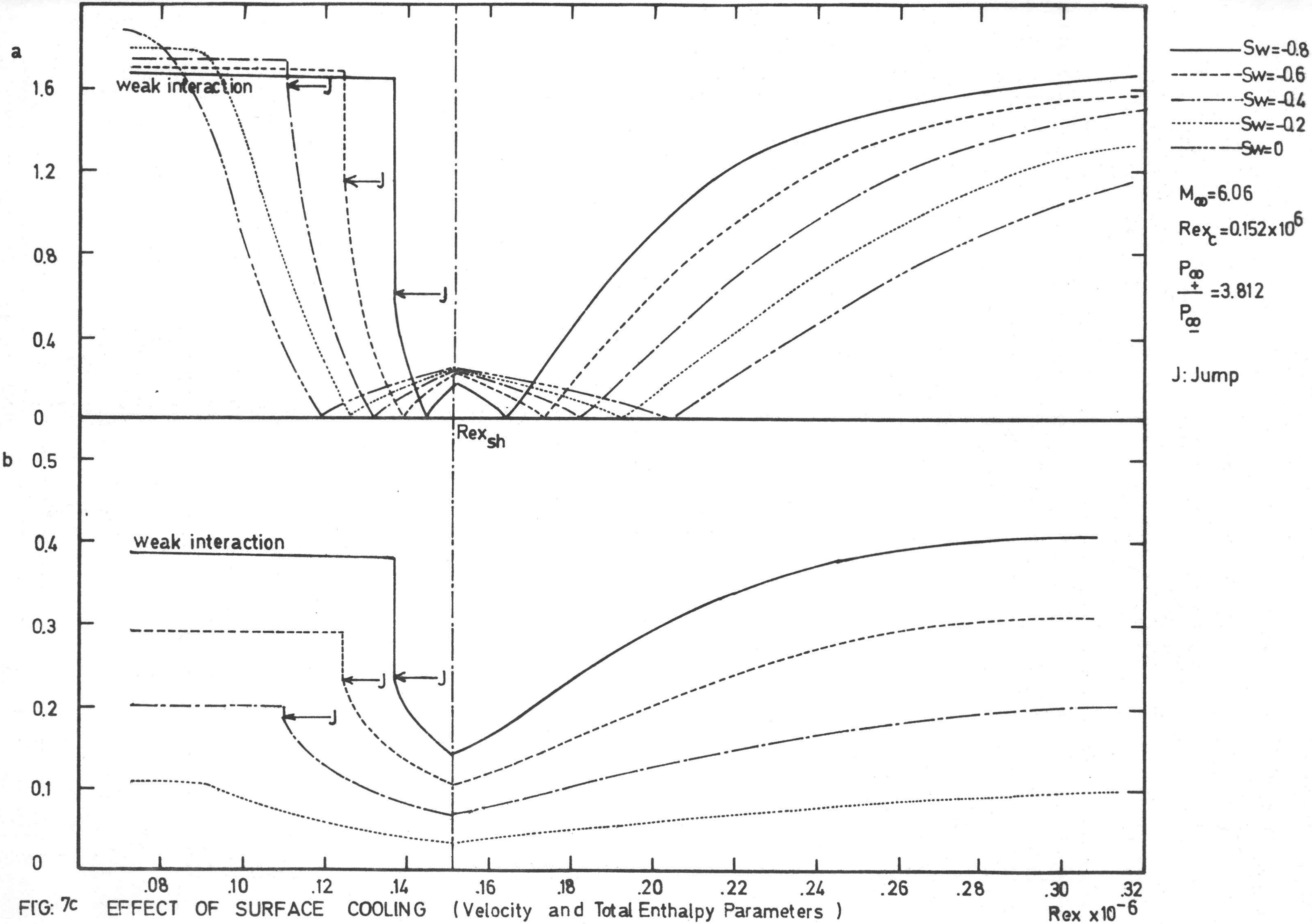

FIG: 7c EFFECT OF SURFACE COOLING (Velocity and Total Enthalpy Parameters)

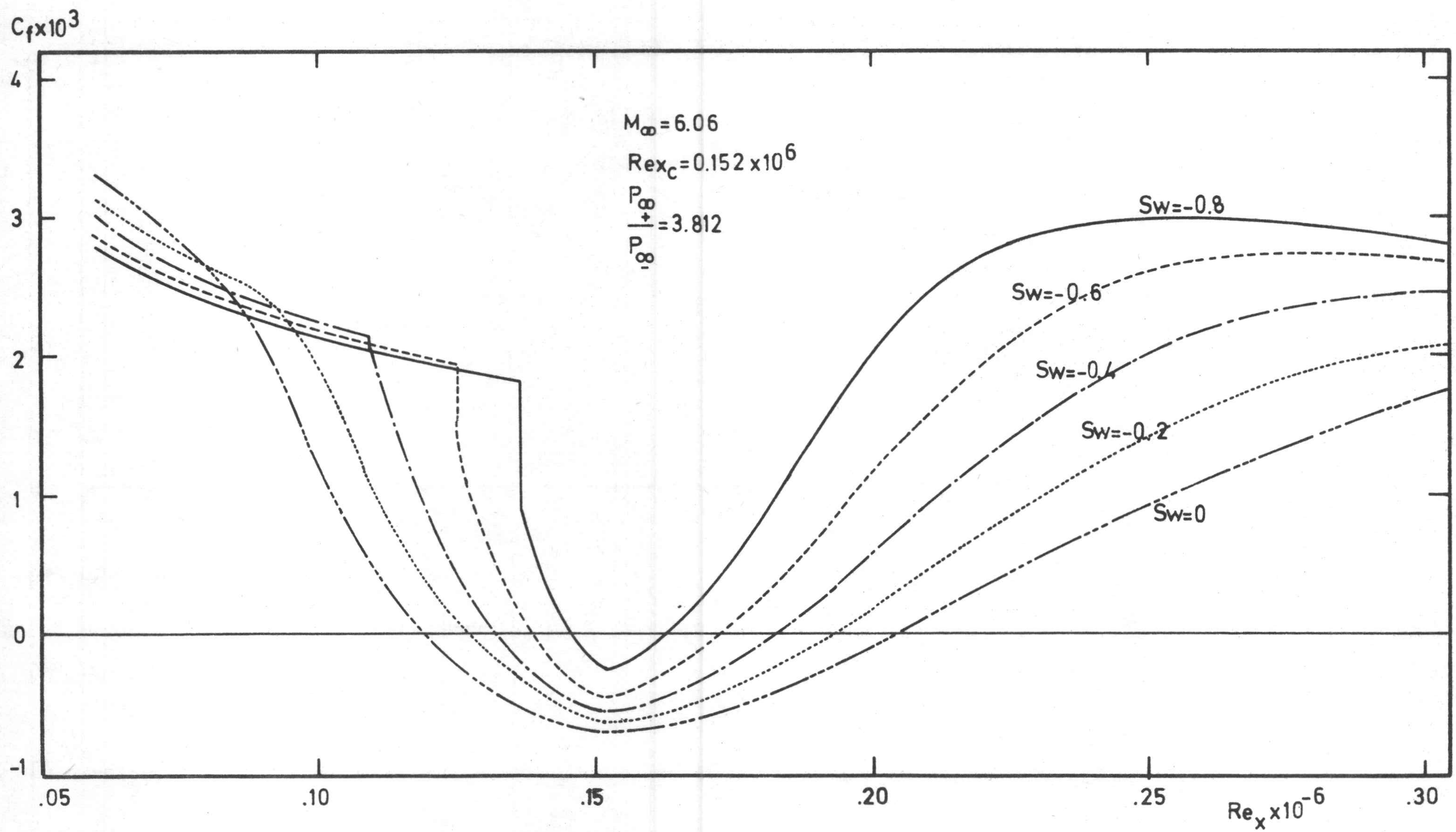

FIG:7d EFFECT OF SURFACE COOLING ON SKIN-FRICTION DISTRIBUTION

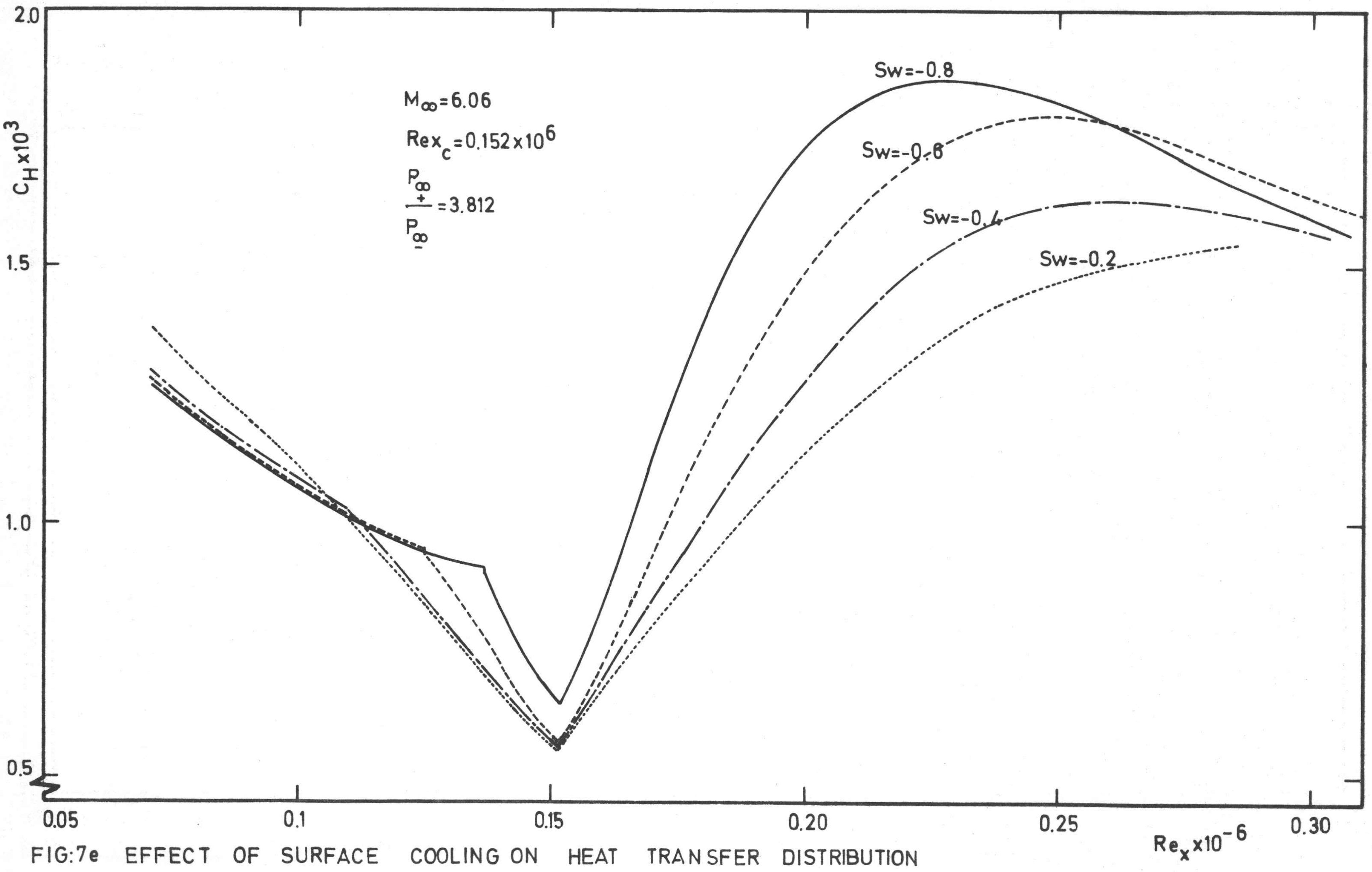

FIG:7e EFFECT OF SURFACE COOLING ON HEAT TRANSFER DISTRIBUTION

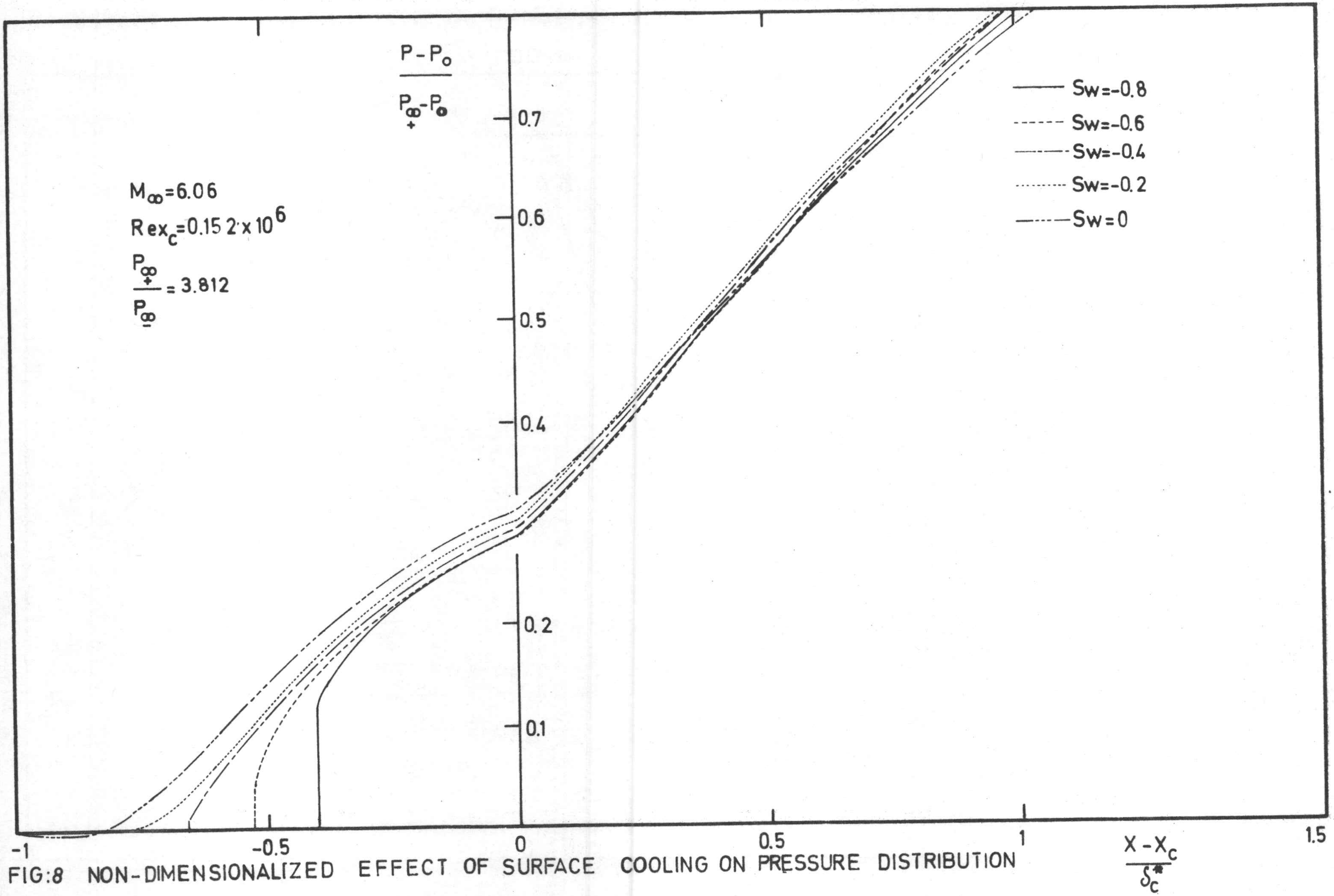

FIG:8 NON-DIMENSIONALIZED EFFECT OF SURFACE COOLING ON PRESSURE DISTRIBUTION

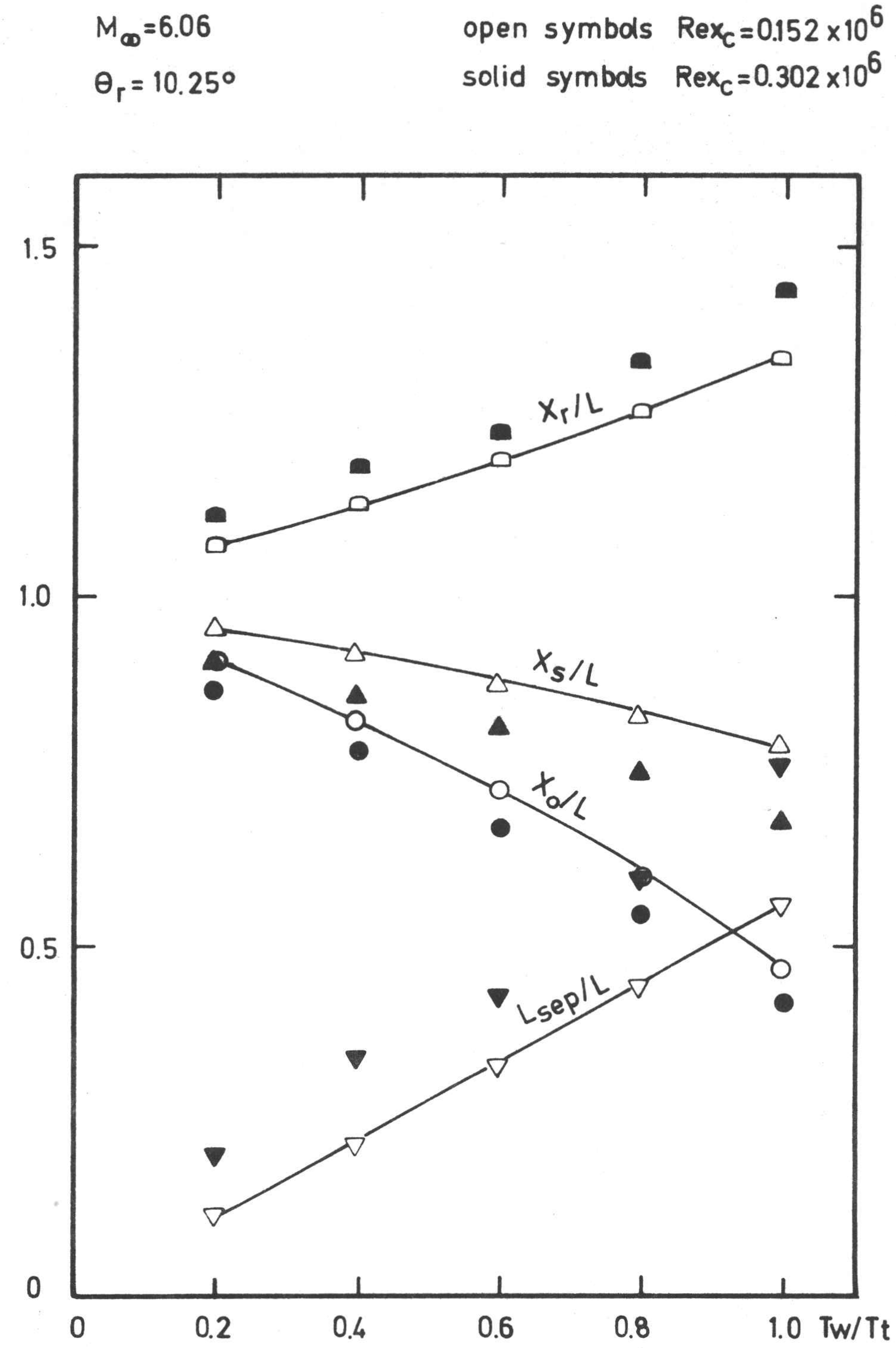

FIG.9a EFFECT OF WALL-TO-STAGNATION TEMPERATURE RATIO ON CHARACTERISTIC LENGTHS OF LAMINAR INTERACTION

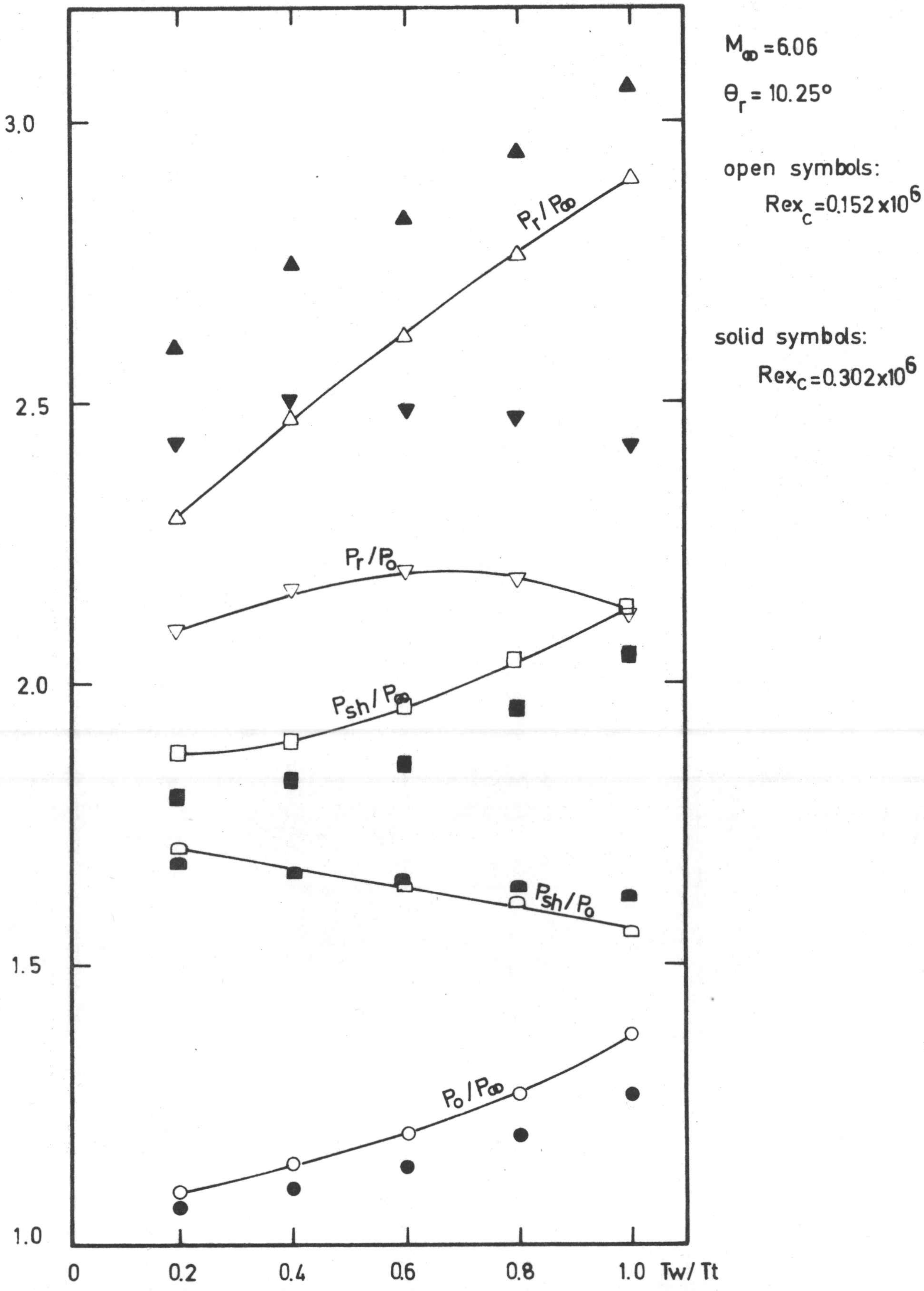

FIG:9b EFFECT OF WALL-TO-STAGNATION TEMPERATURE RATIO ON CHARACTERISTIC PRESSURES OF LAMINAR INTERACTION

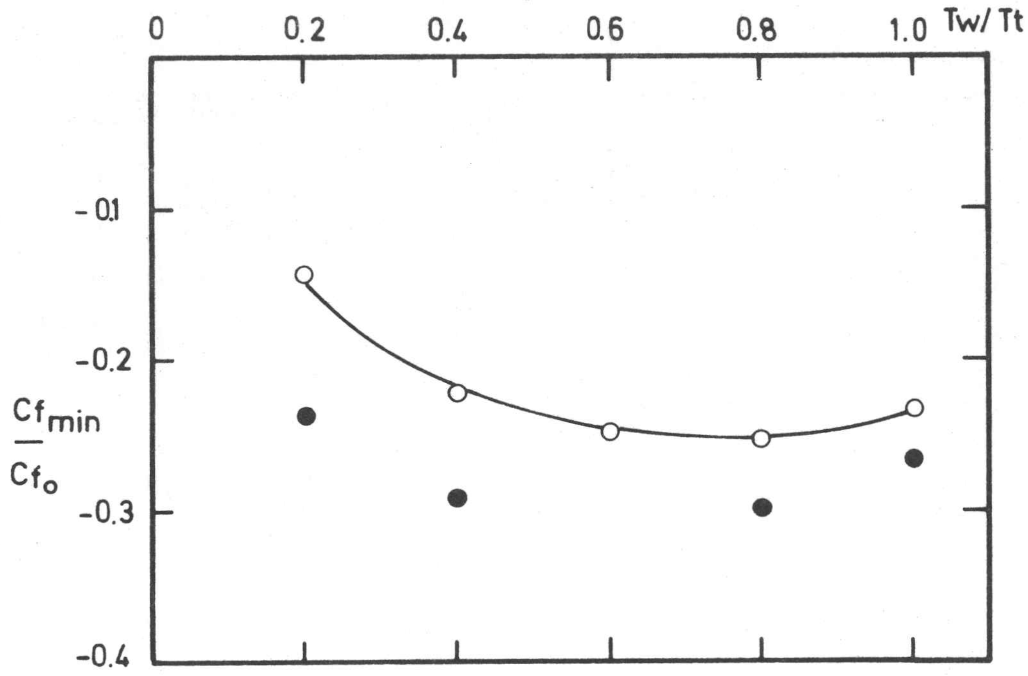

FIG:9c EFFECT OF WALL-TO-STAGNATION TEMPERATURE RATIO ON MINIMUM SKIN-FRICTION

$M_\infty = 6.06$

$\theta_r = 10.25°$

open symbols:
$Re_{x_c} = 0.152 \times 10^6$

solid symbols:
$Re_{x_c} = 0.302 \times 10^6$

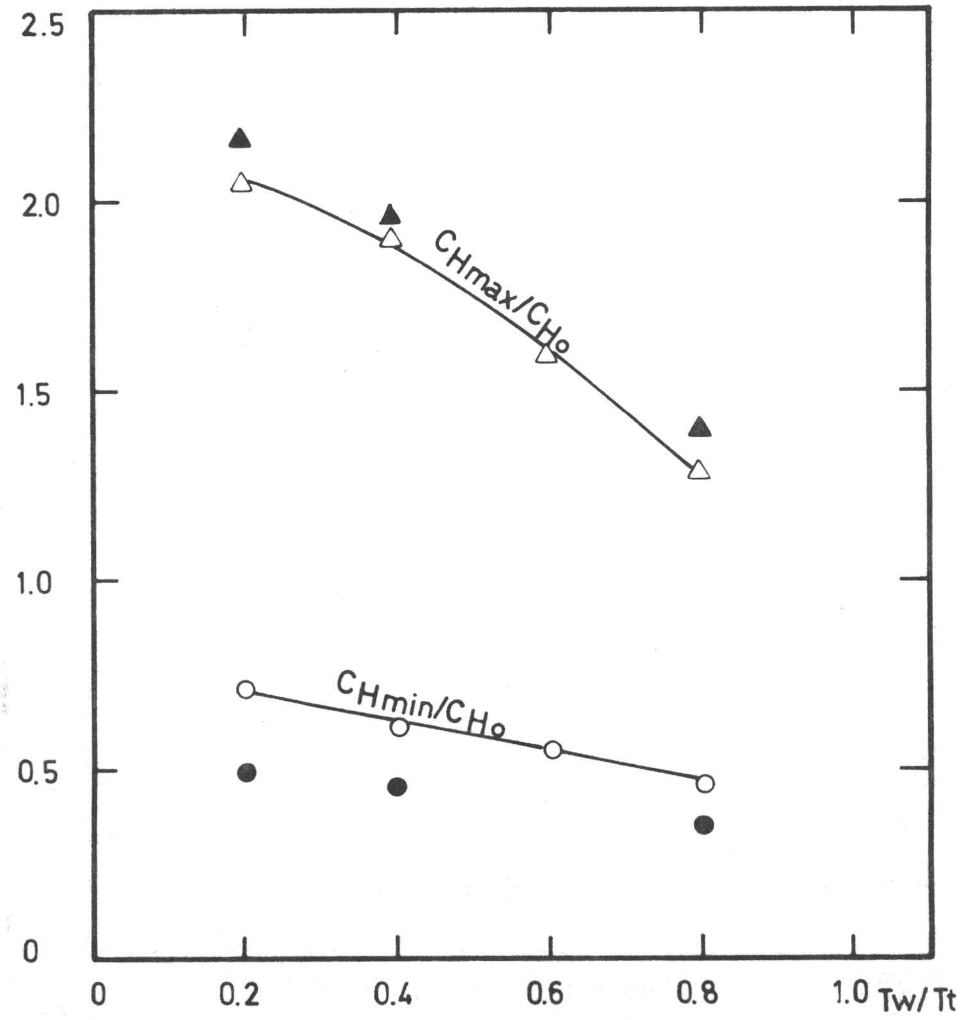

FIG:9d EFFECT OF WALL-TO-STAGNATION TEMPERATURE RATIO ON PEAK AND MINIMUM HEAT TRANSFER

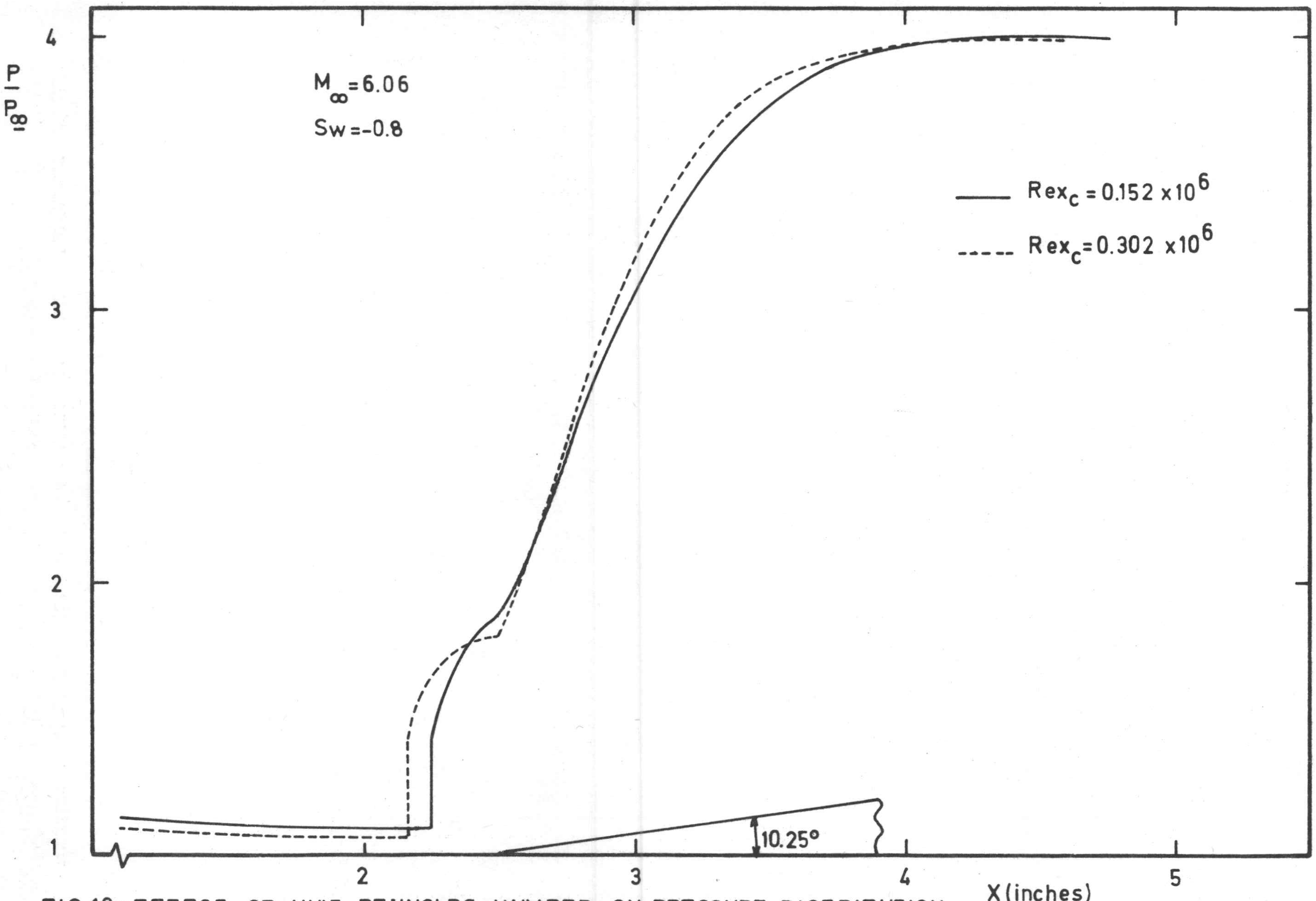

FIG:10a EFFECT OF UNIT REYNOLDS NUMBER ON PRESSURE DISTRIBUTION
(HIGHLY COOLED WALL)

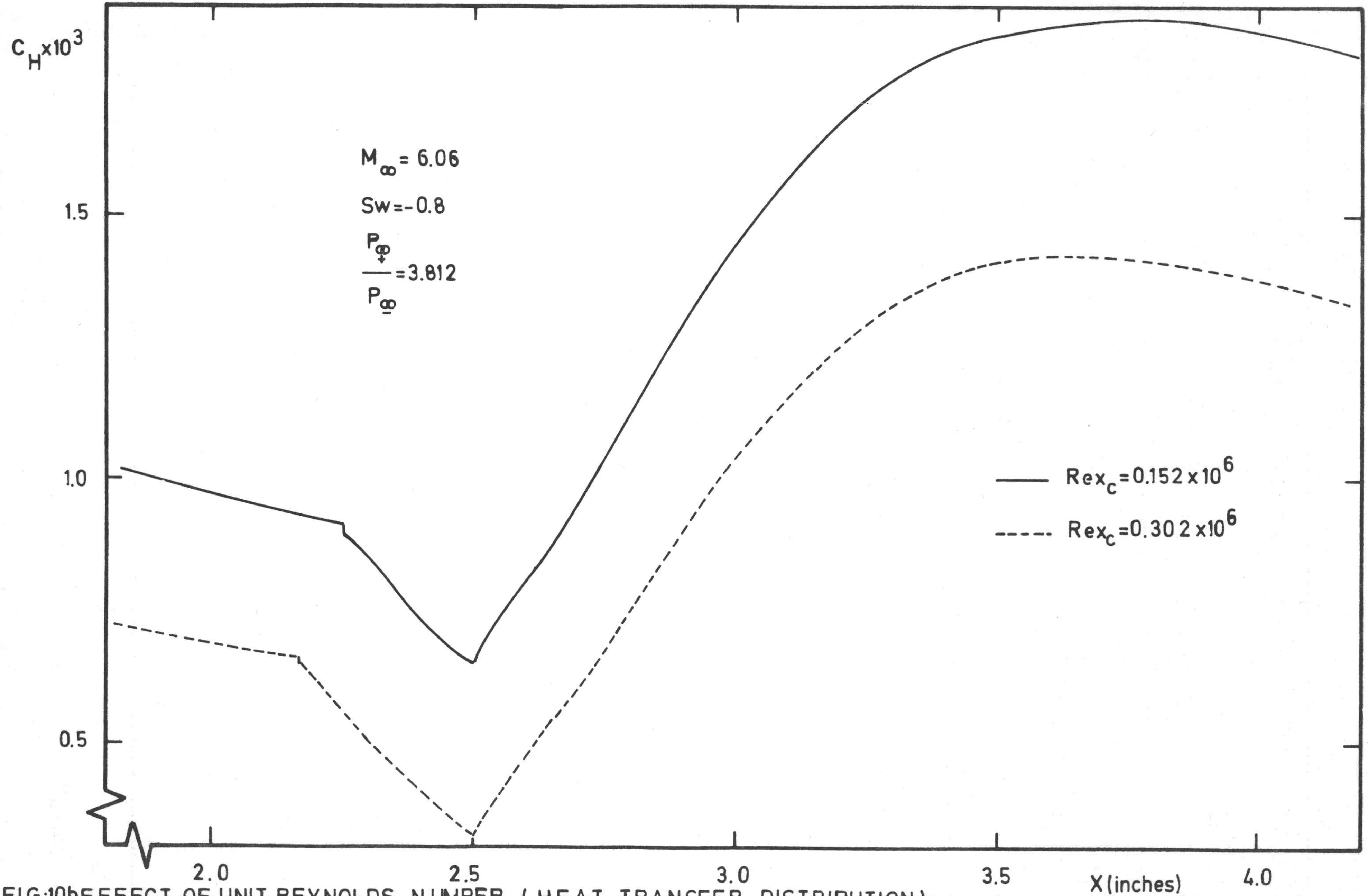

FIG:10b EFFECT OF UNIT REYNOLDS NUMBER (HEAT TRANSFER DISTRIBUTION)

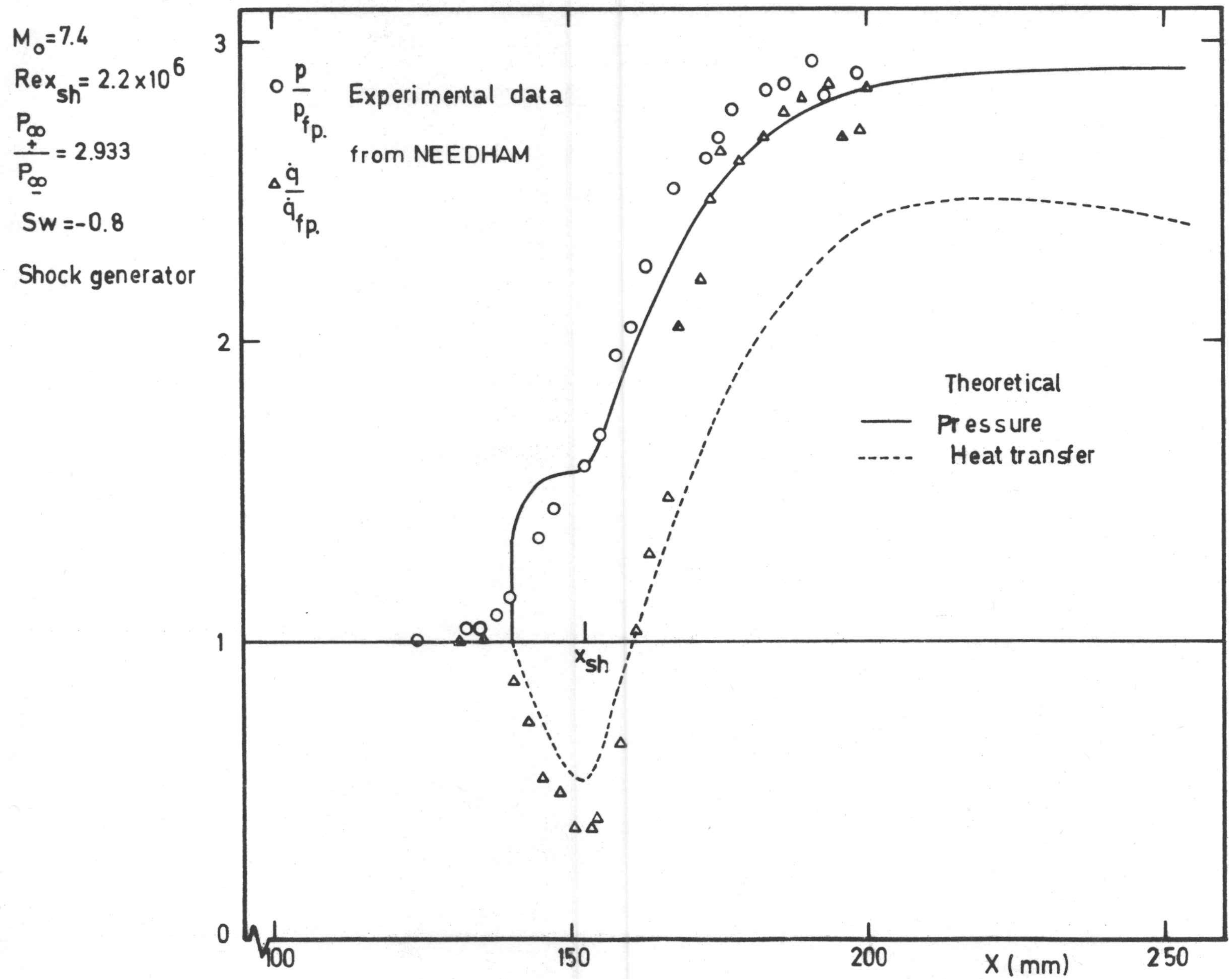

FIG:11a EXPERIMENTAL and THEORETICAL DISTRIBUTIONS OF PRESSURE and HEAT TRANSFER

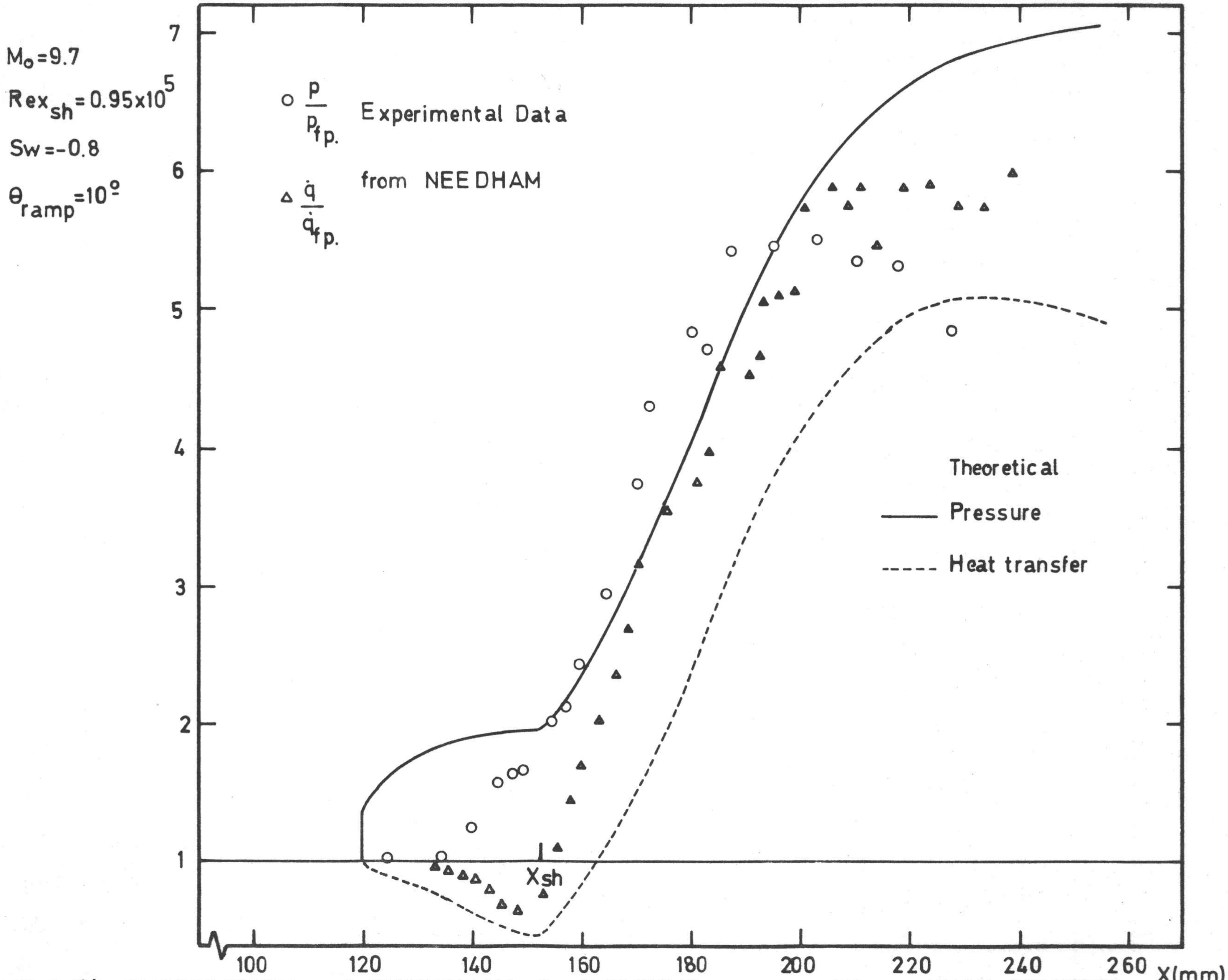

FIG: 11b EXPERIMENTAL and THEORETICAL DISTRIBUTIONS of PRESSURE and HEAT TRANSFER

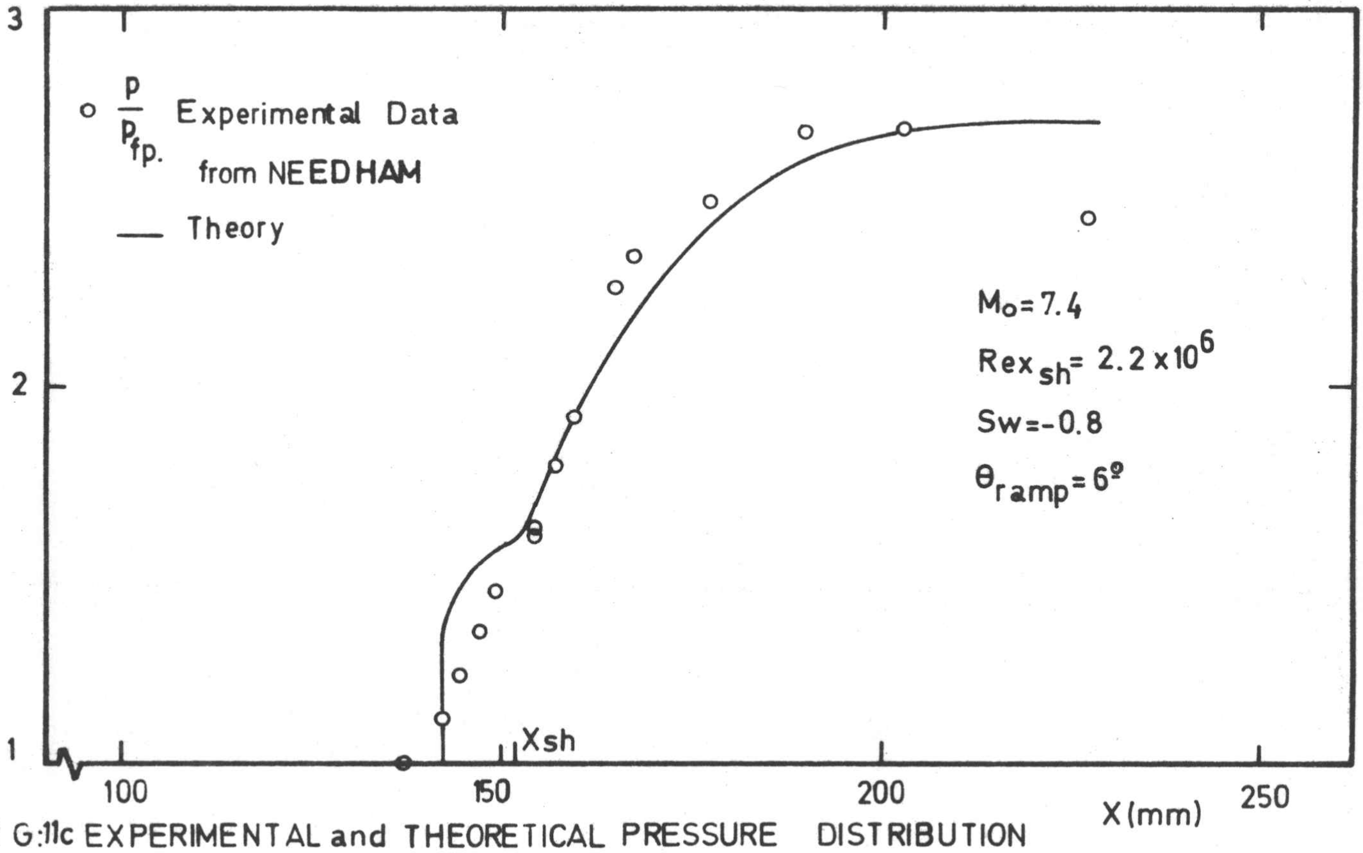

FIG:11c EXPERIMENTAL and THEORETICAL PRESSURE DISTRIBUTION

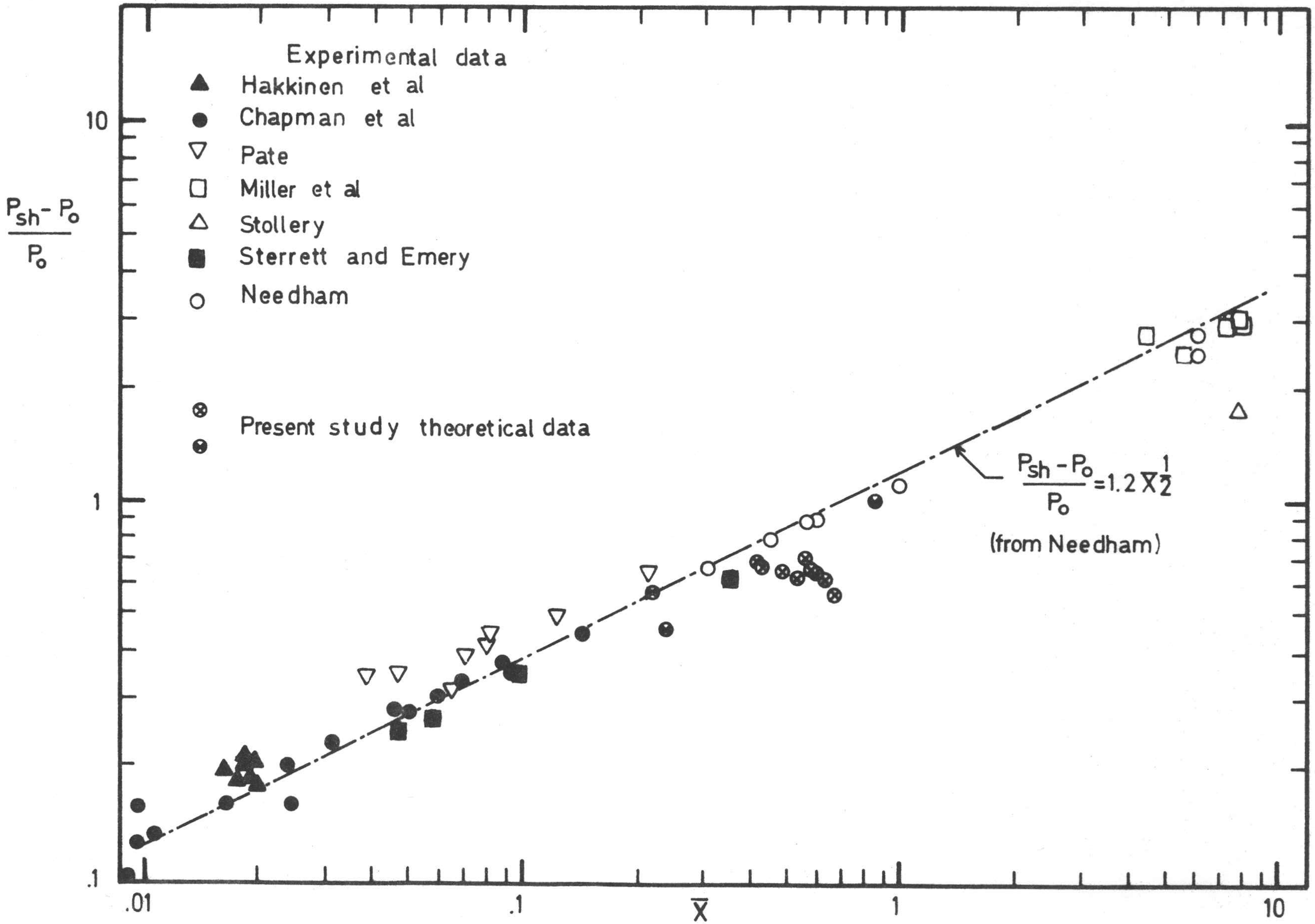

FIG:12 PLATEAU PRESSURE CORRELATION IN TERMS OF VISCOUS INTERACTION PARAMETER

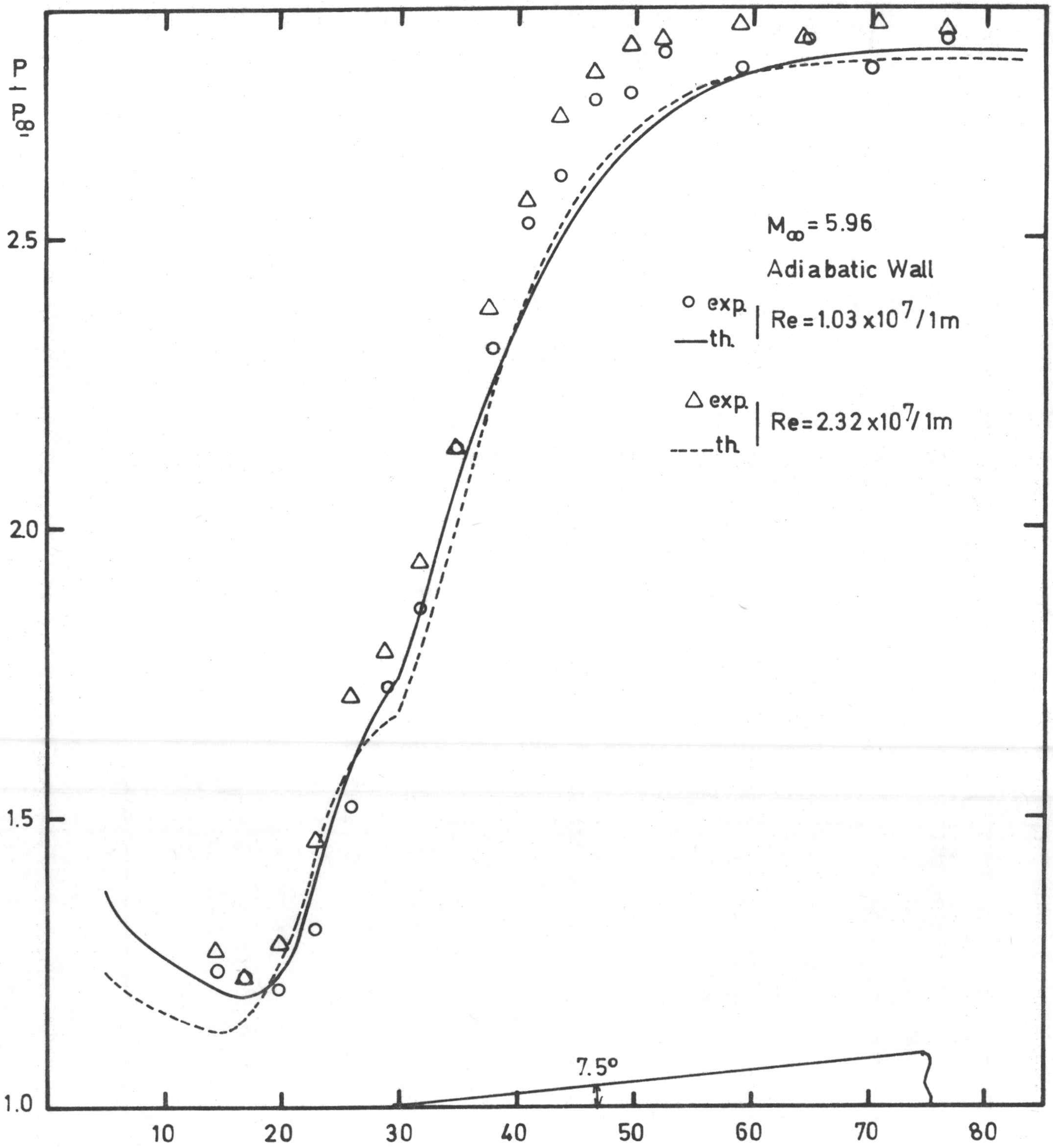

FIG:13 COMPARISON BETWEEN LEES-REEVES-KLINEBERG THEORY and V.K.I MEASUREMENTS ON ADIABATIC WALL